UNIVERSIDAD AUTÓNOMA DE MADRID
FACULTAD DE CIENCIAS
DEPARTAMENTO DE QUÍMICA ORGÁNICA

TUNING PROPERTIES OF "SMART" POLYMERS USING CONTROLLED RADICAL POLYMERIZATION

MARIO LUZÓN COLLADO

CONSEJO SUPERIOR DE INVESTIGACIONES CIENTÍFICAS
INSTITUTO DE CIENCIA Y TECNOLOGÍA DE POLÍMEROS
DEPARTAMENTO DE QUÍMICA MACROMOLECULAR APLICADA

Madrid, septiembre de 2013

Grupo de Fotoquímica de Polímeros
Departamento de Química Macromolecular Aplicada
Instituto de Ciencia y Tecnología de Polímeros
CONSEJO SUPERIOR DE INVESTIGACIONES CIENTÍFICAS

Departamento de Química Orgánica
Facultad de Ciencias
UNIVERSIDAD AUTÓNOMA DE MADRID

Tesis Doctoral

Tuning Properties of "Smart" Polymers using Controlled Radical Polymerization

Mario Luzón Collado
Licenciado en Ciencias Químicas

Dra. Carmen Peinado Margalef
Dra. Teresa Corrales Viscasillas
(Directoras)

Madrid, septiembre de 2013

A Karla y Claudia

A mis padres y a mi hermana

Deseo expresar mi más sincero agradecimiento a las personas que han contribuido de una u otra manera a que este trabajo llegue a su fin. El camino ha sido largo y muchas personas han conseguido que el recorrido sea más liviano pero de lo que no cabe duda es que ha merecido la pena.

En primer lugar quiero hacer una mención especial a mi directora de tesis Dra. Carmen Peinado por transmitirme la motivación por la investigación, por guiarme y respaldarme en los primeros años del doctorado con el rigor científico que la caracterizaba y por poseer la virtud de afrontar todos los obstáculos mostrando siempre una sonrisa. Allá donde estés, mil gracias.

Agradezco a la Dra. Teresa Corrales su esfuerzo, apoyo y comprensión a lo largo de estos años y especialmente este último tramo en el que sin su valiosa ayuda no habría podido concluir este proyecto.

Extiendo este agradecimiento al grupo de fotoquímica, Dra. Paula Bosch y Dr. Fernando Catalina por confiar en mí para disponer de cuanto fuese necesario para desarrollar toda clase de experimentos.

A mi gran amigo Íñigo, por todos estos años de carrera, máster y doctorado que nos ha hecho pasar mucho tiempo estando cerca el uno del otro viviendo experiencias inolvidables tanto dentro como fuera de los laboratorios. Sinceramente, has hecho que todo haya sido infinitamente más fácil. Te deseo lo mejor.

A mis compañeros, desde los primeros a los últimos, por hacer que todas las horas que hemos pasado en el laboratorio se hagan cortas, Verónica, Sara, Jesús, Leví, Gema, Sandra, Felisa, y especialmente a Esther y Quique por tantísimos buenos ratos que hemos pasado y por todas las charlas que hemos tenido sobre química, polímeros o cualquier otro tema.

A lo largo de este proyecto he tenido la oportunidad de visitar laboratorios de otros lugares del mundo donde he podido desarrollarme aún más como investigador y como persona. En todos ellos me han tratado de maravilla y me gustaría dejar constancia de las principales personas que han influido en mi camino: Prof. Tom Davis y Dr. Mikey Whittaker, del Centre for Advance Macromolecular Design (CAMD) de la Universidad de New South Wales (UNSW) en Sydney, Australia; Prof. Craig Hawker y Prof. Ed. Kramer, del Materials Research Laboratory (MRL) de la Universidad de California en Santa Barbara (UCSB), Estados Unidos; Dr. José Martinho y Dr. Jose Paulo Farinha del Instituto Superior Tecnico (UST) de Lisboa, Portugal.

I would like to thank as well to the people that I met in the CAMD, Antoine, David, Jan, Mikey, Tony and especially to Cyrille for all the adventures we have spent together since we met in Australia and for sharing the best of themselves.

También quiero agradecer el esfuerzo que ha realizado la empresa Iberceras para la que trabajo actualmente y en especial a Donato Herrera, Director de I+D+i, por las facilidades que me han dado para la finalización de este proyecto.

Sin duda, las personas que más me han apoyado de una manera incondicional son mis padres, Chema y Paloma, y mi hermana Cristina. Os quiero agradecer vuestra entrega y comprensión en todo momento así como vuestras sabias palabras y consejos en este y cualquier otro proyecto que he afrontado. Os estoy infinitamente agradecido.

Por último, agradezco desde lo más profundo de mi corazón a Karla, mi inseparable compañera, mi medio yo. Tú has sufrido en primera línea la montaña rusa de emociones y sensaciones que ha sido mi vida estos últimos años. Gracias por hacer esfuerzos infinitos por comprenderme y adaptarte a mis necesidades. Gracias por estar llena de vida y por hacerme ser mejor persona.

Y tú, Claudia, has sido la gran motivación para acabar este proyecto.

Tuning Properties of "Smart" Polymers using Controlled Radical Polymerization

GENERAL INDEX

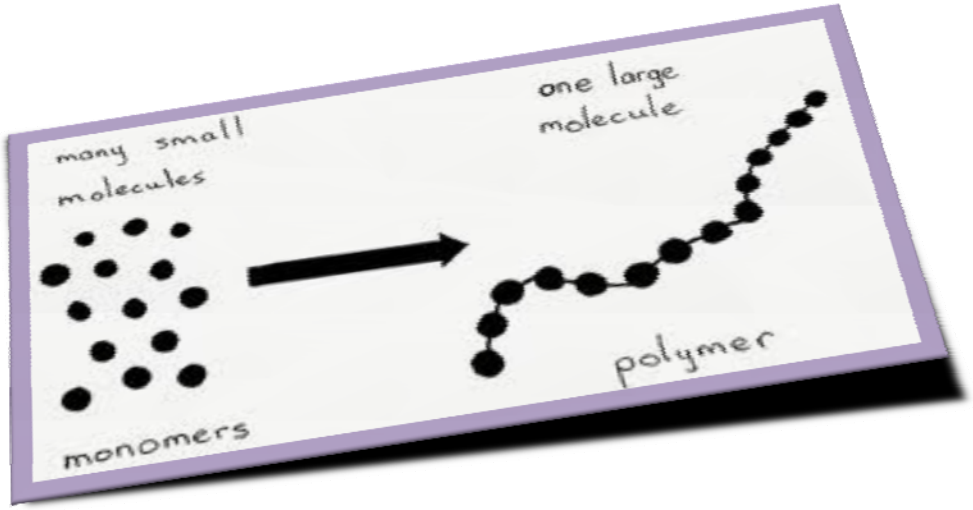

Perspective and Objectives

Chapter 1

1. Perspective

Polymers may be found in every part of the nature and life from the very beginning. The nature has been capable of creating specific polymers for every application. The polymers may come from mineral, vegetable or animal kingdom. Natural polymers such as cellulose, which is found in the wood and in the stalk of many plants, wool or silk have been extensively used along the history. Animal and vegetable fibers, bones and horn are polymers, and even inside the nucleus and the membrane that separates one cell from another there is a very important polymer, the deoxyribonucleic acid (DNA). And a very improved mechanism for getting energy from vegetal polymers like starch or cellulose has been got.

However, polymer chemistry has started to develop in the last decades. At the beginning around the 1800s, scientists tried to modify polymers that already exist in the nature and first complete synthetic polymer, rayon, is dated in 1911. It is not possible to talk about the history of the polymers without mentioning to John Wesley Hyatt (celluloid), Leo Baekelan (bakelite), Hermann Staudinger (demonstrated the existence of macromolecules) or Wallace Hume Carothers (nylon).

Like many times, the bigger developments of these materials were carried out during the war, specifically during the World War II. In this period the availability of natural sources of wool, latex, silk and other materials was cut off. The need of synthetic materials that supplant the natural polymers was urgent and during these years many polymers were produced from petroleum. It was developed nylon, SBR rubber, acrylic, polyethylene and many other polymers. Since that period the research and innovation in polymer science is the one which grows fastest in the world.

Nowadays polymers are present everywhere, these materials have been developed for many different applications and with very specific characteristics and properties. Polymer can be found in every area such as agriculture, medicine, industry, consumibles, aeronautics, adhesives, sports, construction and renewable energies.

But, what I imagine when I think of a polymer?

When somebody thinks in a polymer first thing that should appear in its mind is a chain. A chain made of repetitive units which are linked each other by a polymerization

process. Normally this backbone is formed by carbon atoms and different moieties can be grafted to. This specific topology provides polymer of singular characteristics which make them so special.

Polymers whether may form crystals or they may be amorphous, in this state they have a special morphology. Due to their high molecular weight, amorphous polymers are interacting all together and because of that they are totally tangled. That is why the morphology they adopt in this state can be compared with a basket with snakes because above the vitreous temperature the chains are moving but if you decrease the temperature below the vitreous temperature you can think of polymer more statics like spaghettis looks on a plate.

In **Chapter 2** it is included an extended introduction where is described the state of art of most relevant synthetic approaches that have been employed for the synthesis of functional polymers. Such strategies are mostly based on controlled polymerization techniques.

The controlled polymerization techniques are an important family of polymerization reactions that allow the preparation of interesting macromolecular structures. Polymers produced using these techniques are characterized by narrow molecular weight distribution, predictable molecular weight and end groups where chain growth can be restarted to give block copolymers and material with attractive architectures.

2. Objectives

The objective of this thesis was to prepare well-defined thermoresponsive “smart” polymers by controlled radical polymerization. Responsive or “smart” materials have been an increasing focus for chemists in the pharmaceutical and biomedical sectors. Potential applications for these materials include drug, gene, and cell delivery, surface engineering, sensing and actuation, water remediation. For these applications the polymers have to be soluble in water.

The polymers synthesized in this study have been achieved by reversible addition-fragmentation chain transfer (RAFT) polymerization, atom transfer radical polymerization (ATRP) and ring opening polymerization (ROP) and they have very specific characteristics for many different applications.

The main objectives of the work undertaken in this thesis are detailed below:

Chapter 3, *Hierarchically Organized Micellization of Thermoresponsive Rod-coil Copolymers based on Poly[oligo(ethylene glycol) methacrylate] and Poly(ε-*caprolactone). This work is related to the synthesis of a series of amphiphilic triblock copolymers, poly[oligo(ethylene glycol) methacrylate]$_x$-block-poly(ε-caprolactone)-block-poly[oligo(ethylene glycol) methacrylate]x. Self-assembly behaviour of water solutions was studied by several techniques. It is worth recalling that the interplay of the two hydrophobic and one thermoresponsive macromolecular chains as long with the specific architecture (topology, relative block lengths) and the nature of the blocks of the macromolecule give rise to hierarchically organized micellization.

Two main features are of relevance: the use of a novel methodology based on Modulated Temperature Differential Scanning Calorimetry to determine critical micellar temperature (cmt) and the detection of cubic structures by HRTEM and STEM.

Chapter 4, *Water-soluble, Thermoresponsive, Hyperbranched Copolymers based on PEG- Methacrylates: Synthesis, Characterization and LCST Behavior.* The aim of this work was to achieve a fine-tuning of the LCST of PEGMA by varying the composition of copolymers and changing the length of PEG chains and study the impact of the topology on LCST of these interesting copolymers based on PEGMA. Different polymers have been synthesized and LCST was determined as function of the architecture and composition. It has been demonstrated that the architecture of the polymers has an important influence in its characteristics.

Chapter 5, *Thermal studies and chromium removal efficiency of thermoresponsive hyperbranched copolymers based on PEG-methacrylates.* In this paper we describe an application for the thermoresponsive hyperbranched polymers. Due to their characteristic they have the ability of encapsulating heavy metal atoms inside the micelles. Using this methodology it could be possible to obtain chromium-free water increasing the temperature above the LCST of the polymer, making them collapse and forming the aggregates where the chromium will introduce. In this study, the thermal behavior and thermal stability of the copolymers is also evaluated.

Chapter 6, *Design and Synthesis of Dual Thermo-Responsive and Anti- Fouling Hybrid Polymer/Gold Nanoparticles.* The intention of this paper was to obtain thermosensitive gold nanoparticles and evaluate the properties of these hybrid materials in solution using dynamic light scattering and UV-vis spectroscopy. The thermoresponsive copolymers were based on PEGMA with narrow polydispersities using reversible addition-fragmentation chain transfer polymerization (RAFT). The range of the LCST of these copolymers is from 15 to 90 °C dependent on their monomer compositions. Subsequently, these copolymers were grafted onto gold nanoparticle (GNP).

At the end, in **Chapter 7** the general conclusions drawn from all the work that has been carried out in this thesis are collected.

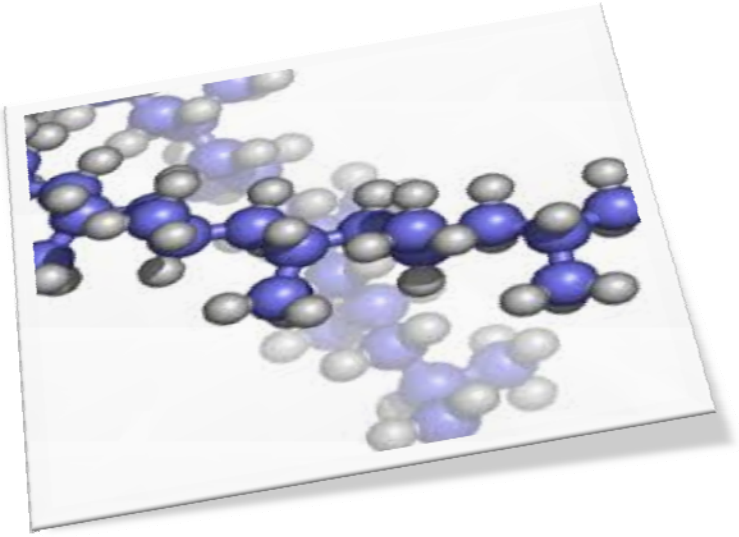

General Background

Chapter 2

1. Introduction

The main aim of this chapter is to describe the most relevant synthetic approaches that have been developed for synthesis of functional polymers. On the last decades, strategies are mostly based on controlled polymerization techniques, and a general description of such synthetic techniques is reported here.

1.1. Radical polymerization overview

Radical polymerization was developed in the 1950's while living anionic vinyl polymerization was being discovered. Exhaustive studies of the radical process was carried out by Michael Szwarc[1-8] followed by the study of the analysis of the active species involved including the mechanism of the reaction, relationship between structure and reactivity, kinetic and thermodynamic parameters for rate constant.[9-13]

Radical polymerization mechanism proceeds by adding organic free radicals which are the active species of the reaction. As all chain polymerization the resulting polymers by RP are high molecular weight from the beginning and during the reactions at any a time only exist monomer, high molecular weight polymers and growing chains. In spite of this polymerization could seem uncontrolled, final polymers show good selectivity (regio and chemo) due to the head to tail addition of the monomers. The head to tail addition is favored on both steric and resonance reasons.

Radical chain polymerization, like any chain polymerization, consists in a sequence of three elementary reactions: initiation, propagation and termination. The initiation step involves two different reactions, first one the homolitic rupture of the initiator to produce the free radicals which is usually, similar to termination process, a slow step in comparison with the propagation process. Secondly the reaction of the free radical created from the initiator with the first monomer, which is added to the chain is considered as a part of the initiation step. Choosing the radical initiator the initiation rate may be adjusted. One characteristic of the chain radical polymerization is that may be initiator left at the end of the polymerization because of the long half life of them. Propagation step consists in the addition of monomers on the growing chain. This addition occurs to the carbon with less steric impediment obtaining usually head

to tail linkages and every time a monomer is added to the polymer chain, it creates a new radical, with same identity than the one before, which will react with a new monomer. At a certain moment, the propagating chain stops adding monomer and start the termination process. Termination step occurs when two radical reacts with each other in two different possible ways, by coupling or by disproportionation. In the first way, which is more common both radicals react and form a unique polymer chain and in the second way the hydrogen beta of one radical is transferred to the other radical resulting in the formation of two polymer molecules.

Since the propagation step is extremely fast the life of a propagating chain is too short, $\sim$ 1 s, in order to make any external manipulation, which means that is not possible any end functionalization or addition of other monomers to obtain pure block copolymers. The kinetic of this polymerization is described by Eq. (1), where the rate of polymerization is a function of the efficiency of initiation (f) and the rate constants of radical initiator decomposition (k_d), propagation (k_p) and termination (k_t). The final molecular weight depends on the termination rate and on the rate of transfer. If the contribution of the transfer process can be neglected, the degree of polymerization depends reciprocally on the square root of radical initiator concentration, as shown in Eq. (2).

$$R_p = k_p[M](f\, k_d[I]_0/k_t)^{1/2} \qquad [1]$$

$$DP_n = k_p[M](f k_d[I]_0 k_t)^{-1/2} \qquad [2]$$

Radical polymerization can be carried out of both, homogeneous (mass and solution polymerization) and heterogeneous (suspension and emulsion) type. Bulk or mass polymerization is the simplest process although there is not good control of the parameters of the reaction and the characteristics of the final polymer. Solution polymerization avoids the mass polymerization limitations by decreasing the viscosity of the system making it easier for stirring and transferring the heat more efficiently. In solution polymerization the critical point is the solvent to be used, it must be very well selected to not interfere in the radical process. Heterogeneous polymerizations, where

suspension and emulsion polymerization are included, are used to control the homogeneous limitations such as thermal or viscosity issues.

Conventional radical polymerization has a significance use in the industry since circa 50 % of all commercial polymers produced are synthesized by this procedure. Typical polymers obtained by radical polymerization are low density polyethylene, polystyrene, vinyl polymers (poly(vinyl chloride), poly(vinyl acetate), poly (vinylidene chloride), acrylate and methacrylate polymers, fluoropolymers among others.

Radical polymerization like others chain polymerization system cannot produce block copolymers or other polymers with specific architectures mainly due to its intrinsic characteristics in terms of termination process.

1.2. Controlled radical polymerization techniques (CRP)

Polymers obtained by chain polymerization techniques like radical or ionic polymerization do not have controlled topologies. It was developed in 1950s the anionic living polymerization which permit to control the structure of the final polymers. Using this technique it is possible to determine the monomer composition and therefore the molecular weight and polydispersity. However it was not until the 1990s when other techniques with the ability of control the structure of the polymer were developed.[14,15] These new polymerization systems (Stable Free Radical Polymerization (SFRP),[16] reversible addition-fragmentation chain transfer polymerization (RAFT),[17] atom transfer radical polymerization (ATRP)[18]) and its main characteristic will be discussed below.

The aim of design new polymers with specific architecture and therefore with desirable features such as block copolymers are of high commercial interest. Much of the driving force for the effort derives from the belief that well defined materials from controlled radical polymerization will offer substantial advantages to build nanostructures for microelectronics, biotechnology, and other areas.

1.2.1. Fundamentals of CRP

One of the principal objectives of controlled radical polymerization is to minimize the chain breaking reactions that contribute to end the growing polymers. On the other

hand a fast initiation is crucial for controlling de polymer length and therefore the molecular weight. The combination of simultaneous initiation and no termination leads to a process in which all the polymer chains grow at the same time. Another feature of these systems is the presence of a compound that reacts with the growing chain capturing the propagating radical becoming a dormant specie (Schemes 2.1). This reversible reaction is regulated by an equilibrium constant which is shifted to the dormant species. Thus, the synthesis of the polymers occurs by an intermittent formation of active propagation species. The introduction of the dormant state suppress the bimolecular termination of living polymers, and increase the average lifetime for living polymers by at least 4 orders of magnitude.

The equilibrium between the dormant species and the propagating radicals is essential to all controlled radical polymerization systems[19,20] although the reversibly may either be governed by an deactivation/activation process according to Scheme 2.1a, or they can be involved in a ‘‘reversible transfer’’, degenerative exchange process according to Scheme 2.1b.

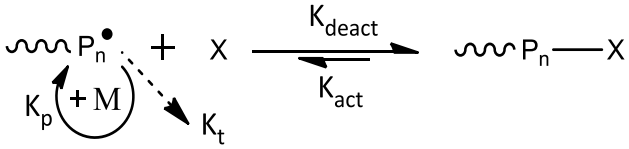

Scheme 2.1a. Mechanism of radical polymerization by deactivation/activation process

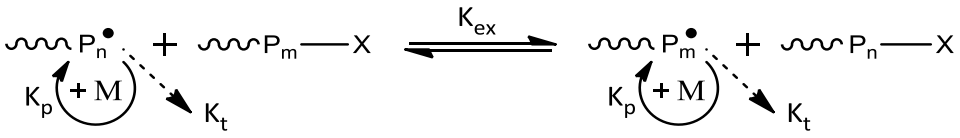

Scheme 2.1b. Mechanism of radical polymerization by degenerative exchange process

The approach detailed in scheme 2.1a relies on the persistent radical effect (PRE).[20-23] The stable radical is often called persistent radical and its suppression of termination is known as PRE, which is a peculiar kinetic feature which provides a self-regulating effect in certain CRP systems. Propagating radicals Pn• are rapidly captured in the deactivation process (with a rate constant of deactivation, k_{deact}) by species X, which is

typically a stable radical. The dormant species are activated (with a rate constant k_{act}) to reform the growing centers. Radicals can propagate (k_p) but also terminate (k_t). Persistent radicals (X) can only cross-couple reversibly with the growing species (k_{deact}) thus a steady state of growing radicals is established through the activation–deactivation process rather than initiation–termination as in conventional RP. Therefore, every time that occur a radical–radical termination there is an irreversible accumulation of X. The concentration of X progressively increases with time, and consequently, the concentration of radicals as well as the probability of termination decreases with time.

Systems that obey PRE include stable free radical polymerization (SFRP) and atom transfer radical polymerization (ATRP). Since all dormant chains are capped by the trapping agent a stoichiometric amount of mediating species is required. Although ATRP operates via the PRE the amount of transition metal catalyst can often be substoichiometric due to the combination of catalytic process and redox reaction.

On the other hand, processes dependent on approach shown in scheme 2.1b are based on degenerative transfer (DT). CRP processes based on DT do not obey the PRE. In DT processes the equilibrium of the transfer reaction should be the unity since a steady state concentration of radicals is established via initiation and termination processes. The transfer agents interchange a group or an atom with all the propagating chains and this agent controls the molecular weights and polydispersity of the final polymer. In order to have a good control the exchange should be faster than the propagation process and the degree of polymerization is defined by regulating the ratio monomer-transfer agent-initiator.

Comparing the lifetime of a chain in the active state in a CRP process with the lifetime of a propagating chain in conventional RP similar values are found, however due to the time that the growing radicals remain in the dormant state, the whole propagation process may take $\sim$ 1 h in CRP, therefore exists the opportunity to perform synthetic procedures, including chain-end functionalization or chain extension.[24]

Summarizing, the key for efficient controlling of polymer architecture as well as molecular weight and polydispersity of all CRP system, is required fast exchange between active and dormant species, and the compounds involved in the reaction should be perfectly chosen for creating a growing radical which react only with a few

monomer units (within a few milliseconds) before it is deactivated to the dormant state (where it remains for several seconds).

1.2.2. Comparison of radical polymerization and controlled radical polymerization

Both systems are based on radical generation process sharing mechanism, selectivity among other characteristics. However, as it has been discussed above there are important differences between those polymerizations being the fundamentals detailed below:

1. Initiation step: In RP system the radical initiation is slow whereas in most CRP systems, the initiation step is very fast, in some cases the initiator create the starting radical at once achieving an instantaneous growth of all chains.
2. Propagating step: In RP system, the lifetime of growing chains is ~ 1 s whereas in CRP it could take more than 1 h, as dormant species are involved and reversible activation is intermittent.
3. Termination step: In RP system almost all chains are dead, whereas in CRP the dead chains reach usually 10 %.

1.2.3. Stable-free radical polymerization (SFRP)

This polymerization following PRE approach is based on the employment of stable radicals, usually nitroxide radical (most commonly used, TEMPO; 2,2,6,6-tetramethyl-1-piperidinyloxy) for trapping reversibly the growing chain resulting the dormant specie (Scheme 2.2). Like other CRP systems, the equilibrium is shifted strongly toward the dormant species so that the propagating radical stays most of the time linked to the stable radical being activated every 10^2-10^3 s for a short period of time enough to add 1 to 5 monomers units before deactivation.

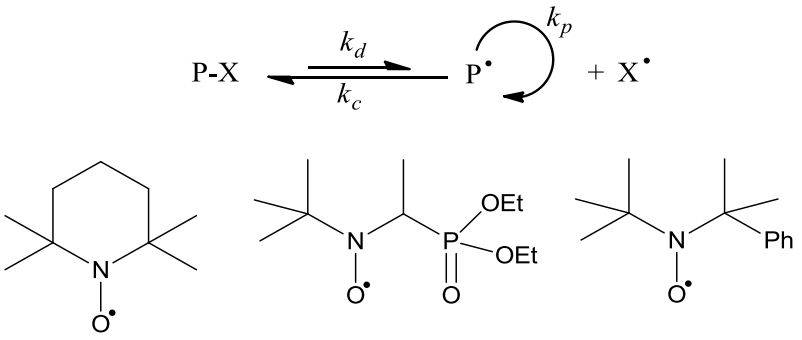

Scheme 2.2. Stable-free radical polymerization (SFRP) mechanism and stable nitroxide compounds typically employed

In SFRP polymerization, it is crucial to set appropriate reaction condition since those are the responsible of minimizing the termination rate, which leads to dead chains and broadening of the molecular weight distribution. Termination also results in accumulation of nitroxide, which shifts the equilibrium toward the dormant state, thereby lowering the radical concentration and the polymerization rate.

1.2.4. Atom transfer radical polymerization (ATRP)

ATRP consists on the transfer of a halide atom from a catalyst/ligand complex to a propagating macroradical (Scheme 2.3). To form the catalyst/ligand complex a transition metal in its lower oxidation state is needed, being copper the most commonly used. This complex is the reliable of activates a halide-terminated polymer chain (or alkyl halide initiator) to yield a radical capable to add monomers and a catalyst complex in a higher oxidation state.

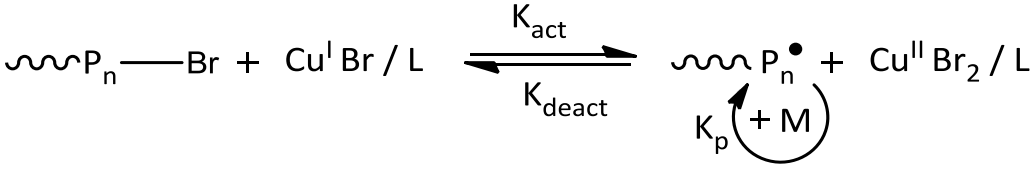

Scheme 2.3. Simplified reaction scheme for ATRP

It is important to choose a determined metal/ligand complex due to its decisive role in the reactivity of the catalyst complex towards various monomers as well as affecting its solubility in the reaction medium. Advantages of ATRP are that it does not require high temperatures, and the range of monomers it can polymerize is much more versatile than other controlled radical polymerizations.

1.2.5. Reversible addition–fragmentation chain transfer polymerization (RAFT)

First mention of reversible addition–fragmentation chain transfer polymerisation was made in 1998 by CSIRO[17] who developed this new technique and is currently amongst the most popular CRP processes due to its versatility for polymerizing a wide range of monomers.[17,25,26]

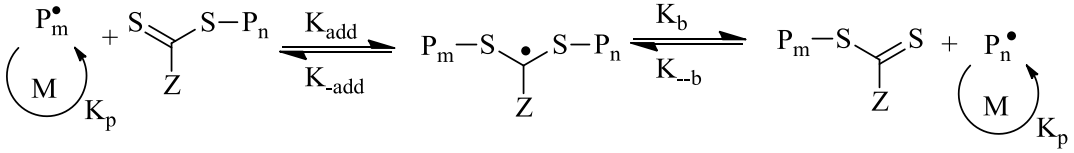

Scheme 2.4. Simplified mechanism of RAFT polymerisation.

It is shown in Scheme 2.4 the simplified mechanism of RAFT polymerisation which involves a sequence of addition-fragmentation equilibrium.[27] In this system, is essential a skilled choice of RAFT agent for achieving a good control over the macromolecular features for a given polymerisation system. This polymerization is widely studied and there are many advances in this field but some aspects of the kinetics of RAFT polymerisation still requires further investigation.

Below is detailed the controlled radical polymerizations, including mechanism and control parameters, which have been utilized in this thesis for preparing the different polymer structures.

2. Atom Transfer Radical Polymerization (ATRP)

2.1. Introduction and background

It was in 1995 when a new class of controlled radical polymerization was reported by the groups of Matyjaszewski[28] and Sawamoto[29]. Atom transfer radical polymerization (ATRP) is a controlled radical polymerization which has had a tremendous impact on the synthesis of macromolecules with well-defined compositions, architectures and functionalities.[29-31] Radical generation in ATRP involves an organic halide undergoing a reversible redox process catalyzed by a transition metal compound such as Ti, Mo, Re, Fe, Ru, Os, Rh, Co, Ni, Pd and Cu.[32,33] After studying these metals for polymerizing different monomers in diverse media, it has been found that complexes of copper are the most efficient catalysts.

ATRP has become a very popular system which is confirmed by the increasing ATRP-related publications over the last 18 years (Fig. 2.1).

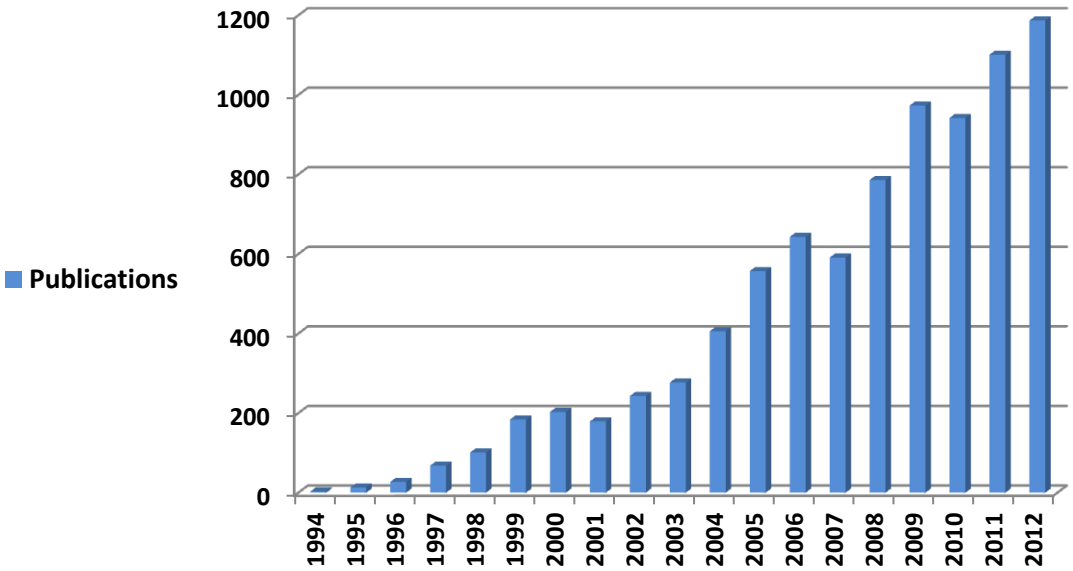

Figure 2.1. Publications per year indexed using the words ATRP and Polymerization

ATRP, like others CRP, is based on two fundamental characteristic, quantitative initiation step to create the starting radicals at once keeping the concentration of growing polymers chains constant, and well selected metal/ligand system capable of retaining the growing chains mostly of the time of reaction by the dynamic equilibrium between the activated and the dormant species. The general mechanism of ATRP is shown in Scheme 2.5. Taking into account that the radical termination reactions are mostly suppressed it is possible to calculate the final molecular weight, and due to the simultaneous formation of the polymer chains narrow molecular weight distribution are reached, this way the structure as well the composition and therefore, the features and properties may be precisely defined. In the literature are described different polymers with diverse architectures, functionalities and composition synthesized by ATRP (Figure 2.2).[12,18,34-37]

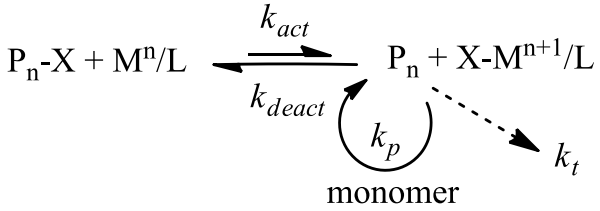

X is a halide, M is a metal and L is a ligand

Scheme 2.5. Schematic illustration of ATRP process.

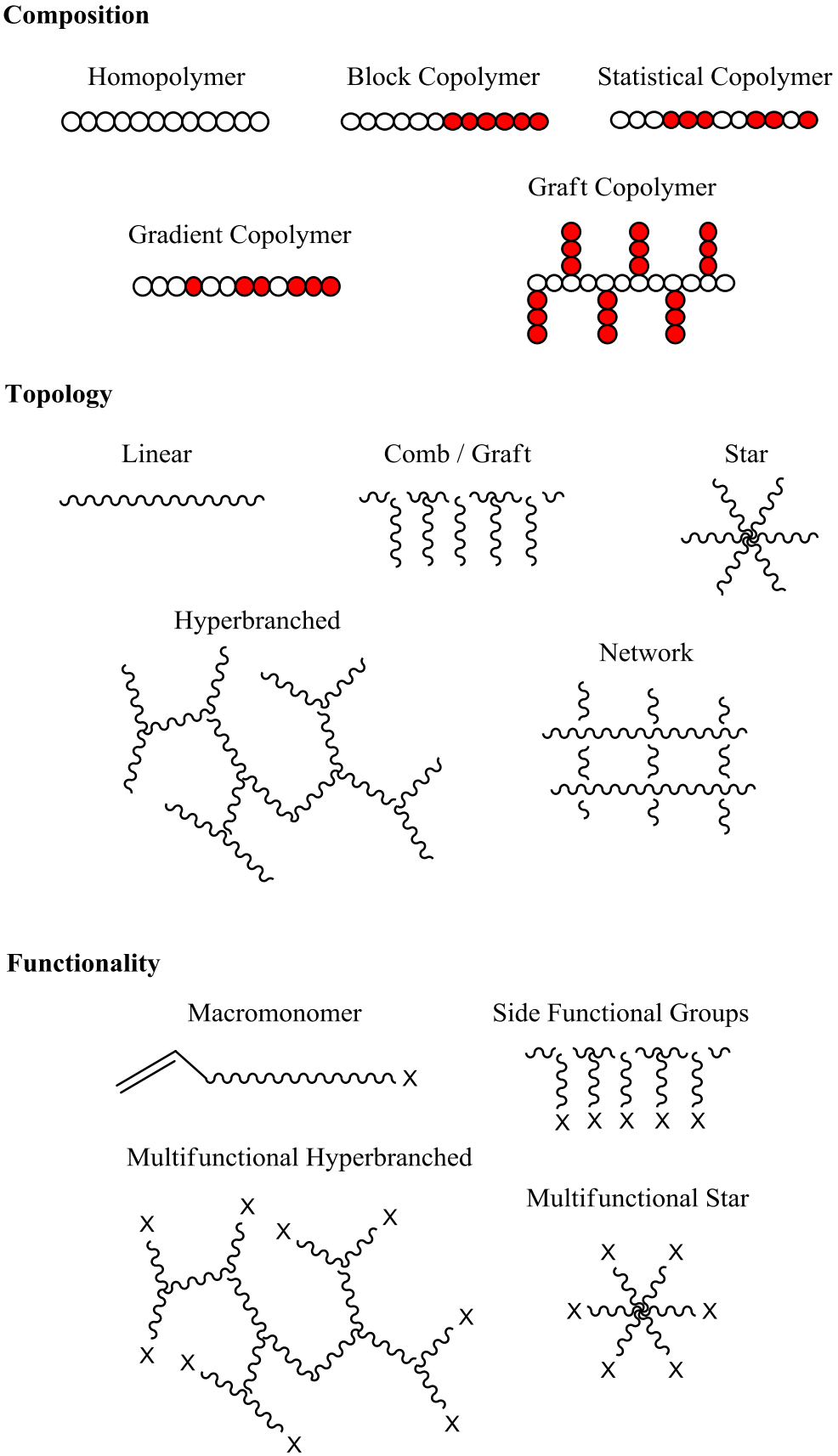

Figure 2.2. Schematic representation of polymers with controlled topology, composition and functionality synthesized using copper-mediated ATRP.

2.2. Architecture

Many different architectures may be prepared by ATRP with diverse properties depending on the application. By changing the composition it is possible to produce homopolymers, statistic copolymers, block copolymers, graft copolymers, by changing the topology of the system lineal, star, brush or dendritic polymers may be prepare and furthermore, varying the functionality of the polymeric chain telechelic polymers, macroradicals, multifunctional polymers, miktoarms polymers among other architecture could be design.[38,39]

In this thesis comb-like copolymers have been prepared. There are three different techniques for the preparation of comb-like polymers. When the side chains grow starting from the polymer backbone is considered grafting from approach. If the comb-like structure is achieved by coupling polymer already synthesized to the polymer backbone the approach is called grafting onto. The grafting through approach consists in the addition vinyl macromonomers to the growing chain. For the synthesis of comb-like polymers of chapter 3 grafting through approach have been followed. This approach offers the advantage on the precise control of side chain polydispersity and grafting density.

Hyperbranched structures may be obtained using divinyl monomers. This polymerization should be carefully controlled in terms of concentration of difunctionalized compound and monomer conversion to assure that hyperbranched architecture has been achieved. In this systems, the degree of polymerization determine the branching degree.[36]

2.3. Composition

A variety of monomers can be polymerized by ATRP such as styrene, acrylonitrile, (meth) acrylates, (meth) acrylamides and 1,3-dienes among others. Their functional groups which form the structure are fundamental for predicting the final properties of the material. ATRP is very versatile as many functional groups[34] are tolerated during the reaction without interfering in the polymerization reaction. In ATRP reaction various components are involved, initiator, monomer, catalyst, ligand, solvent,

therefore the basis of a successfully ATRP polymerization is to match all those components so that the deactivated species concentration exceeds the propagation radical chain by a factor of 10^6 approximately which is the fundamental characteristic of the controlled radical system.

By ATRP is possible to prepare polymers by segments (ABA, ABCD, etc), comb-like polymer by grafting from, grafting onto or grafting through approaches, hyperbranched or gels may be also obtained by this technique by adjusting the feed of every monomer and multifunctionalized monomer present in the reaction. Hybrid materials, by combining organic and inorganic compounds as well as biodegradable structures have been synthesized by ATRP.

2.4. Copper catalyst system

2.4.1. Basic components of copper-catalyzed ATRP

Copper-catalyzed ATRP is a multicomponet system formed by an initiator, a monomer and copper system formed by a ligand and a metal in its lower oxidation state. One of the most important compounds in ATRP is the copper complex, which is usually utilized copper(I) halide and the corresponding nitrogen based ligand. The complex acts as a catalyst and is the responsible of the reversible activation (homolitic rupture) of carbon-halogen bond present in the initiator, creating a radical with latent activity by redox reaction. In this process the metal is oxidized by the transfer of an electron followed of the capture of the halogen atom, thus a radical is created giving rise to the propagation reaction between the just created radical and monomers. Later, the metal complex is reduced when reacts with the growing chain coupling the halogen atom to the propagating radical. Therefore, this metal complex is the determinant compound in the sense that is the main responsible of the establishment of the dynamic equilibrium between dormant/latent and active species.

An advantage of ATRP mechanism is that all the reactive needed for the polymerization are commercially available including alkyl halides, ligands and transition metals. The common monomers that are used in ATRP, shown in figure 2.3, are styrenes, (meth)acrylates, meth(acrylamides), acrylonitrile and (meth)acrylic acids. Typical initiators are halogenated alkanes, benzylic halides, α-haloketones, α-

halonitriles and sulfonyl halides some of them are shown in figure 2.3. Beside, the dynamic equilibrium between latent species and growing radicals for a particular system is easily adjusted by modifying the ligand of the metal complex. Commonly used ligands to form the metal complex are shown in figure 2.3.[40]

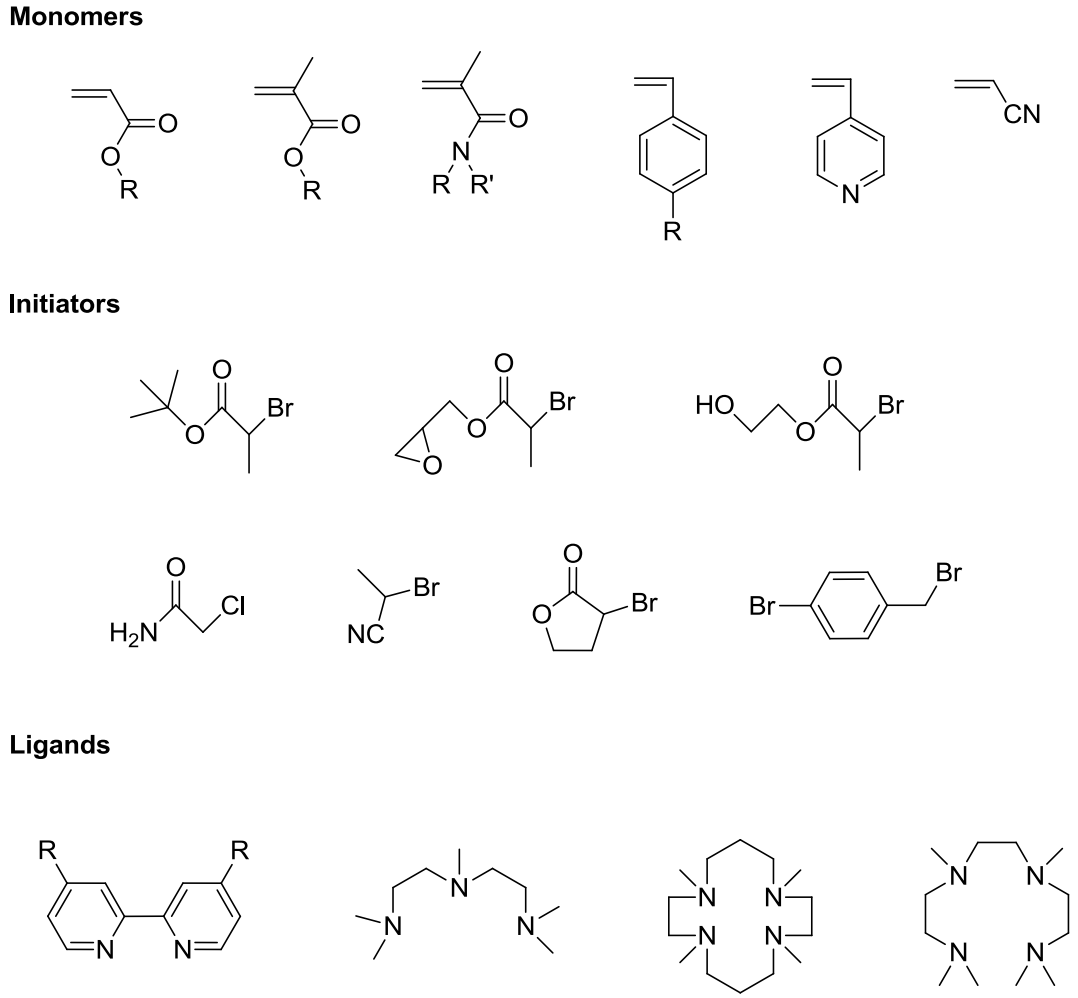

Figure 2.3. Typical monomers, initiators and ligands used in ATRP polymerization

2.4.2. Kinetics of ATRP. Molecular weight and molecular weight distribution.

The analysis of the kinetics has been extensively studied for homogeneous, copper based polymerizations. The kinetic and the control of the reaction is not only persistent radical dependence but also the activator metal complex is involved, then several requirements are needed to achieve a successful ATRP process.

Initiation should be fast and need to occur in the early stages of polymerization so that the propagation chains consume monomers simultaneously leading to polymers with similar degrees of polymerization (DP) which have been previously defined. This hypothesis neglects the contribution of termination reactions due to the persistent radical effect.

The molecular weight, and therefore the degree of polymerization, is calculated by the ratio on the feed of initiator-monomer and they are not affected by metal complex concentration.

The molecular weight distribution or polydispersity, which is the index of the lenght distribution of the polymer chains, in a well controlled polymerization is usually circa 1.1. For a given system the faster the metal complex capture the growing polymers the narrower polydispersity is obtained.

Considering that termination reactions are suppressed because of the persistent radical effect the rate law for ATRP can be derived as is detailed in equation [3]

$$\frac{-d[M]}{dt} = k_p[M][P^{\bullet}] = \frac{k_p K_{ATRP}[M][PX][Cu^I]}{[X - Cu^{II}]} \qquad [3]$$

where $K_{ATRP} = k_a/k_d$. According to equation (1), polymerization rate in ATRP depends on the equilibrium constant for ATRP (K_{ATRP}), concentrations of dormant species (PX) and monomer (M), propagation rate constant of monomer (k_p), and the ratio of concentrations of activator (Cu^I) and deactivator ($X - Cu^{II}$). On the other hand, molecular weight distribution or polydispersity index ($PDI = M_w/M_n$) in ATRP depends on the propagation rate constant (k_p), deactivation rate constant (k_d), monomer conversion (p), and concentrations of dormant species, monomer and deactivator ($X - Cu^{II}$) according to equation (4)[40]

$$\frac{M_w}{M_n} = 1 + \left(\frac{[PX]k_p}{k_d[X - Cu^{II}]}\right)\left(\frac{2}{p} - 1\right) \qquad [4]$$

In ATRP, a semilogarithmic plot of ($\ln[M]_0/[M]$) versus time (Fig. 2.4a) yields a straight line which means that concentration of active species remain constant during the polymerization and the first order kinetic with respect to the monomer. However, experimentally may be observed a slightly deviation at high conversions produced by the increase of oxidized metal species due to the termination process. Figure 2.4b shows the linear increment of the molecular weight depending on the conversion. This linearity indicates that the number of growing polymer chains is constant. Furthermore, the molecular weight distribution (M_w/M_n) or polydispersity index (PDI) decrease while the conversion increase (Fig. 2.4c). In adequate selected parameters and components ATRP process the final value of polydispersity is near 1.1.[32]

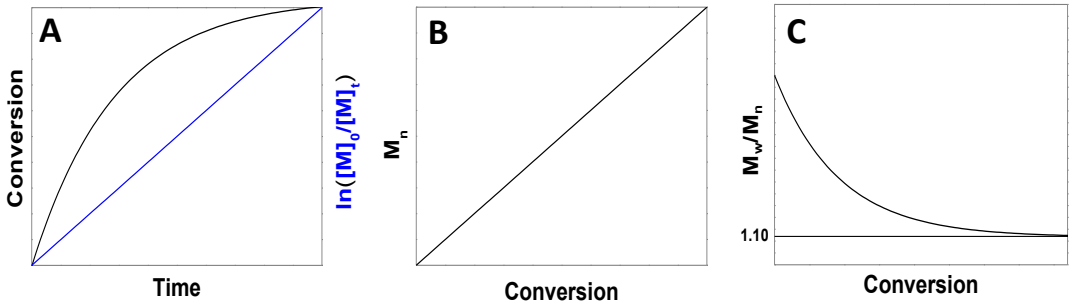

Figure 2.4. Typical kinetic features of copper-mediated ATRP.

In spite of all the advantages of ATRP system which permit to produce polymeric materials controlling composition, topology and functionality there is a critical point where many research groups are working. All the studies are focused on the development of an ATRP system where the amount of copper is reduced which is the handicap of the system due to the environmental and health impact. This is why it is investing great effort to develop a "greener" copper mediated ATRP with the minimal quantity of metal involved in the process.[33,35,41-46] This motivation has encouraged investigation groups to design processes using environmentally benign reducing agents for regenerating the catalyst and decrease the amount utilized.

2.5. AGET ATRP

AGET ATRP[47] (**A**ctivators are **G**enerated by **E**lectron **T**ransfer) consists in using oxidized transition metal complexes instead of the reduced species. Therefore a reducing agent is needed to activate the activator and for this purpose other component is added to the reaction such as tin 2-ethylhexanoate,[48] ascorbic acid[49]. The reducing agents react by electron transfer with the oxidized metal complex and generate the activator in its lower oxidation state ready to react with the alkyl halide and create the growing radical.

2.6. ARGET ATRP

ARGET ATRP (**A**ctivators **R**e**G**enerated by **E**lectron **T**ransfer) is the most benign in environmentally terms because a much lower concentration of metal catalyst is utilized for the polymerization.

In this system, unlike the conventional ATRP polymerization where the metal complex is irreversible oxidized and cannot be reduced to generate new activators, a reducing agent added to the reaction. This reducing agent is constantly regenerating the metal complex to its reduced state producing species that are able to generate new chains. The use of compounds approved by FDA such as tin^{II} 2-ethylhexanoate ($Sn(EH)_2$), glucose,[50,51] or ascorbic acid,[52] hydrazine and phenyl hydrazine[53] as reducing agents make possible to reduce the metal concentration to a few ppm in the case of styrene polymerization.

2.7. ICAR ATRP

ICAR ATRP (**I**nitiators for **C**ontinuous **A**ctivator **R**egeneration) could be considered a "reverse" ARGET ATRP. In ICAR ATRP the regeneration of the metal activator is achieved by employing organic free radicals which are responsible of continuous regenerating of the catalyst allowing the decreasing of the metal concentration to a very low concentration.

This relatively new techniques, AGET ATRP, ARGET ATRP and ICAR ATRP, are being under deep investigation in order to the low amounts of catalyst employed in the reaction.[40,54-57]

3. Reversible Addition-Fragmentation Chain Transfer Polymerization (RAFT)

3.1. Introduction and background

Reversible addition-fragmentation chain transfer polymerization is a controlled radical polymerization (CRP) technique,[25,31,32,58-62] that, unlike conventional radical polymerization, monomer composition, architecture and thus, molecular weight and molecular weight distribution can be perfectly predetermined allowing to prepare polymers with defined characteristics and properties. RAFT polymerization has evolved and is becoming the most versatile CRP system due to the wide range of functional monomers may be polymerized and its mild reaction conditions. First report describing this new technique was made by CSIRO group[17,65] in 1998 making this methodology the most recent CRP, however simultaneously, other research group in France developed a process involving Xanthates (MADIX)[63,64] as controlling agents with same mechanism than RAFT polymerization. Comparing RAFT with other CRP as SFRP or ATRP, the fundamental difference is inherent to the transfer mechanism. Whereas the transfer step in SFRP and ATRP relies on the persistent radical effect, RAFT polymerization makes use of degenerative transfer process to establish the dynamic equilibrium control of the reaction. RAFT polymerization has become a very powerful tool for the synthesis of polymer with complicated structures due to the high tolerance to functional monomers.

The growing interest in the RAFT process is represented by the increasing number of studies on this topic. Figure 2.5 shows the number of publications related to RAFT polymerization over the last 15 years. It is clear that research groups are making strong efforts on the understanding which results in many publications concerning the mechanism, solvent dependent behavior, reaction simulations and other parameters of the RAFT process[25,60-62,65-75] Additionally, the RAFT technology has been meticulous analyzed in the book entitled Handbook of RAFT Polymerization.[76]

This RAFT introduction is organized into sections that first introduce briefly the different polymer architectures that we can achieve with this technique, then describe the chain transfer agent (CTA) structures necessary for controlled polymerization and the RAFT mechanism, and finally the control of molecular weight is described.

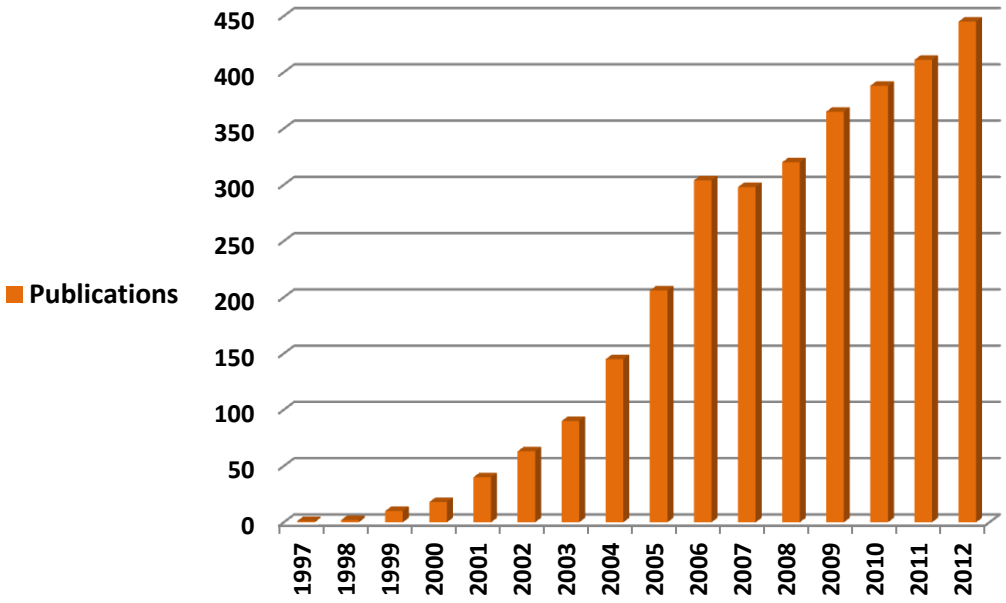

Figure 2.5. Publications per year indexed using the words RAFT and Polymerization

3.2. Polymer architectures

3.2.1. Functional polymers

One of the advantages of RAFT polymerization is its compatibility with a wide range of unprotected functionality in the monomer and RAFT agent. In RAFT polymerization, the chain transfer agent ends attached to the polymer in such a way that the functional group present in the initial RAFT agent, commonly thiocarbonylthio groups, are maintained in the final polymer. This feature is at the same time a disadvantage because the presence of thiocarbonylthio groups gives odour, colour and toxicity to the final product, therefore transformation or even removal of these terminal groups is part of many polymer syntheses. Since the chemistry of the thiocarbonylthio group has been deeply investigated,[77-79] different reactions may be used to transform or

remove the end group.[80] Some of the methodologies used for terminal group removal/transformation are summarized in figure 2.6.

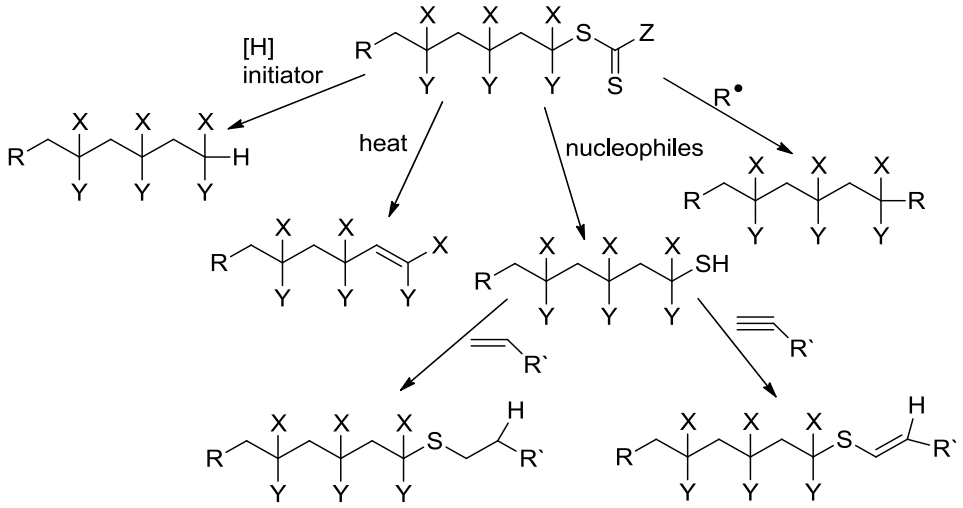

Figure 2.6. Schematic end group reactions for polymers synthesized by RAFT polymerization

3.2.2. Comb polymers

Comb polymers consist in a linear backbone from where a number of branches are pendant. These polymers can be made following diverse strategies and combining different polymerization methodologies. They may be made either in one single step or in a multistep process. One strategy is the attachment of the raft agent in the synthesis of the backbone and in a second step, growing the side chains from the principal structure. Second approach, which is the approach used for preparing the polymers of Chapter 3, is based on the use of macromonomers. This method allows a precise control of the concentration and length of the branches. There are other approaches such as the later attachment of the initiator to the backbone or the combination of several techniques.

3.2.3. Gradient copolymers

Gradient polymers are those that the monomer composition is continuously changing along the polymer which results in a wide range of properties. The basis of the synthesis relies on different consumption rates of the monomers, which are influenced by the steric impediment and the electronic properties of the system. The reactivity

ratios are generally unaffected by the RAFT process and the final polymers are not homogeneous at the molecular level due to the succession of single monomers.

3.2.4. Block copolymers

Since RAFT polymerization is a very versatile process, it offers several methods for the synthesis of block copolymer and due to the potential applications of these structures numerous examples of block synthesis may be found in the literature. The most common way to prepare block copolymers by RAFT polymerization proceeds by the addition of a second monomer once the first monomer is totally consumed (figure 2.7).[81,82] This method is possible due to the retention of the thiocarbonylthio group in the extreme of the polymer. This pathway is an easy method for the synthesis of AB diblock copolymers although other block copolymers are also possible using same methodology.

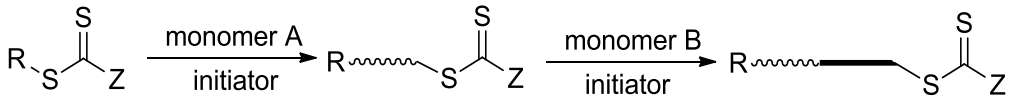

Figure 2.7. Schematic route for synthesis of diblock copolymers

For more complex block copolymer synthesis ABA, ABC, etc, different RAFT agents are needed. Taking into account that the order of the blocks plays an important role, a well synthesis path is imperative.[81,83] Then, by choosing determined and more complex RAFT agents considering the position of 'Z' or 'R' groups, synthesis of more complicated block structures can be achieved. For instance, the use of a bis-RAFT agent allows the direct synthesis of triblock copolymers in a 'one-pot' reaction (ABA figure 2.8, BAB figure 2.9).[66]

Based on the tolerance to monomers with diverse functional groups, RAFT polymerization posses the ability to make amphiphilic polymers without the necessity of carry out additional protect/unprotect steps. Hence, this characteristic makes it attractive for making hydrophobic/hydrophilic, and other combinations of moieties, polymers.

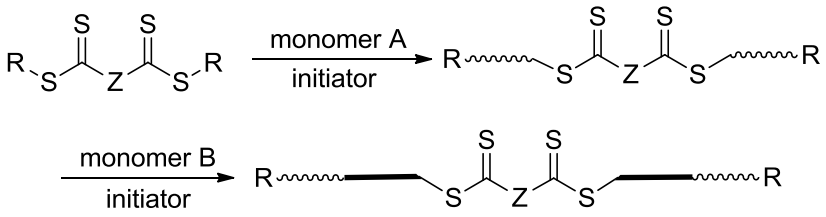

Figure 2.8. A-B-A triblock synthesis from "Z-connected" Bis-RAFT agent.

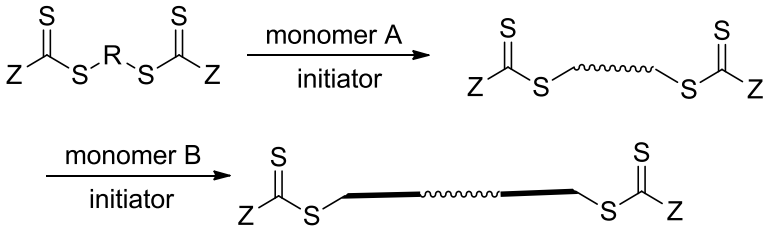

Figure 2.9. B-A-B triblock synthesis from "R-connected" Bis-RAFT agent

3.2.5. Star polymers

There are many studies regarding the synthesis of star polymers by RAFT polymerization.[69,84-91] One of the most utilized is the core first approaches, and among the different possible pathways, the use of a multi-RAFT agent, containing multiple thiocarbonylthio groups is preferred, however other synthesic routes such as arm first may be used for the same purpose.

3.3. RAFT chain transfer agent structure

RAFT agent, also known as Chain Transfer Agents (CTA), plays a very important role in the mechanism of RAFT polymerization.[83,92] The CTA should be carefully selected depending on the reaction conditions as well as the monomers and other compounds present in the reaction. Various families of compounds have been used as CTA for controlled polymerization including dithioesters, xanthates, dithiocarbamates, and trithiocarbonates.

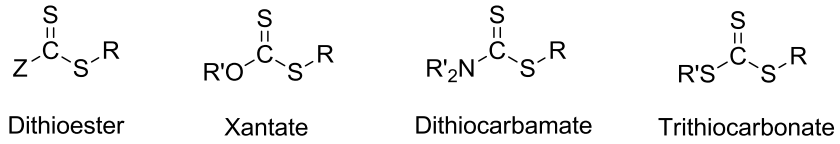

Figure 2.10. Generic structures of chain transfer agents

Although the most widely CTA utilized are dithioesters compounds which general structure is illustrated, together with other generic structures of CTAs, in the figure 2.10, the CTAs used for the RAFT polymerization carried out in Chapter 4 and Chapter 6 are trithiocarbonates compounds.

The appropriate selection of a CTA is so critically important that a bad choice could cause a loss of control of the kinetics which might lead to an unrestrained final polymer. Some specific examples of, already described, CTAs employed in the synthesis of polymers are illustrated in figure 2.11. The design of the transfer agent includes the specific selection of the group Z and the free radical leaving group R is crucial for the reason that they are the responsible of the activation/deactivation of thiocarbonyl double bond and the modification of the stability of the intermediate radicals, which means that the effectiveness of the CTA depends strongly of them.

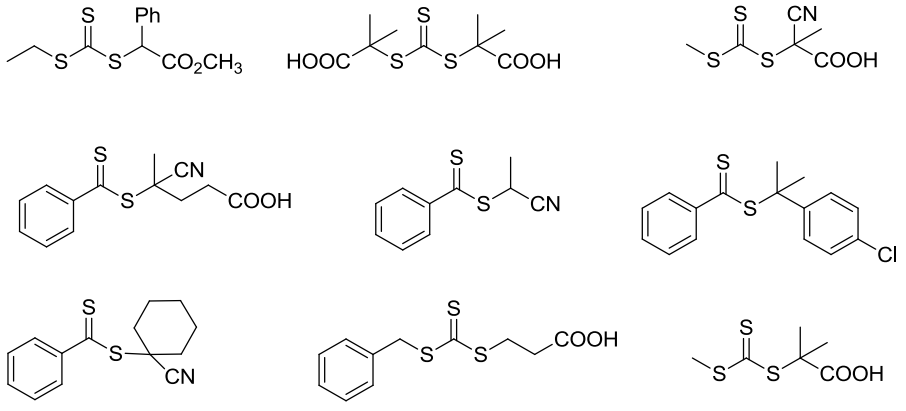

Figure 2.11. Commonly chain transfer agents employed in RAFT polymerization

The free radical leaving group R must be effective in reinitiating polymerization since, once it is fragmented from the CTA is rapidly converted to a propagating species, thus

the selection of characteristics of R group should be balanced between the leaving group ability and the reinitiation efficiency.[83] Therefore, for efficiently fragmentation in the desired direction, R must be a good homolytic leaving group relative to the attacking group, hence this balance varies for every particular system. As an example of this balance between the function of the R group, Chong et al.[83] observed that a certain RAFT agent with R = CH_2Ph is suitable for polymerizing styrene and acrylic monomers whereas is not suitable for methacrylic monomers. This is because the benzyl radical is good leaving group compared with the styryl and acrylyl radicals but if it is compared with methacrylyl is a poor leaving group. Could be even possible that a RAFT agent is suitable chain transfer agents in polymerization with a monomer and absolutely inert with other monomer.

The group Z modifies the addition and fragmentation rates by activating the thiocarbonyl double bond. These in turn affect the rates of the elementary reactions in the pre- and main-equilibrium of the polymerization. If the double bond is highly activated the propagating chains will add to the transfer agent very fast reducing the time to attach enough number of monomers to the growing chain. On the other hand, if the double bond is too stable the fragmentation event goes very slow retarding the polymerization[93] and increasing the likelihood of termination process.[94,95]

3.4. The RAFT mechanism

The mechanism of RAFT polymerization is well known since 1998 when first publication about this topic was published. The mechanism is composed of several steps, initiation, propagation, reversible chain transfer, reinitiation, main equilibrium and termination (scheme 2.6). The only difference between conventional radical polymerization and RAFT polymerization is that the latter uses a CTA compound.

Initiation step, as other polymerization, requires a source of radicals created from traditional initiators such as azo compound, peroxides, photoinitiators and redox initiating systems. Typical initiatiors in RAFT polymerization are shown in figure 2.12.

Generally, in RAFT polymerization the concentration of initiator is minimum, tipically is ten times less than the concentration of RAFT agent. The reaction begins with the homolitic rupture of initiator forming the primary radical, I•, which reacts with several

monomers (Pn•) during the propagation step before the addition to the CTA. In some cases, when the concentration of monomer is very low or the RAFT agent is very reactive the radical I• does not add any monomer and reacts directly with the CTA. However, undesired reaction involving the initiator or the radical derived from the initiator might occur. A good choice of the initiator is important to avoid transfer reaction of the active radical or unfavorable reaction with the RAFT agent which would lead to dead polymers.

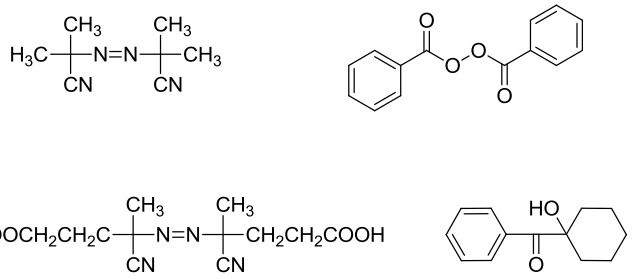

Figure 2.12. Typical initiators utilized in RAFT polymerization.

The propagating oligomeric specie, Pn•, reacts with the CTA producing the reversible chain transfer process. The reactions occur through an intermediate radical which release a new radical specie, R•, capable to restart the polymerization, hence it adds monomer units to form propagation chains Pm•. This step should take place quantitatively and instantaneously at early stage in the reaction so that all the chains grow at the same time obtaining narrow molecular weight distributions.

The main equilibrium stage, governed by the four rate constants k_{add}, k_{-add}, k_{β} and $k_{-\beta}$, involves the degenerative process of the thiocarbonylthio end group between propagating chains through the formation and fragmentation of an intermediate radical. The ability of the fragmentation and formation of the radical is the base of the controlled polymerization since it establishes the exchange between active and latent chains allowing the alternating addition of monomer units to each chain with equal probability. Therefore, is expected that the majority of monomer is consumed during this step.

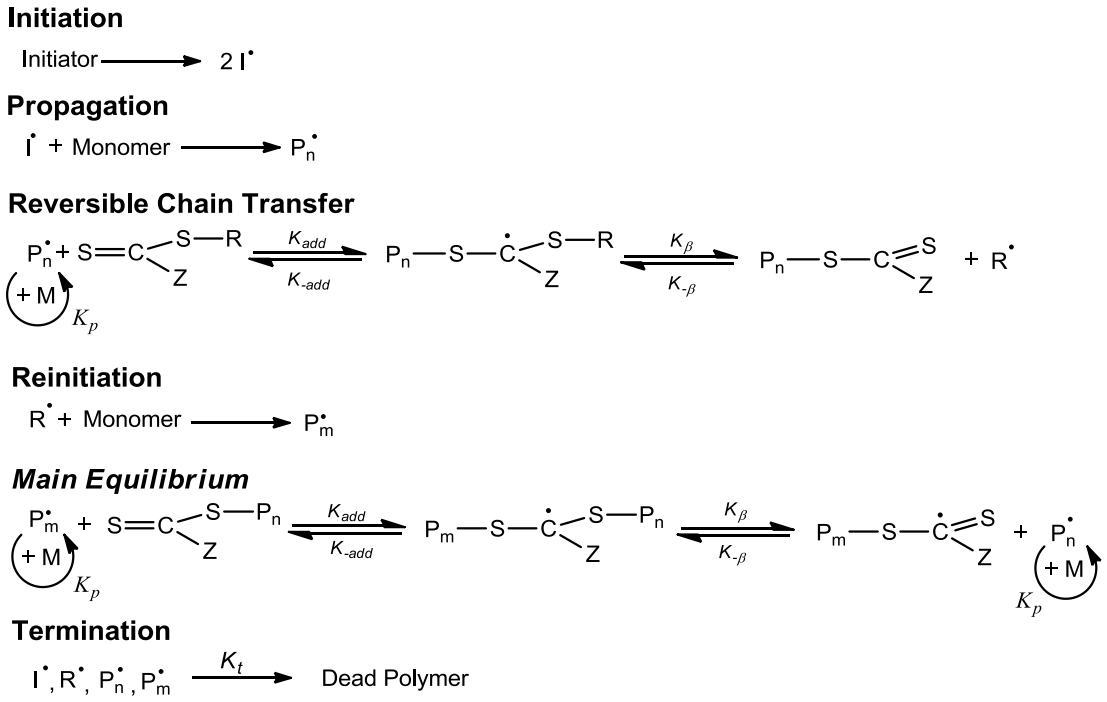

Scheme 2.6. Mechanism of RAFT polymerisation

The termination process, similar to all controlled polymerization techniques, is minimized, however bimolecular termination occur either by combining or by disproportionation of two growing chains. When the polymerization is complete (or stopped), most of the chains retains the thiocarbonylthio end group and can be isolated as stable materials. In order to decrease at a minimum the termination events, high ratio CTA-initiator must be used and commonly the number of dead chain does not exceed 5 %.

3.4.1. Molecular weight control by RAFT polymerization

In RAFT polymerization, like other controlled radical polymerizations, the molecular weight, and thus, the degree of polymerization, can be predetermined as shown in equation [5]:

$$M_{n,th} = \frac{[M]_0 M_{Mw} \rho}{[CTA]_0 + 2f[I]_0(1-e^{-k_d t})} + CTA_{Mw} \qquad [5]$$

where $[M]_0$ is the initial monomer concentration, $M_{Mw}$is the molecular weight of the monomer, ρ is the monomer conversion, $[CTA]_0$ is the initial CTA concentration, f is the initiator efficiency, $[I]_0$ is the starting initiator concentration, k_d is the initiator decomposition rate constant, and CTA_{Mw} is the molecular weight of the CTA.[25,60] According to this equation, it is of crucial importance to make a good selection of the CTA, which depends on the monomer, and to use a much higher concentration of CTA than monomer. In a RAFT polymerization that accomplished this conditions the termination of the fraction of initiator-derived chains can be neglected since it is considered less than 5%.[25] Then, the equation [5] may be simplified to obtain equation [6]:

$$M_{n,th} = \frac{[M]_0 M_{Mw} \rho}{[CTA]_0} + CTA_{Mw} \qquad [6]$$

These equation suggest that a plot of molecular weight versus conversion should be linear, meaning that the molecular weight increase proportionally as the reaction progress. This feature allows the synthesis of predefined polymers with determined molecular weight.

4. Self-organization Behavior

Polymers with self-associative behavior attract considerable interest due to their potential in several applications such as drug delivery, water treatment,[96,97] drugs and cosmetics, electronics. Synthesis, morphology and aggregation behavior is widely investigated in order to understand the self-assembly mechanism. The origin of such singular behavior is the presence of both hydrophilic and hydrophobic moieties in the same polymer chain.

The structures formed when are diluted in water depends, among other factors, on polymer concentration, hydrophobic-hydrophilic balance, physical bonds strength. Self-assembly phenomenon might take place in polymer solution leading to a partial collapse or an aggregation of several molecules to form ordered particles called

micelles which, in turn, may form more complex morphologies with potential applications.

Furthermore, chemists have interest in design and synthesize macromolecules with controlled self assembly behavior. It has been found that determined monomers have the capacity of responding to external signals such as temperature, pH, electrolytes, light, mechanical stress, etc. Those stimuli-responsive polymers, known as “smart” polymers, are very useful in biomedicine, electronic, pharmacology and cosmetics. Among all smart polymers, those which temperature variations trigger changes of the polymer configuration are called thermo-responsive polymers.

Controlled radical polymerization is a powerful synthetic methodology to develop polymers with perfectly defined and complex architecture and composition with the purpose of determine the response to external stimuli.

4.1. Lower critical solution temperature (LCST)

The lower critical solution temperature (LCST) transition is a fundamental mechanism by which many stimuli responsive polymers react to environmental temperature changes. This feature has drawn great interest for developing synthetic “smart polymers” and many polymers utilized in biomedical applications make use of it. LCST physics drive two qualitatively distinct but related behaviors. For solutions of uncrosslinked polymers with a concentration exceeding the chain overlap concentration, above the LCST the system presents a macro-scale phase separation which means that the polymer is dehydrated, becomes hydrophobic and precipitates whereas below the LCST, the polymer is in the hydrated state and therefore it is soluble (figure 2.13).

First and most relevant thermo-responsive polymer for biomedical applications was poly(N-isopropylacrylamide) (PNIPAAm)[98] because it possesses a sharp phase transition or a lower critical solution temperature (LCST) around 32 °C in aqueous solutions, although poly(ethylene glycol) methacrylate (PEGMA) nowadays is becoming of interest due to its versatility, biocompatibility and solution properties.

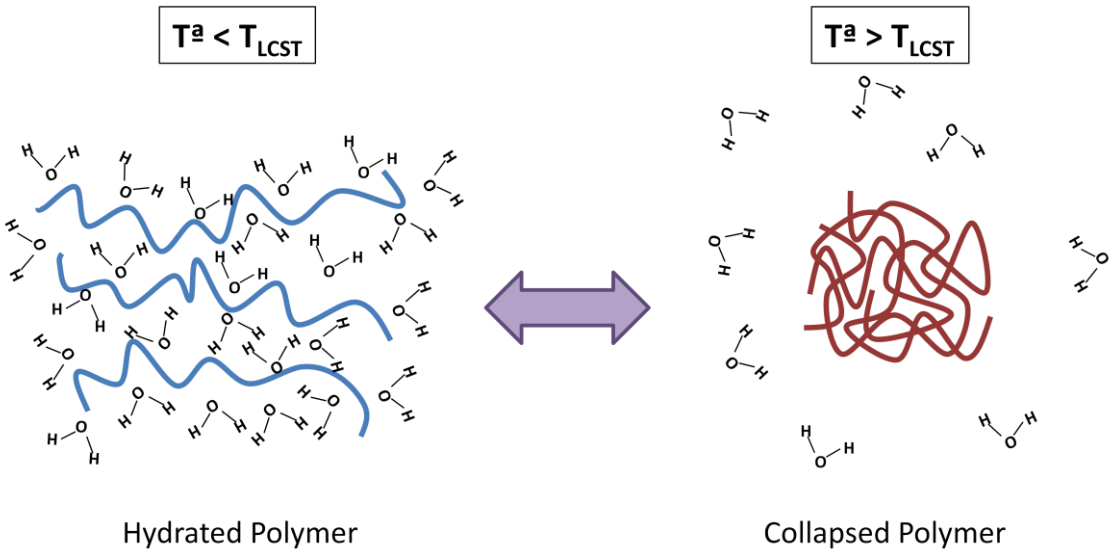

Figure 2.13. Schematic LCST transition

4.2. Poly(ethylene glycol) methacrylate (PEGMA)

Linear polymers such as poly(ethylenglycol) or poly(lactide-*co*-glycolide) have been productively used in several applications related with bioscience and biotechnology however. There is a need of polymers materials with sophisticated properties in order to cover challenging applications on the field of diagnostics, gene- or protein- therapy, controlled release, implants, bioseparation. In this scenario, the requirement of "smarter" materials is required, therefore the synthesis of macromolecular structures with the ability of making relatively fast changes in response to external stimuli has become a goal.[99,100] In that sense, polymers that response to changes of temperature, pH, ionic strength or irradiation are being developed.[98,101,102]

Chapter 4, chapter 5 and chapter 6 focus on the synthesis, characterization and application of "smart" polymers which present fast response to slight changes of temperature.

During the last fifteen years it has been demonstrated that amphiphilic polymers that are composed of a hydrophobic backbone and a hydrophilic grafted chain exhibit temperature responsive behavior. Different methodologies may be utilized in order to achieve these special structures being grafting through the most common by using macromonomers formed by a polymerizable vinyl group attached to the side chain

creating a suitable block for this purpose. Hence, vinyl monomers from which ethylene glycol units are pendant are perfect macromonomers to prepare this sort of amphiphilic polymers. The first examples of grafting-through polymerization by various mechanisms using PEG macromonomers have been reported more than 20 years ago.[101-103]

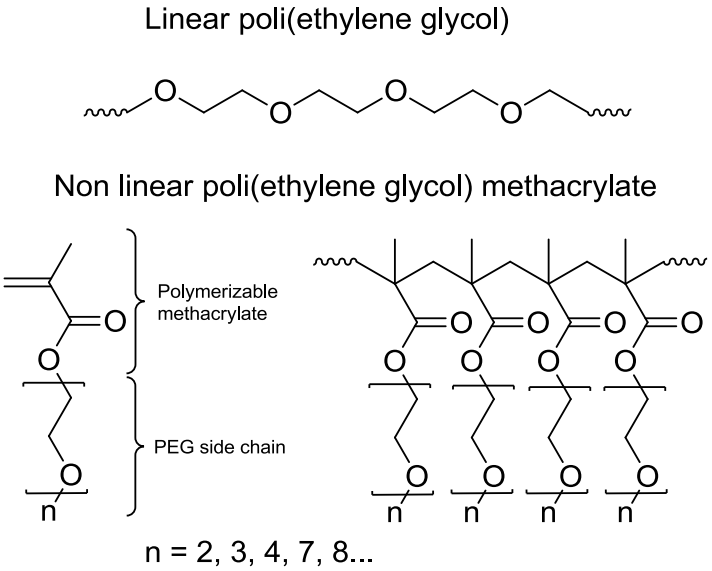

Scheme 2.7. Molecular structure of linear and non linear PEG analogues

The polymerization of PEG macromonomers produce water soluble materials that generally display a lower critical solution temperature (LCST) in pure water or in physiological medium[104-108] and they are very versatile since the units of the ethylene glycol side chains may be tuned in order to adjust the resulting behavior and, therefore, the final properties of the "smart" polymer.

4.2.1. Polymerization and macromolecular engineering

PEG macromonomers allow the design of innovative macromolecule structure, mainly comb-like polymers with defined architecture. By changing the length of the lateral chain the resulting polymer will have different properties, specially its behavior when diluted in water. In order to produce novel tailor made polymers, the monomer composition, combining various monomers with different length, of the product may

be also varied. First report in scientific literature in this regard appeared during the 1980s.[109-111]

The polymerization of the PEG macromonomers may be carried out by a variety of methodologies such as anionic, cationic, ring opening metathesis, or free radical polymerization.[112-115] It has been also successfully utilized, for the preparation of PEGMA polymers, controlled radical polymerization techniques including atom transfer radical polymerization (ATRP), nitroxide mediated polymerization (NMP), and reversible addition-fragmentation transfer polymerization (RAFT), obtaining in all the cases good results.[31,32,37,58,66,116-118] Despite the fact that methacrylate and acrylate derivatives are the most studied PEG macromonomer, other PEG macromonomers derivatives can be found in the literature.[105,106,108,119-121] Among PEG methacrylate derivatives, the most frequent are those with methoxy, ethoxy or hidroxy as terminal group due to its commercial availability. In table 2.1 are represented the molecular structures of various PEG-methoxy methacrylates and their properties in aqueous solution.

Tabla 2.1. Molecular structures of various oligo(ethylene glycol) methacrylates.

Polymer	**PMMA**	**MEMA**	**MEO_2MA**	**MEO_3MA**	**$PEGMA_{300}$**	**$PEGMA_{475}$**
Structure	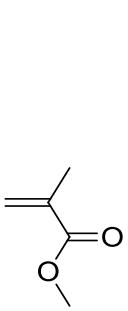	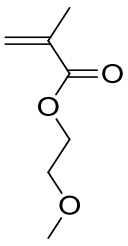	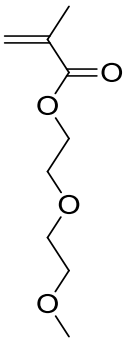	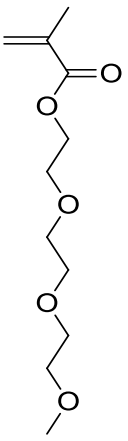	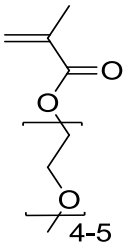	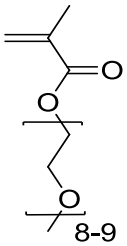
Hydrophilicity						
Properties in Aqueous Solution	Hydrophobic	Slightly Hygroscopic	LCST ≈ 26 °C	LCST ≈ 52 °C	LCST ≈ 64 °C	LCST ≈ 90 °C

As has been mentioned previously, controlled radical polymerization has been used for the preparation of PEGMA based polymers with a narrow molecular weight distribution. Successfully ATRP of an oligo(ethylene glycol) methyl ether methacrylate (OEGMA) with 7/8 ethylene oxide units was described in 1999 by Armes' research group.[122,123] Matyjaszewski and coworkers have confirmed that ATRP of (ethylene glycol) methyl ether methacrylates, independently of the number of ethylene glycol units in the side chain, leads to well defined PEGMA polymers in organic solvent.[124-126] It has been verified that ATRP in aqueous solution make a more complicated system which understanding continues under study.

RAFT technique has been also successfully used for polymerizing PEGMA monomers achieving polymers with perfectly determined molecular weight and well defined topology.[127,128]

Other controlled radical polymerizations technique, particularly, nitroxide mediated polymerization (NMP) cannot be used for polymerizing MEO_2MA, MEO_3MA, or OEGMA since this method is generally problematic for methacrylate monomers, however, polymers based on other macromonomers such as acrylate or styrene derivatives may be accomplished.[108,119,129]

Therefore, the combination of CRP techniques and PEG macromonomers create a powerful strategy to prepare complex structures. The potential of this system is translated into an enormous variety of possibilities on the polymer architecture control which allow to achieve telechelics polymers,[130] macromolecular brushes,[126] amphiphilic block copolymers,[131,132] or random copolymers[105,133,134] Beside these structures, CRP approaches, as it is described on chapter 6, can be exploited for modifying organic or inorganic surfaces.[135,136] These hybrid materials have received considerable interest for several application and many studies are focused on this topic, including planar inorganic substrates (e.g., gold or glass surfaces),[137-139] solid or soft-matter nanoparticles (e.g., nanocarriers, contrast agents),[140-143] or biological structures (e.g., proteins).[144-146]

Furthermore, polymers obtained by any CRP technique can be modified after polymerization.[34,147-149] There are various methods for polymer functionalization, among them, the most promising methodology in order to make modifications on final structures is the highly known as "click" chemistry which encompass several

reactions.[150-153] Other reactions such as copper catalyzed 1,3-dipolar cycloaddition of azides and alkynes (CuAAC) have been also utilized.[130]

Summarizing, CRP techniques, which most important are ATRP, RAFT, or NMP, permit to control variables such as chain-length, polydispersity, functionality, composition, and architecture, therefore, numerous possibilities of macromolecular engineering appear for the synthesis of tailor-made polymers.[37,151-153]

5. Chromium Adsorption from Aqueous Solution

Many industrial manufacturing processes generate wastewaters that contain dissolved heavy metals as a result of their activity. Among them, the most relevant metals are mercury, lead, arsenic, cadmium, silver, copper and chromium. Heavy metals are a highly toxic contaminant therefore they are a very great environmental concern, in fact, many dissolved metals have been found in harmful concentrations in groundwaters which are destined for potable drinking water. However, there are many industrial manufacturing processes which produce residual metals including printed circuit board manufacturing, metal finishing, semiconductor manufacturing, automotive, aerospace, electroplated metal parts/washing, textile dyes and steel.

Since the environmental regulation is becoming stricter related with the removal of heavy metals from water, extensive research on water remediation has been carried out in order to discharge those pollutants from water. Several techniques have been developed and multiple systems and materials have been used to accomplish this complicated process. After wastewater treatment through the purification system, the water obtained need to achieve a determined quality level for reuse and recycling.

Chromium is one of the heavy metals most utilized in industrial activities such as textile dyeing,[154] leather tanning process[155] or electroplating[156] and is present in effluents waters. Many investigation have focused on the removal of Cr(VI) because it is hazardous due to its affection to the human physiology, accumulates in the food chain and causes several diseases. The toxicological effects of Cr(VI) is originated from the action of its form itself as an oxidizing agent, as well as the formation of free radicals during the reduction of Cr(VI) to Cr(III) that occurs inside the cell. Another

reason of the higher toxicity of Cr(VI) is that chromate ions pass quicker through cellular and nuclear membranes than trivalent species.

The most employed technologies to remove Cr(VI) are electrochemical precipitation,[157] phytoextraction,[158,159] reverse osmosis,[160] ultrafiltration[161] and evaporative recovery.[162] In the last years, it have been demonstrated that the adsorption of the metal ion onto substrates is one of the most effective techniques for water remediation. Many substrates have been studied for this purpose such as bacteria, fungal biomass, alga biomass, chemicals components from agricultural products, hybrid materials, polymers or resins.[163-172]

In this thesis, the employment of polymers with specific architecture has been proposed for water remediation. The thermoresponsive hyperbranched polymers based on PEG-methacrylates synthesized and characterized in Chapter 4 have been used as chromium capturing substrate. The efficiency of these materials in chromium removal from aqueous solution has been investigated and summarized in Chapter 5.

6. References

(1) Szwarc, M.; Ghosh, B. N.; Sehon, A. H. *J. Chem. Phys.* **1950**, *18*, 1142.

(2) Szwarc, M.; Taylor, J. W. *J. Chem. Phys.* **1954**, *22*, 270.

(3) Szwarc, M. *J. Polym. Sci. Part A: Polym. Chem.* **1955**, *16*, 367.

(4) Szwarc, M. *J. Chem. Phys.* **1951**, *19*, 256.

(5) Buckley, R. P.; Szwarc, M. *J. Am. Chem. Soc.* **1956**, *78*, 5690.

(6) Buckley, R. P.; Rembaum, A.; Szwarc, M. *J. Polym. Sci. Part A: Polym. Chem.* **1957**, *24*, 135.

(7) Buckley, R. P.; Leavitt, F.; Szwarc, M. *J. Am. Chem. Soc.* **1956**, *78*, 5557.

(8) Binks, J. H.; Szwarc, M. *Proceedings of the Chemical Society* **1958**, 226.

(9) *Free Radicals in Solution.*; Walling, C. T., Ed., 1957.

(10) *The kinetics of vinyl polymerization by radical mechanisms*; Bamford, C. H.; Barb, W. G.; Jenkins, A. D.; Onyon, P. F., Eds.; Academic Press: New York, 1958.

(11) *Theory of radical polymerization*; Bagdasaria, H. S., Ed.; Izd. Akademii Nauk: Moscow, 1959.

(12) *Handbook of Radical Polymerization*; Matyjaszewski, K.; Davis, T. P., Eds.; Wiley: Hoboken, 2002.

(13) *The chemistry of radical polymerization*; Moad, G.; Solomon, D. H., Eds.; Elsevier: Oxford, UK, 2006.

(14) Walling, C. T. *Free Radicals in Solution*, 1957.

(15) Bamford, C. H.; Barb, W. G.; Jenkins, A. D.; Onyon, P. F. *The Kinetics of Vinyl Polymerization by Radical Mechanisms*, 1958.

(16) Grubbs, R. B. *Polymer Reviews* **2011**, *51*, 104.

(17) Chiefari, J.; Chong, Y. K.; Ercole, F.; Krstina, J.; Jeffery, J.; Le, T. P. T.; Mayadunne, R. T. A.; Meijs, G. F.; Moad, C. L.; Moad, G.; Rizzardo, E.; Thang, S. H. *Macromolecules* **1998**, *31*, 5559.

(18) Matyjaszewski, K. *Macromolecules* **2012**, *45*, 4015−4039.

(19) Greszta, D.; Mardare, D.; Matyjaszewski, K. *Macromolecules* **1994**, *27*, 638.

(20) Goto, A.; Fukuda, T. *Progress in Polymer Science* **2004**, *29*, 329.

(21) Fischer, H. *Chem. Rev.* **2001**, *101*, 3581.

(22) Tang, W.; Tsarevsky, N. V.; Matyjaszewski, K. *J. Am. Chem. Soc.* **2006**, *128*, 1598.

(23) Tang, W.; Fukuda, T.; Matyjaszewski, K. *Macromolecules* **2006**, *39*, 4332.

(24) Matyjaszewski, K. *Macromolecules* **1999**, *32*, 9051.

(25) Moad, G.; Rizzardo, E.; Thang, S. H. *Australian Journal of Chemistry* **2005**, *58*, 379.

(26) Destarac, M.; Taton, D.; Zard, S. Z.; Saleh, T.; Yvan, S. *ACS Symposium Series* **2003**, *854*, 536.

(27) Rizzardo, E.; Chiefari, J.; Mayadunne, R. T. A.; Moad, G.; Thang, S. H. *Book of Abstracts, 218th ACS National Meeting, New Orleans, Aug. 22-26* **1999**, POLY.

(28) Wang, J.-S.; Matyjaszewski, K. *Journal of the American Chemical Society* **1995**, *117*, 5614.

(29) Kato, M.; Kamigaito, M.; Sawamoto, M.; Higashimura, T. *Macromolecules* **1995**, *28*, 1721.

(30) K. Matyjaszewski and J. Xia *Chem. Rev.* **2001**, *101*, 2921.

(31) Kamigaito, M.; Ando, T.; Sawamoto, M. *Chem. Rev.* **2001**, *101*, 3689.

(32) Matyjaszewski, K.; Xia, J. *Chem. Rev.* **2001**, *101*, 2921.

(33) Patten, T. E.; Matyjaszewski, K. *Acc. Chem. Res.* **1999**, *32*, 895.

(34) Coessens, V.; Pintauer, T.; Matyjaszewski, K. *Progress in Polymer Science* **2001**, *26*, 337.

(35) Braunecker, W. A.; Matyjaszewski, K. *Progress in Polymer Science* **2007**, *32*, 93.

(36) *Macromolecular Engineering-Precise Synthesis, Materials Properties, Applications*; Matyjaszewski K.; Gnanou Y.; Leibler L., Eds.; Wiley-VCH: Weinheim, 2007.

(37) Matyjaszewski, K. *Progress in Polymer Science* **2005**, *30*, 858.

(38) Li, Y.; Zhang, B.; Hoskins, J. N.; Grayson, S. M. *Journal of Polymer Science: Part A: Polymer Chemistry* **2012**, *50*, 1086.

(39) Huang, W.; Yang, H.; Xue, X.; Jiang, B.; Chen, J.; Yang, Y.; Pu, H.; Liu, Y.; Zhang, D.; Kong, L.; Zhai, G. *Polymer Chemistry* **2013**, Accepted Manuscript.

(40) Pintauer, T.; Matyjaszewski, K. *Chemical Society Reviews* **2008**, *37*, 1087.

(41) Tsarevsky, N. V.; Matyjaszewski, K. *Chem. Rev.* **2007**, *107*, 2270.

(42) Pintauer, T.; Matyjaszewski, K. *Coord. Chem. Rev.* **2005**, *249*, 1155.

(43) Pintauer, T.; McKenzie, B.; Matyjaszewski, K. *ACS Symp. Ser.* **2003**, *854*, 130.

(44) Matyjaszewski K.; Tsarevsky N. V.; Braunecker W. A.; Dong H.; Huang J.; Jakubowski W.; Kwak Y.; Nicolay R.; Tang W.; A., Y. J. *Macromolecules* **2007**, *40*, 7795.

(45) Tsarevsky, N. V.; Matyjaszewski, K. *J. Polym. Sci. Part A: Polym. Chem.* **2006**, *44*, 5098.

(46) Lou, Q.; Shipp, D. A. *Chem. Phys. Chem.* **2012**, *13*, 3257

(47) Bai, L.; Zhang, L.; Cheng, Z.; Zhu, X. *Polymer Chemistry* **2012**, *3*, 2685.

(48) Jakubowski, W.; Matyjaszewski, K. *Macromolecules* **2005**, *38*, 4139.

(49) Min, K.; Gao, H.; Matyjaszewski, K. *Journal of the American Chemical Society* **2005**, *127*, 3825.

(50) Jakubowski, W.; Min, K.; Matyjaszewski, K. *Macromolecules* **2006**, *39*, 39.

(51) Jakubowski, W.; Matyjaszewski, K. *Angew. Chem. Int. Ed.* **2006**, *45*, 4482.

(52) Min, K.; Gao, H.; Matyjaszewski, K. *Macromolecules* **2007**, *40*, 1789.

(53) Matyjaszewski, K.; Jakubowski, W.; Min, K.; Tang, W.; Huang, J.; Braunecker, W. A.; Tsarevsky, N. V. *Proceedings of the National Academy of Sciences U.S.A.* **2006**, *103*, 15309.

(54) Dong, H.; Matyjaszewski, K. *Macromolecules* **2008**, *41*, 6868.

(55) Tanaka, K.; Matyjaszewski, K. *Macromolecular Symposia* **2008**, *261*, 1.

(56) Chan, N.; Cunningham, M. F.; Hutchinson, R. A. *Macromol. Chem. Phys.* **2008**, *209*, 1797.

(57) Yamamoto, S.-i.; Matyjaszewski, K. *Polymer Journal* **2008**, *40*, 496.

(58) Hawker, C. J.; Bosman, A. W.; Harth, E. *Chem. Rev.* **2001**, *101*, 3661.

(59) Chung, T. C.; Janvikul, W.; Lu, H. L. *J. Am. Chem. Soc.* **1996**, *118*, 705.

(60) Moad, G.; Rizzardo, E.; Thang, S. H. *Aust. J. Chem.* **2006**, *59*, 669.

(61) Lowe, A. B.; McCormick, C. L. *Progress in Polymer Science* **2007**, *32*, 283.

(62) McCormick, C. L.; Lowe, A. B. *Acc. Chem. Res.* **2004**, *37*, 312.

(63) Corpart, P.; Charmot, D.; Zard, S.; Franck, X.; Bouhadir, G. *WO 9935177* **1999**.

(64) Charmot, D.; Corpart, P.; Adam, H.; Zard, S. Z.; Biadatti, T.; Bouhadir, G. *Macromol. Symp.* **2000**, *150*, 23.

(65) Moad, G.; Rizzardo, E.; Thang, S. H. *Acc. Chem. Res.* **2008**, *41*, 1133.

(66) Moad, G.; Rizzardo, E.; Thang, S. H. *Polymer* **2008**, *49*, 1079.

(67) Perrier, S.; Takolpuckdee, P. *J. Polym. Sci. Part A: Polym. Chem.* **2005**, *43*, 5347.

(68) Favier, A.; Charreyre, M. T. *Macromol. Rapid Commun.* **2006**, *27*, 653.

(69) Barner, L.; Davis, T. P.; Stenzel, M. H.; Barner-Kowollik, C. *Macromol. Rapid Commun.* **2007**, *28*, 539.

(70) Barner-Kowollik, C.; Davis, T. P.; Heuts, J. P. A.; Stenzel, M. H.; Vana, P.; Whittaker, M. *J. Polym. Sci. Part A: Polym. Chem.* **2003**, *41*, 365.

(71) Barner-Kowollik, C.; Buback, M.; Charleux, B.; Coote, M. L.; Drache, M.; Fukuda, T.; al., e. *J. Polym. Sci. Part A: Polym. Chem.* **2006**, *44*, 5809.

(72) McLeary, J. B.; Klumperman, B. *Soft Matter* **2006**, *2*, 45.

(73) Save, M.; Guillaneuf, Y.; Gilbert, R. G. *Aust. J. Chem.* **2006**, *59*, 693.

(74) Coote, M. L.; Barner-Kowollik, C. *Aust. J. Chem.* **2006**, *59*, 712.

(75) Coote, M. L.; Krenske, E. H.; Izgorodina, E. I. *Macromol. Rapid Commun.* **2006**, *27*, 473.

(76) *Handbook of RAFT polymerization*; Barner-Kowollik, C., Ed.; Wiley-VCH: Weinheim, Germany, 2007.

(77) Kato, S.; Ishida, M. *Sulfur Rep* **1988**, *8*, 155.

(78) Zard, S. Z. *Aust. J. Chem.* **2006**, *59*, 663.

(79) Quiclet-Sire, B.; Zard, S. Z. *Topics in Current Chemistry* **2006**, *264*, 201.

(80) Chiefari, J.; Chong, Y. K.; Ercole, F.; Krstina, J.; Jeffery, J.; Le, T. P. T.; al., e. *Macromolecules* **1998**, *31*, 5559.

(81) Chong, B. Y. K.; Le, T. P. T.; Moad, G.; Rizzardo, E.; Thang, S. H. *Macromolecules* **1999**, *32*, 2071.

(82) Rizzardo, E.; Mayadunne, R.; Moad, G.; Thang, S. H. *Macromol. Symp.* **2001**, *174*, 209.

(83) Chong, Y. K.; Krstina, J.; Le, T. P. T.; Moad, G.; Postma, A.; Rizzardo, E.; al., e. *Macromolecules* **2003**, *36*, 2256.

(84) Barner-Kowollik, C.; Davis, T. P.; Stenzel, M. H. *Aust. J. Chem.* **2006**, *59*, 719.

(85) Moad, G.; Chiefari, J.; Krstina, J.; Postma, A.; Mayadunne, R. T. A.; Rizzardo, E.; al., e. *Polymer International* **2000**, *49*, 993.

(86) Rizzardo, E.; Chiefari, J.; Mayadunne, R. T. A.; Moad, G.; Thang, S. H. *ACS Symp. Ser.* **2000**, *768*, 278.

(87) Moad, G.; Mayadunne, R. T. A.; Rizzardo, E.; Skidmore, M.; Thang, S. *Macromol. Symp.* **2003**, *192*, 1.

(88) Mayadunne, R. T. A.; Jeffery, J.; Moad, G.; Rizzardo, E. *Macromolecules* **2003**, *36*, 1505.

(89) Boschmann, D.; Vana, P. *Macromolecules* **2007**, *40*, 2683.

(90) Chaffey-Millar, H.; Stenzel, M. H.; Davis, T. P.; Coote, M. L.; Barner- Kowollik, C. *Macromolecules* **2006**, *39*, 6406.

(91) Frohlich, M. G.; Vana, P.; Zifferer, G. *Macromol. Theory Simul.* **2007**, *16*, 610.

(92) Chiefari, J.; Mayadunne, R. T. A.; Moad, C. L.; Moad, G.; Rizzardo, E.; Postma, A.; al., e. *Macromolecules* **2003**, *36*, 2273.

(93) Mayadunne, R. T. A.; Rizzardo, E.; Chiefari, J.; Chong, Y.; Moad, G.; Thang, S. H. *Macromolecules* **1999**, *32*, 6977.

(94) Kwak, Y.; Goto, A.; Tsujii, Y.; Murata, Y.; Komatsu, K.; Fukuda, T. *Macromolecules* **2002**, *35*, 3026.

(95) Barner-Kowollik, C.; Quinn, J. F.; Nguyen, T. L. U.; Heuts, J. P. A.; Davis, T. P. *Macromolecules* **2001**, *34*, 7849.

(96) Rösler, A.; Vandermeulen, G. W. M.; Klok, H. A. *Advanced Drug Delivery Reviews* **2012**, *64*, 270.

(97) Jing, G.; Wang, L.; Yu, H.; Amer, W. A.; Zhang, L. *Colloids and Surfaces A: Physicochemical and Engineering Aspects* **2013**, *416*, 86.

(98) Gil, E. S.; Hudson, S. M. *Progress in Polymer Science* **2004**, *29*, 1173.

(99) Langer, R.; Tirrell, D. A. *Nature* **2004**, *428*, 487.

(100) Klok, H.-A. *J. Polym. Sci. Part A: Polym. Chem.* **2005**, *43*, 1.

(101) Capek, I.; Riza, M.; Akashi, M. *Die Makromolekulare Chemie* **1992**, *193*, 2843.

(102) Geetha, B.; Mandal, A. B.; Ramasami, T. *Macromolecules* **1993**, *26* 4083.

(103) Xiao, H.; Pelton, R.; Hamielec, A. *Polymer* **1996**, *37*, 1201.

(104) Lutz, J. F.; Akdemir O.; Hoth A. *J. Am. Chem. Soc.* **2006**, *128*, 13046.

(105) Lutz, J.-F.; Hoth, A. *Macromolecules* **2006**, *39*, 893.

(106) Han, S.; Hagiwara, M.; Ishizone, T. *Macromolecules* **2003**, *26*, 8312.

(107) Kitano, H.; Hirabayashi, T.; Gemmei-Ide, M.; Kyogoku, M. *Macromol. Chem. Phys.* **2004**, *205*, 1651.

(108) Zhao, B.; Li, D.; Hua, F.; Green, D. R. *Macromolecules* **2005**, *38*, 9509.

(109) Masson, P.; Beinert, G.; Franta, E.; Rempp, P. *Polymer Bulletin* **1982**, *7*, 17.

(110) Hamaide, T.; Mariaggi, N.; Foureys, J. L.; LePerchec, P.; Guyot, A. *J. Polym. Sci. Part A: Polym. Chem.* **1984**, *22*, 3091.

(111) Ito, K.; Tsuchida, H.; Hayashi, A.; Kitano, T.; Yamada, E.; Matsumoto, T. *Polymer Journal* **1985**, *17*, 827.

(112) Neugebauer, D. *Polymer International* **2007**, *56*, 1469.

(113) Biagini, S. C. G.; Parry, A. L. *J. Polym. Sci. Part A: Polym. Chem.* **2007**, *45*, 3178.

(114) Jiang, X.; Vogel, E. B.; Smith, M. R., III; ; Baker, G. L. *J. Polym. Sci. Part A: Polym. Chem.* **2007**, *45*, 5227.

(115) Jiang, X.; Smith, M. R.; Baker, G. L. *Macromolecules* **2008**, *41*, 318.

(116) Lacroix-Desmazes, P.; Lutz, J.-F.; Chauvin, F.; Severac, R.; Boutevin, B. *Macromolecules* **2001**, *34*, 8866.

(117) Lutz, J.-F.; Neugebauer. D.; Matyjaszewski, K. *J. Am. Chem. Soc.* **2003**, *125*, 6986.

(118) Lutz, J.-F.; Pakula, T.; Matyjaszewski, K. *ACS Symp. Ser.* **2003**, *854*, 268.

(119) Hua, F.; Jiang, X.; Li, D.; Zhao, B. *J. Polym. Sci. Part A: Polym. Chem.* **2006**, *44*, 2454.

(120) Oh, J. K.; Min, K.; Matyjaszewski, K. *Macromolecules* **2006**, *39* 3161.

(121) Skrabania, K.; Kristen, J.; Laschewsky, A.; Akdemir, O.; Hoth, A.; Lutz, J.-F. *Langmuir* **2007**, *23*, 84.

(122) Wang, X.-S.; Lascelles, S. F.; Jackson, R. A.; Armes, S. P. *Chem. Commun.* **1999**, 1817.

(123) Wang, X.-S.; Armes, S. P. *Macromolecules* **2000**, *33*, 6640.

(124) Yamamoto, S. I.; Pietrasik, J.; Matyjaszewski, K. *J. Polym. Sci. Part A: Polym. Chem.* **2008**, *46*, 194.

(125) Neugebauer, D.; Zhang, Y.; Pakula, Y., T., ; Sheiko, S. S.; Matyjaszewski, K. *Macromolecules* **2003**, *36*, 6746.

(126) Yamamoto, S. I.; Pietrasik, J.; Matyjaszewski, K. *Macromolecules* **2007**, *40*, 9348.

(127) Mertoglu, M.; Garnier, S.; Laschewsky, A.; Skrabania, K.; Storsberg, J. *Polymer* **2005**, *46*, 7726.

(128) Garnier, S.; Laschewsky, A. *Macromolecules* **2005**, *38*, 7580.

(129) Jiang, X.; Zhao, B. *J. Polym. Sci. Part A: Polym. Chem.* **2007**, *45*, 3707.

(130) Lutz, J.-F.; Börner, H. G.; Weichenhan, K. *Macromolecules* **2006**, *39*, 6376.

(131) Holder, S. J.; Rossi, N. A. A.; Yeoh, C. T.; Durand, G. G.; Boerakker, M. J.; Sommerdijk, N. *J. Mater. Chem.* **2003**, *13*.

(132) Street, G.; Illsley, D.; Holder, S. J. *J. Polym. Sci. Part A: Polym. Chem.* **2005**, *43*, 1129.

(133) Ali, M. M.; Stover, H. D. H. *Macromolecules* **2004**, *37*, 5219.

(134) Zhang, D.; Macias, C.; Ortiz, C. *Macromolecules* **2005**, *38*, 2530.

(135) Pyun, J.; Kowalewski, T.; Matyjaszewski, K. *Macromol. Rapid Commun.* **2003**, *24*, 1043.

(136) Lutz, J.-F.; Borner, H. G. *Progress in Polymer Science* **2008**, *33*, 1.

(137) Ma, H. W.; Hyun, J. H.; Stiller, P.; Chilkoti, A. *Advanced Material* **2004**, *16*, 338.

(138) Jonas, A. M.; Glinel, K.; Oren, R.; Nysten, B.; Huck, W. T. S. *Macromolecules* **2007**, *40*, 4403.

(139) Lee, B. S.; Lee, J. K.; Kim, W. J.; Jung, Y. H.; Sim, S. J.; Lee, J.; Choi, I. S. *Biomacromolecules* **2007**, *8*, 744.

(140) Hu, F. X.; Neoh, K. G.; Cen, L.; Kang, E.-T. *Biomacromolecules* **2006**, *7*, 809.

(141) Lee, H.; Lee, E.; Kim, D. K.; Jang, N. K.; Jeong, Y. Y.; Jon, S. *J. Am. Chem. Soc.* **2006**, *128*, 7383.

(142) Yusa, S. I.; Fukuda, K.; Yamamoto, T.; Iwasaki, Y.; Watanabe, A.; Akiyoshi, K.; Morishima, Y. *Langmuir* **2007**, *23*, 12842.

(143) Ishii, T.; Otsuka, H.; Kataoka, K.; Nagasaki, Y. *Langmuir* **2004**, *20*, 561.

(144) Bontempo, D.; Maynard, H. D. *J. Am. Chem. Soc.* **2005**, *127*, 6508.

(145) Lele, B. S.; Murata, H.; Matyjaszewski, K.; Russell, A. J. *Biomacromolecules* **2005**, *6*, 3380.

(146) Nicolas, J.; San Miguel, V.; Mantovani, G.; Haddleton, D. M. *Chem. Commun.* **2006**, 4697.

(147) Xu, J.; Tao, L.; Boyer, C.; Lowe, A. B.; Davis, T. P. *Macromolecules* **2010**, *43*, 20.

(148) Hoyle, C. E.; Lowe, A. B.; Bowman, C. N. *Chem. Soc. Rev.* **2010**, *39*, 1355.

(149) Tsarevsky, N. V.; Bencherif, S. A.; Matyjaszewski, K. *Macromolecules* **2007**, *40*, 4439.

(150) Kolb, H. C.; Finn, M. G.; Sharpless, K. B. *Angew. Chem. Int. Ed.* **2001**, *40*, 2004.

(151) Fournier, D.; Hoogenboom, R.; Schubert, U. S. *Chem. Soc. Rev.* **2007**, *8*, 1369.

(152) Lutz, J.-F. *Angew. Chem. Int. Ed.* **2007**, *46*, 1018.

(153) Lutz, J. F. *Angew. Chem. Int. Ed.* **2008**, *47*, 2182.

(154) *Chromium(VI) Handbook, CRC Press, New York*; Jacobs, J. A.; Testa, S. M.; in: J. Guertin, J. A. J., C.P.Avakian (Eds), Eds., 2004.

(155) *Prevention and Determination of Cr(VI) in Leather, United Nations Industrial Development Organization*; Hauber, C., Ed., 2000.

(156) *Materials and Process in Manufacturing 9th Ed., Wiley, New York*; Paul, D. E.; Black, J. T.; Kohser, A. R., Eds., 2003.

(157) Kongsricharoern, N.; Polprasert, C. *Water Science and Technology* **1996**, *34*, 109.

(158) Ali H; Khan E; MA, S. *Chemosphere* **2013**, *91*, 869.

(159) Garbisu, C.; Alkorta, I. *Bioresource Technology* **2001**, *77*, 229.

(160) Mousavi Rad, S. A.; Mirbagheri, S. A.; Mohammadi, T. *World Academy of Science, Engineering and Technology* **2009**, *57* 348.

(161) Ghosh, G.; Bhattacharya, P. K. *Chemical Engineering Journal* **2006**, *119* 45.

(162) Aksu, Z.; Özer, D.; Ekiz, H. I.; Kutsal, T.; Çaglar, A. *Environ. Technol.* **1996**, *17*, 215.

(163) Levankumar, L.; Muthukumaran, V.; Gobinath, M. B. *Journal of Hazardous Materials* **2009**, *161*, 709.

(164) Garg, U. K.; Kaur, M. P.; Sud, D.; Garg, V. K. *Desalination* **2009**, *249*, 475.

(165) Gupta, V. K.; Rastogi, A.; Nayak, A. *Journal of Colloid and Interface Science* **2010**, *342*, 135.

(166) Neagu, V.; Mikhalovsky, S. *Journal of Hazardous Materials* **2010**, *183*, 533.

(167) Narayanan, N. V.; Ganesan, M. *Journal of Hazardous Materials* **2009**, *161*, 575.

(168) Larraza I; López-Gónzalez M; Corrales T; G., M. *J. Colloid. Interf. Sci.* **2012**, *385*, 24.

(169) Ghoul, M.; Bacquet, M.; Morcellet, M. *Water Research* **2003**, *37*, 729.

(170) Huang R; Yang B; Q, L. *J Applied Polym Sci.* **2013**, *129*, 908.

(171) Kanwal F; Imran M; Mitu L; Rashid Z; Razzaq H; UA, Q. *E-Journal of Chemistry* **2012**, *9*, 621.

(172) Zuo X; R., B. *Carbohydrate polymers* **2013**, *92*, 2181.

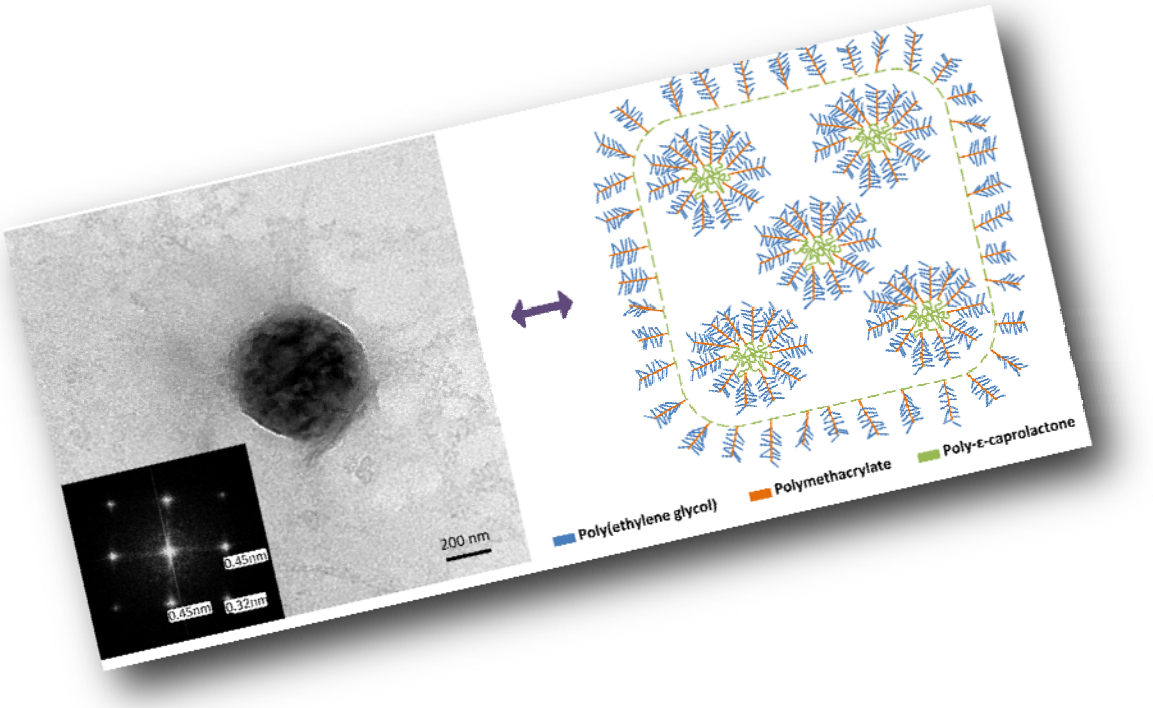

Hierarchically Organized Micellization of Thermoresponsive Rod-coil Copolymers based on Poly[oligo(ethylene glycol) methacrylate] and Poly(ε-caprolactone)

Chapter 3

Published in
Journal of Polymer Science Part A: Polymer Chemistry

Hierarchically Organized Micellization of Thermoresponsive Rod-coil Copolymers based on Poly[oligo(ethylene glycol) methacrylate] and Poly(ε-caprolactone)

Mario Luzón[1], Teresa Corrales[1], Fernando Catalina[1], Verónica San Miguel[2], Carmen Ballesteros[3] and Carmen Peinado[1,]*

Abstract. A series of amphiphilic triblock copolymers, poly [oligo(ethylene glycol) methacrylate]$_x$ - *block* - poly (ε-caprolactone) – *block* – poly [oligo(ethylene glycol) methacrylate]$_x$, POEGMA$_{Co}$(x), were synthesized. Formation of hydrophobic domains as cores of the micelles was studied by fluorescence spectroscopy. The critical micelle concentrations in aqueous solution were found to be in the range of circa 10^{-6} M. A novel methodology by modulated temperature differential scanning calorimetry was developed to determine critical micelle temperature. A significant concentration dependence of cmt was found. Dynamic light scattering measurements showed a bidispersed size distribution. The micelles showed reversible dispersion/aggregation in response to temperature cycles with lower critical solution temperature between 75 and 85 ºC. The interplay of the two hydrophobic and one thermoresponsive macromolecular chains offers the chance to more complex morphologies.

Keywords**:** *Biodegradable, block copolymer, cmc and cmt, comb-like polymer, grafting through, highly branched polymers, hierarchically self-assembly, micelles, thermoresponsive.*

[1] Instituto de Ciencia y Tecnología de Polímeros, C.S.I.C. c/ Juan de la Cierva 3, ES28006 Madrid, Spain
[2] Max Planck Institute for Polymer Research, Ackermannweg 10, DE55128 Mainz, Germany
[3] Universidad Carlos III de Madrid, Avda. de la Universidad 30, ES28911 Leganés, Madrid, Spain
*Correspondence to: C. Peinado (E-mail: cpeinado@ictp.csic.es)

1. Introduction

Highly branched architectures are attracting a growing interest in the design of new polymers due to their behavior, structure and, specially, properties on various surfaces and interface in relationship to their structure.[173] In particular the control of the number of the branches allows fine-tuning physical properties and processing conditions. In addition to regular dendrimers, a wide variety of highly branched structures have been designed being one of the simplest graft polymers, also called molecular brush or comb-like polymers. In contrast to typical graft copolymers, which are loosely grafted, the characteristic feature of brush molecules is high grafting density, currently one graft per backbone repeat unit.[174] The dense spacing of the side chains results in steric repulsion that induces an increase of the persistent length as well as the contour length of the polymer backbone.

The self assembly behaviour of block copolymers is attracting considerable attention as a powerful strategy in the preparation of functional materials. Several authors have pointed out the importance of the architecture of copolymers in the self-organization behaviour[175,176] although the studies were restrained due to the lack of controlled synthetic routes for the preparation of well-defined block copolymers with low polydispersities. The development of new polymerization techniques, such as ATRP (Atom Transfer Radical Polymerization), RAFT (Reversible Addition-Fragmentation chain Transfer) and grafting-through, has allowed the synthesis of well-defined block copolymers with novel architectures giving rise to a growing number of papers devoted to their aggregation both in selective solvents and solid state. However, there is still a need to achieve more studies of self-assembly behaviour of block copolymers with novel architectures to gain a deep knowledge of the relationship between the architecture of the copolymers and their self-assembly behaviour. For instance, graft copolymers and rod-coil copolymers possess a complex structure giving rise to a complicated self-assembly behaviour in solution and only, recently, the investigations are centred in these complex structures.[177]

ATRP is one of the most efficient methods to produce polymers with controlled molecular weight and polydispersity.[178] The combination of this method with grafting approaches has been successfully employed to prepare molecular brushes.[179-181] In

particular macromonomer polymerization offers advantages on the control of both side chain polydispersity and grafting density over “grafting onto” and “grafting from” strategies.[182,183] For instance, polymers of high branch density and uniform branch length can be obtained, which would not be easy to prepare by other synthetic approaches. Moreover, when macromonomer polymerization is carried out by ATRP the control of the reaction enables to obtain low main chain polydispersities.

Poly(ethylene glycol), PEG, is one of the most successful synthetic polymers in biotechnological and medical applications due to its biocompatibility and physiological solubility. The upcoming of oligo(ethylene oxide)-based macromonomers has allowed different macromolecular architectures that have been recognized as “smart” biorelevant materials.[184-190] The polymerization of (meth)acrylates with PEG side chains has been carried out by ATRP under different conditions, showing high polymerization rates in aqueous media.[191] The limit of ATRP control has been explored through a detailed study of the solvent effects on ATRP of oligo(ethylene glycol) methacrylate.[192] In a new way of initiation process, ascorbic acid was used as a reducing agent of the Cu(II) complex, resulting in generation of an active catalyst activator generated by electron transfer (AGET ATRP).[193,194] Besides ATRP, other controlled radical polymerization methods were employed such as reversible addition fragmentation transfer polymerization (RAFT) and nitroxide mediated polymerization.[195,196] Macromolecular engineering was performed by combination of PEG macromonomers polymerization with “click chemistry”.[197] A critical review of polymerization procedures of PEG-based macromonomers has been recently published by Neugebauer.[198]

In an attempt to obtain cylindrical brush-linear chain hybrid structures ATRP of a macromonomer, oligo(ethylene oxide) methacrylate (M_n= 475 g/mol), was carried out using a bifunctional macroinitiator based on low molecular weight (M_n= 2000 g/mol) poly(ε-caprolactone), PCL. Following this procedure we have prepared a new series of comb-like block copolymers. These macromolecules consist of a triblock polymeric backbone and oligo(ethylene oxide), oEO, grafted side chains (with identical chain length) in the end-blocks. A central block of poly(ε-caprolactone) is connected to both terminal blocks which are poly[oligo(ethylene glycol) methacrylate]. In this series the chain length of the central PCL block was maintained constant and varied that of the terminal fragments. Diblock and triblock copolymers containing poly[oligo(ethylene glycol methyl ether) methacrylate] blocks have been synthesized previously[199,200] but

not containing a central biodegradable block such as poly(-caprolactone). Lately, with an increase in environmental awareness, amphiphilic biodegradable copolymers offer interesting properties for biotechnological applications.[201]

These amphiphilic block copolymer brushes should exhibit interesting phase behavior. Thus, fluorescence spectroscopy, dynamic light scattering, TEM and MTDSC studies were carried out to have a detailed knowledge of their self-organization behavior, including critical micelle concentration and temperature (cmc and cmt), micellar size and aggregate morphology.

These block copolymers are of interest both due to their practical applications, and from a fundamental perspective addressing hydrophobic-hydrophilic interactions, cloud points, gelation phenomena, and critical micelle concentrations. All the studies were carried out on the dilute region and thus, gelation process will be studied further.

2. Experimental

Materials

Poly(ε-caprolactone) diol (Aldrich, M_n ~2000), 2-bromo-2-methylpropionyl bromide (Aldrich, 98%), triethylamine (TEA, Fischer, 99%, stored over potassium hydroxide pellets), 2,2´-bipyridine (Aldrich, ≥99%). Monomethoxy-capped oligo(ethylene glycol) methacrylate (OEGMA; mean degree of polymerization is 8-9, Aldrich). Copper bromide (Cu(I)Br) (Aldrich, 99%) was purified according to the method of Keller and Wycoff.[202] Toluene (Merck, ≥99.9%) was degassed by bubbling with nitrogen for thirty minutes and water used in all experiments was MilliQ-grade. Acetonitrile (Panreac 99.7%). Pyrene was recrystallized from ethanol.

Synthesis of Amphiphilic Copolymers

ABA triblock copolymers with different polymerization degrees of OEGMA were synthesized via a two-step reaction (Fig. 1). Firstly, a dihydroxy-terminated poly(-caprolactone) was end-functionalized using 2-bromoisobutyryl bromide. The resulting polymer was used as macroinitiator in the polymerization of OEGMA leading to triblock copolymers with a central core of PCL and POEGMA as terminal blocks of different lengths. A similar experimental procedure was recently reported.[203]

Synthesis of Macroinitiator

2-Bromoisobutyryl bromide (9.3 mL, 75 mmol) and triethylamine (10.5 mL, 75 mmol) were added to an anhydrous THF solution (300 mL) of α,ω-hydroxy terminated poly-ε-caprolactone (M_n= 2000 g/mol) under a nitrogen atmosphere. The reaction was carried out at ambient temperature overnight. The precipitated salts were removed via filtration and volatiles eliminated under reduced pressure. The obtained viscous oil product was dissolved in dichloromethane and washed with saturated $NaHCO_3$ solution. The organic phase was dried over anhydrous magnesium sulphate and removed. The white solid product was eluted through a basic alumina column with dichloromethane (yield = 70%).

^{1}H-NMR ($CDCl_3$, 400 MHz): δ (ppm): 1.37 [m, 17 OC-$(CH_2)_2$-C$\underline{H}_2$-$(CH_2)_2$O $_{PCL}$, 34H], 1.63 [m, 17 OC-CH_2-(C$\underline{H}_2$) -(CH_2) -(C$\underline{H}_2$)-$(CH_2)_2$-O $_{PCL}$, 68H], 1.92 (s, 1 (C$\underline{H}_3)_2$-C(Br)(CO)-$_{PCL}$, 12H), 2.30 [t, 17 OC-C$\underline{H}_2$-$(CH_2)_4$-O-$_{PCL}$, 34H], 4.05 [t, 27 OC-$(CH_2)_4$-C$\underline{H}_2$-OCO$_{PCL}$, 34H].

Synthesis of Triblock Copolymers

Four block copolymers were synthesized by changing the feed composition. The ratio between the concentrations of initiator, catalyst and ligand were maintained constant in all the polymerizations ([I]:[C]:[L] = 1:2:4.2). The ratios of monomer concentration to initiator were 27:1 for $POEGMA_{Co}$(13); 40:1 for $POEGMA_{Co}$(21); 70:1 for $POEGMA_{Co}$(29) and 75:1 for $POEGMA_{Co}$(39).

A typical polymerization procedure is detailed below. PCL based macroinitiator (1 g, 0.45 mmol) was placed in a Schlenk tube and dissolved in deoxygenated toluene (30 mL). Oligo(ethylene glycol) methyl ether methacrylate (9.9 mL, 22.5 mmol) was added to the solution. Then, the tube was sealed using a rubber septum and the mixture degassed *via* three freeze-pump-thaw cycles. Cu(I)Br (0.13 g, 0.91 mmol) was added to the frozen mixture and it was deoxygenated by three vaccuum-N_2 cycles. The reaction mixture, under nitrogen atmosphere, was heated at 80 ºC. When the temperature is reached, 2, 2´-bipyridine (0.30 g, 1.91 mmol) (t=0) was added. The reaction mixture immediately turned dark brown in colour in addition of the ligand. Samples for analysis were taken periodically throughout the reaction in order to follow the polymerization by ^{1}H-NMR in $CDCl_3$ and GPC. Termination reaction occurred rapidly on exposure to air, as indicated by the colour change from brown to green (oxidation of Cu (I) to Cu (II)). Catalyst residues were eliminated by filtering through an activated basic alumina

column. The volatiles were removed from the solution by rotary evaporation and under high vacuum at ambient temperature, yielding a colourless polymer.

Bulk homopolymerization was carried out using essentially the same conditions as described above but using 2-bromoisobutyryl bromide as initiator instead of PCL-based macroinitiator.

^{1}H-NMR ($CDCl_3$, 400 MHz): δ (ppm): 0.84-1.05 (m, 27 $C\underline{H}_3$-C $_{OEGMA}$, 81H), 1.37 [m, 17 OC-$(CH_2)_2$-$C\underline{H}_2$-$(CH_2)_2$O $_{PCL}$, 34H], 1.63 [m, 17 OC-CH_2-$(C\underline{H}_2)$ -(CH_2) -$(C\underline{H}_2)$-$(CH_2)_2$-O $_{PCL}$, 68H], 1.92 (s, 1 $(C\underline{H}_3)_2$-C(Br)(CO)-$_{PCL}$, 12H), 2.30 [t, 17 OC-$C\underline{H}_2$-$(CH_2)_4$-O-$_{PCL}$, 34H], 3.37 [s, 27 $C\underline{H}_3$-O-$_{OEGMA}$, 81H], 3.64 [m, 8 x 27 -O-$(C\underline{H}_2)$-$C\underline{H}_2$-O- $_{OEGMA}$, 864H], 4.00-4.11 [m, 27 -OC-O-$(C\underline{H}_2)$-CH_2-O- $_{OEGMA}$, 54H]+[t, 17 OC-$(CH_2)_4$-$C\underline{H}_2$-OCO_{PCL}, 34H].

Nuclear Magnetic Resonance

^{1}H-NMR and spectra were recorded in $CDCl_3$ solution on a *Varian INOVA-400* instrument operated at 400 MHz.

Gel Permeation Chromatography

Molecular weights and polydispersity measurements were carried out using a *Waters 1515 Isocratic HPLC Pump* system equipped with a *Waters 2414 Refractive Index Detectors*. Calibration was carried out using linear poly(ethylene oxide) standards (Polymer Standards Service Gmbh), ranging from $2.4x10^4$ to $5.7x10^5$ g·mol^{-1}. The mobile phase was ACN/Water (15 % v/v) at a flow rate of 0.5 mL·min^{-1}. The system was equipped with a guard column Ultrahydrogel 6x40 mm and two Ultrahydrogel 7.8x300 mm mixed columns in series, thermostated at 25 °C.

Optical Transmittance Measurements

Optical transmittance of block copolymer was measured at 550 nm with a Lambda 35 UV–Vis spectrometer (Perkin-Elmer). The sample cell was thermostated in a refrigerated circulator bath *Thermomix 1441* (B.BRAUN) at different temperatures from 10 to 90 °C prior to measurements. The lower critical solution temperature (LCST) of the polymer solution was defined as the temperature at the onset of the decrease in optical transmittance. This method seems to be accurately utilized only when two prerequisites are satisfied. The first prerequisite is that all the initial transmittance

values of the curves are the same. The second is that the phase-transition ranges of all the curves are similar.[204]

Fluorescence Spectroscopy Measurements

The cmc's were determined by a fluorescence probe technique using pyrene as a fluorescent probe. Pyrene stock solutions were prepared in acetonitrile. Fluorescence emission spectra were recorded on a Perkin-Elmer LS-55 spectrofluorimeter. Sample solutions were prepared by dissolving a known amount of polymer in water. The effective concentration of probe was maintained at 10^{-6} M in all the aqueous solutions. Fluorescence emission spectra of the probe were recorded in the range 350-700 nm using a fixed excitation wavelength of 337 nm. All the spectra were corrected using the response curve of the photomultiplier. The temperature was controlled with a thermostate *Thermomix 1441* (B.BRAUN).

The cmc was determined from the plot of the I_1/I_3 versus copolymer concentration following the sigmoidal Boltzman fitting procedure used by Leiva and col.[205]

The partition coefficient of pyrene in copolymer solutions were determined by the method described by Kabanov and col.[206,207] The fraction of hydrophobic pyrene that was incorporated in the micelles (α) was determined from fluorescence intensity at 392 nm, as a function of copolymer concentration, according to the equation [7]:

$$\alpha = \frac{I - I_{\min}}{I_{\max} - I_{\min}} \qquad [7]$$

where I is the fluorescence intensity at 392 nm, I_{min} is the intensity in water and I_{max} is the maximum intensity.

The partition coefficient, P, and the volume fraction of the micellar phase, ϑ, for a specific copolymer concentration is given by equation [8]:

$$\alpha = \frac{P\theta}{P\theta + 1 - \theta} \qquad [8]$$

where $P = C_m / C_w$ and C_m and C_w are the pyrene concentration in the micellar microphase and in the water phase, respectively. The volume fraction of micellar phase is given by equation [9]:

$$\theta = 0.01(C - cmc)\upsilon \qquad [9]$$

where C is the total concentration of copolymer, υ is the partial volume fraction of copolymer, and *cmc* is critical micellar concentration. By combining the equations [7] and [8], equation [9] is obtained:

$$\frac{1}{\alpha} = \frac{1}{0.01P\upsilon(C - cmc)} + 1 - \frac{1}{P} \qquad [10]$$

In accord with equation [10], plots of 1/α vs 1/(C − cac) yield straight lines with slopes equal to 1/(0.01Pv), from which the partitioning coefficient can be determined. In their determination of the partitioning coefficient of benzo[a]pyrene into poly(caprolactone)–block-poly(ethylene oxide) micelles, Lim Soo and co-workers[208] used a value of 1.0 cm^3/g for v.

Calorimetry Measurements

Differential Scanning Calorimetry (DSC) measurements were performed by using a DSC 823^e-Mettler Toledo equipped with sample robot and cooled by Julabo FT400 intracooler and controlled with a STARe software 9.10 version. Aluminium standard crucibles with 20 µl of sample were used for analyses that were carried out under a nitrogen atmosphere. Indium and water were used for temperature and enthalpy calibration.

TOPEM mode was chosen as temperature modulated DSC method. Instead of being based upon a periodic modulation of the heating rate, as is the situation with temperature modulated DSC (MTDSC) techniques, TOPEM uses a stochastic modulation of the heating or cooling rate by means of random pulses of temperature. This feature has the advantage that a set of experiments require only scan of the

samples but not for the blank as in other MTDSC techniques.[209] The parameters selected were: temperature range for the scan was from 10 to 50 °C in order to cover the cmt; the underlying heating rate was 0.1 K min^{-1}; the amplitude of the temperature pulse took values of 0.05 K; and the switching time range, which limits the duration of the pulses, had a minimum of 30 s and a maximum of 60 s.

Data analysis was carried out using TOPEM software. To calculate the response function for the system, the evaluation window was selected covering a region of the data in which there is no transition. The TOPEM evaluation yields the curve of *c*p0, the 'quasi-static' specific heat capacity and the separation of correlated and non-correlated components of the heat flow with respect to the heating rate, which are related to the reversing and non-reversing heat flows in the usual MTDSC terminology.

Dynamic Light Scattering

Solutions for light scattering measurements were prepared by dissolving the triblock copolymer in double filtered Millipore water and filtered again after solution preparation with PTFE filters (pore diameter 0.45 μm). DLS measurements were performed using a Malvern Zetasizer Nano spectrometer equipped with a 4 mW helium neon laser operating at 633 nm. All measurements were carried out with 1 g/L copolymer solution at a scattering angle of 173°. Temperature in the cells was kept constant to 18 °C for the determination of micelle sizes. Also temperature was varied between 10-50 °C allowing equilibration for at least 30 min at each temperature prior to measurement using 0.01 g/L copolymer solution. For each of these conditions a minimum of three measurements was made. The correlation function from DLS was analyzed by the CONTIN algorithm to obtain distributions of decay rate.[210] The decay rate distributions provided distributions of apparent diffusion coefficient,

$$D = \Gamma / q^2 \qquad [11]$$

where $q = (4\pi n/\lambda)\sin(\theta/2)$; n is the refractive index and θ is the angle of measurement.

The apparent hydrodynamic diameter was obtained through the Stokes-Einstein equation [12]:

$$D_h = \frac{kT}{3\pi nD} \qquad [12]$$

2.6. Transmission Electron Microscopy Measurements.

Transmission Electron Microscopy (TEM) with high resolution (HRTEM) was carried out in a Philips Tecnai 20F FEG microscope operating at 200 kV, equipped with a Scanning Transmission Electron Microscopy (STEM) module, with a dark field high angle annular detector for Z-contrast imaging. Aggregation studies were carried out by electron diffraction pattern simulation, using Fast Fourier Transform (FFT) of the HRTEM images. To prepare the TEM samples, 5 microlitres of an aqueous solution (0.1 g/L) of block copolymer micelles was dropped onto a carbon-coated copper grid and the water droplet was allowed to evaporate slowly in air.

3. Results

The “grafting through” approach, combined with Atom Transfer Radical Polymerization (ATRP), was successfully used for the synthesis of a new series of comb-like triblock copolymers. The synthetic route exploited a preformed, terminally functionalized polymer chain that formed the core of the macromolecules, reacting with a methacrylic monomer bearing oligomeric side chains based on poly(ethylene glycol). These macromolecules consist of a triblock ABA polymeric backbone and poly(ethylene glycol) grafted side chains (with identical chain length) in the end-blocks. A central block of poly(ε-caprolactone) was connected to both terminal blocks. In this series the chain length of the central block was maintained constant and varied that of terminal fragments. As the degree of polymerization of the poly[oligo(ethylene glycol) methacrylate] segment increased the main chain became longer than the side chain and the terminal blocks exhibited a cylindrical brush structure.

ABA block copolymers were synthesized from difunctional macroinitiator PCL using copper-mediated Controlled Radical Polymerization (CRP) as shown in figure 3.1. The ATRP macroinitiator was prepared by coupling the hydroxyl functionalities of a commercial α,ω-dihydroxy terminal polycaprolactone with 2-bromo-2-methylpropionyl bromide. Polymerization of oligo(ethylene glycol) methyl ether methacrylate (OEGMA)

was carried out at 80 °C in toluene using bipyridine, bipy, as a ligand and Cu(I)Br as a catalyst. Although OEGMA (8-9 repeat units) is a water-soluble monomer, the polymerization reaction was carried out in toluene due to the hydrophobic character of the PCL macroinitiator. There are several examples of successful polymerization of water-soluble monomers but in non-aqueous media.[211,212]

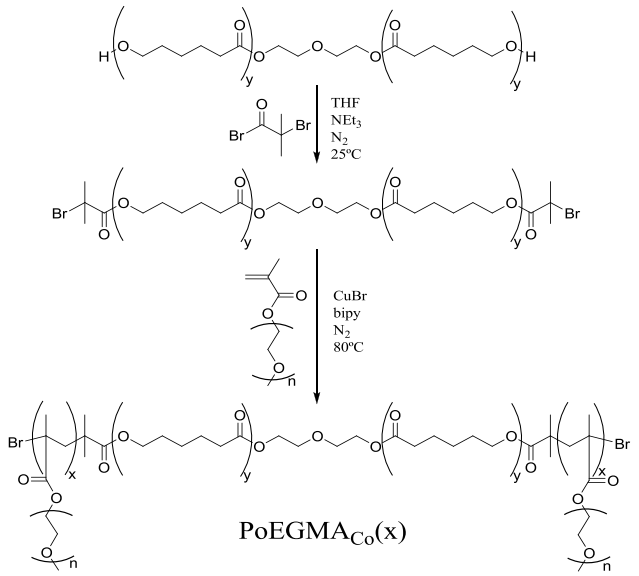

Figure 3.1. Scheme of synthesis of the triblock copolymers $POEGMA_{Co}(x)$.

Table 3.1 summarizes feed and copolymers composition, together with M_n determined by ^{1}H-NMR, GPC and by elemental analysis. The copolymers were named as $POEGMA_{Co}(x)$, where x denoted the polymerization degree of each POEGMA block. In other words, x denote the number of poly(ethylene glycol) side chains in each of the end-blocks. The above procedure was followed for the polymerization of OEGMA (M_n = 475 and DP = 8-9) giving rise to water soluble copolymers at room temperature.

Number average molecular weights, M_n, were determined from ^{1}H NMR spectra on the basis of the intensity ratio of signals at 4.1 ppm assigned to the methylene bond of the methacrylic group and that at 1.63 ppm for two methylenes of PCL. As the signal at 4.1 ppm was also present at the beginning of the reaction the intensity at 1.63 ppm was used as internal reference. These values were fairly close to those theoretically calculated on the basis of the $[M]_0/[I]_0$ and macromonomer conversion. Slight differences increases as degree of polymerization and may be attributed to the

polydispersity of the macromonomer. The commercial macromonomer OEGMA is a mixture of oligomers having a M_n of 475 g/mol. A large discrepancy was observed between GPC and NMR results (Table 3.1) and several reasons may account for these differences. It should be expected large differences between the relationship hydrodynamic volume-molecular weight for these comb-like copolymers compared to that for poly(ethylene oxide) samples used as standards in GPC calibration.[213] Moreover, anomalous elution behaviour has been demonstrated for other cylindrical brushes.[214] All the polymers showed monomodal distributions and a relatively narrow molecular weight distribution by GPC.

Table 3.1. Feed Composition in the ATRP and Composition of Copolymers and Homopolymer, Together with M_n Determined by NMR and GPC

Sample	f_{PoEGMA} [a]	F_{PoEGMA} [b]	$M_{n,NMR}$ [c] (g/mol)	$M_{n,GPC}$ [d] (g/mol)	$M_{n,th}$ [e] (g/mol)	PD	M_w/M_n [f]
$PoEGMA_{Co}$(13)	0.85	0.86	14,350	5,910	13,910	13	1.64
$PoEGMA_{Co}$(21)	0.91	0.91	21,560	9,280	21,770	21	1.47
$PoEGMA_{Co}$(29)	0.93	0.93	29,070	11,270	24,900	29	1.40
$PoEGMA_{Co}$(39)	0.94	0.94	39,050	17,770	36,110	39	1.49
PoEGMA	1.00	1.00	18,700	19,970	20,000	41	1.51

[a] Molar fraction of PoEGMA in the feed.
[b] Molar fraction of PoEGMA in the copolymer.
[c] Determined by NMR.
[d] Determined by GPC, standards of poly(ethylene oxide)s.
[e] $\bar{M}_{n,th}$ = (([Monomer]$_0$ x $M_{w,monomer}$ x Conversion)/[Macroinitiator]$_0$) + $\bar{M}_{n,macroinitiator}$
[f] Polydispersity index determined by GPC.
The copolymers were named as $PoEGMA_{Co}$(x), where x denoted the polymerization degree (PD) of each PoEGMA block.

Kinetics analysis was performed by sampling the reactions at regular time intervals and monitoring monomer conversion by ^{1}H NMR. The signals of the double bond protons (5.6 and 6.1 ppm) disappeared, the peak of the polymethacrylate backbone appeared at 4.1 ppm and the signal at 4.3 ppm (assigned to methylene attached to the ester carbonyl group of the macromonomer) was used as a reference. The comparison of monomer and polymer signals allowed the monomer conversion to be determined with good reliability. A semilogarithmic plot of monomer conversion versus reaction time resulted linear up to high conversions using different composition feeds (Fig. 3.2).

This indicates that the polymerization was first order with respect to monomer and the concentration of growing radicals was constant during the reaction. Kinetic studies showed that polymerization occurred after an induction time but a conversion of nearly 90 % was typically achieved within 120 min, and the polymerization was found to be first order even up to very high conversions. Figure 3.2(b) also shows that the plot of M_n versus conversion is linear with molar mass determined from NMR. All these results suggest a controlled radical mechanism under these conditions.

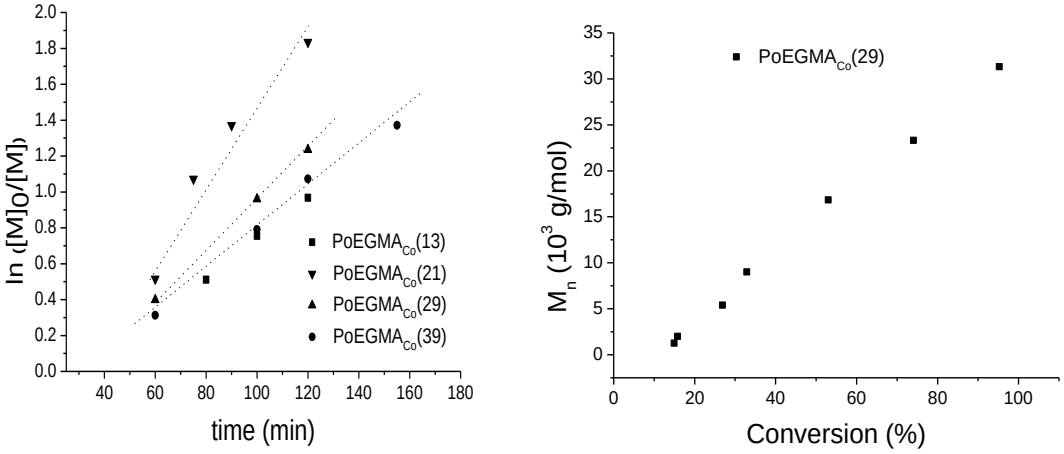

Figure 3.2. Kinetics of polymerization of OEGMA using a bifunctional macroinitiator based in poly(ε-caprolactone) in toluene media at 80 ºC. The relative molar ratios of OEGMA:initiator were 27:1 for $POEGMA_{Co}(13)$; 40:1 for $POEGMA_{Co}(21)$; 70:1 for $POEGMA_{Co}(29)$ and 75:1 for $POEGMA_{Co}(39)$.

The fluorescence emission spectra of pyrene in aqueous solutions of copolymers $POEGMA_{Co}(x)$ were measured at different concentrations. Fluorescence intensity increases as copolymer concentration as is shown in Figure 3.3(a). The ratio between the intensities at two wavelengths, λ_1 = 372 nm and λ_2 = 382 nm, was used to determine cmc at a fixed temperature of 21 °C as far as it senses the micropolarity changes due to the aggregates formation. The ratio of I_1/I_3 versus copolymer concentration is plotted in Figure 3.3(b). The fluorescence intensity ratio decreases as copolymer concentration increases indicating the solubilisation of pyrene in a more hydrophobic environment. Two important features should be pointed out. A drastic change of intensity ratio was observed and it occurred in a wide range of concentration.

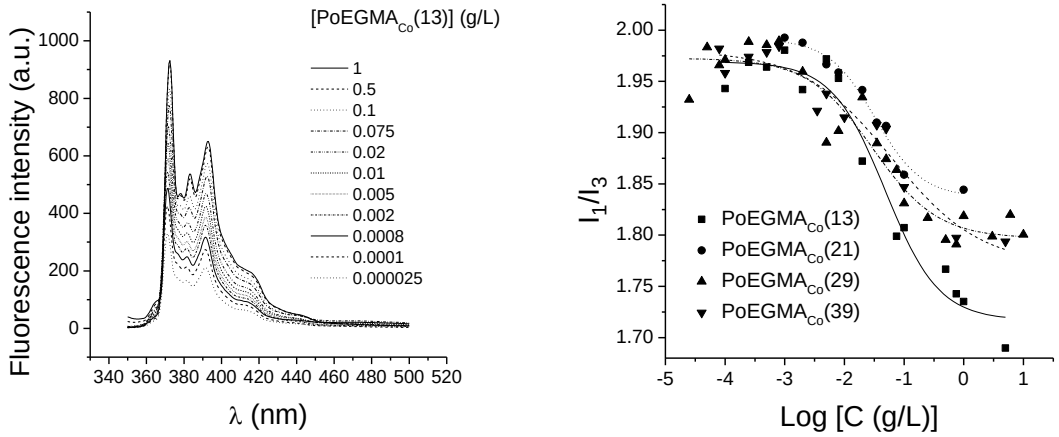

Figure 3.3. (a) Fluorescence intensity versus polymer concentration for PoEGMA $_{Co}$(13). (b) Plot of the I_1/I_3 ratio versus copolymer concentration.

The critical micellar concentration (cmc) and partition coefficients values were determined by fluorescence spectroscopy and are compiled in Table 3.2. As micelles were not formed abruptly, but rather over a concentration range, an onset of micelle formation was determined using a mathematical calculation. When the second derivative of I_1/I_3 to copolymer concentration is calculated, the cmc onset value is obtained from its minimum. All the copolymers displayed very low cmc values with the values in the range circa 10^{-6} M. The cmc values decreased by increasing the degree of polymerization of POEGMA blocks from 13 to 39; which was also accompanied by a decrease of the partition coefficient. This decrease indicates that hydrophobic interactions become stronger as the POEGMA chain length decreases.

Table 3.2. Critical Micellar Concentration, Partition Coefficient of Pyrene between Micelles and Water and Hydrodynamic Diameter of Micelles for the PoEGMA Triblock Copolymers

Sample	$M_{n,NMR}$ (g/mol)	cmc_{onset} (mg/L)	cmc (mg/L)	cmc (10^{-6} M)	Partition coef.	D_h (nm)[a]
PoEGMA$_{Co}$(13)	14,350	12.5	37.2	2.6	3,075	5.5
PoEGMA$_{Co}$(21)	21,560	8.9	32.0	1.6	1,546	10.5
PoEGMA$_{Co}$(29)	29,070	7.2	29.7	1.0	567	16.4

PoEGMA$_{Co}$(39)	39,050	3.9	25.4	0.6	178	23.4

[a] D_h was determined for copolymer solutions of 1 g/L.

The ratio I_1/I_3 verified the apolar nature of the micelle core. Partitioning coefficient also decreased as molecular weight increased indicating that micelle interior become more hydrophilic as a result of the inclusion of some EO units.

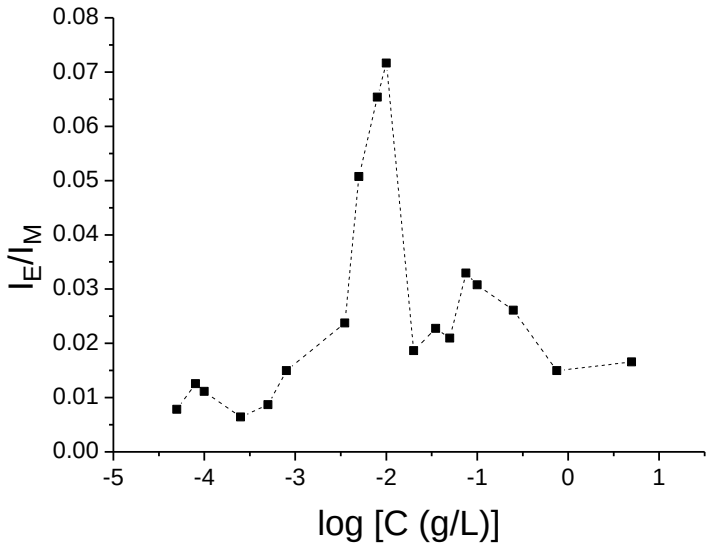

Figure 3.4. Plot of I_E/I_M as a function of the concentration of POEGMA$_{Co}$(39).

The analysis of excimer and monomer emission from pyrene (at 482 and 392 nm, respectively) allowed distinguishing between static and dynamic mechanism of micelles formation. Figure 3.4 shows the plot of I_E/I_M as a function of the concentration of POEGMA$_{Co}$(39). A maximum value of I_E/I_M was observed at 10^{-2} g/L corresponding to the concentration of copolymer at which the number of aggregates increases and gives rise to partitioning of pyrene between different micelles, diminishes the pyrene concentration per micelle and thus, excimer concentration. A dynamic behaviour in micelle formation was confirmed by the overlapping of the excitation spectrum of the monomer with the excitation spectrum of the excimer.[215]

One of the characteristics features of OEGMA based polymers is that their micellization behaviour is strongly temperature dependent in aqueous media. The thermal induced self-organization process of $POEGMA_{Co}$ was studied by differential scanning calorimetry. As it is well-known,[216,217] water of solvation may adopt an ice-like structure around the PEO hydrophilic blocks which disappears as temperature increases. On the other hand, Karlström[218] suggested that the increasing hydrophobicity of PEO blocks was due to a conformational change from polar to non-polar configuration of PEO block that results in reduction in polymer water interaction and the subsequent aggregation. The temperature at which micellization occurs is called critical micellization temperature, cmt, and the surfactant concentration at this temperature is the cmc. The thermally induced association process allows preparing micelles by dissolving the water soluble copolymers precluding the use of more complex methods that involve cosolvents and subsequent dialysis.

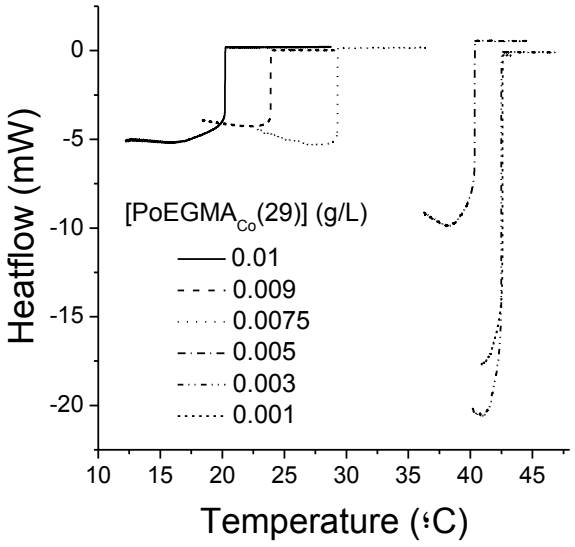

Figure 3.5. Heat flow variations of the non-reversing curve with temperature for a series of $POEGMA_{Co}(29)$ solutions.

The cmt values were determined by temperature modulated DSC using TOPEM technique, in which stochastic temperature modulations are superimposed on the underlying rate of a conventional DSC scan. These modulations consist of temperature

pulses, of fixed magnitude and alternating sign, with random durations within limits specified in the experimental conditions whereas periodic modulation of the heating rate is used in other modulated DSC techniques. The modulation creates high instantaneous heating rates which increases sensitivity. The low underlying constant heating rate is used to get better resolution. Similar experiments using conventional DSC were unsuccessful to determine cmt.

Figure 3.5 shows the heatflow variations of the non-reversing curve with temperature for a series of $POEGMA_{Co}(29)$ solutions. A sharp increase was observed at different temperatures, depending on copolymer concentration. After the rapid increase, heatflow value becomes zero at a certain temperature, which was ascribed to the cmt (Table 3.3).

Table 3.3. The cmt Values Determined by MTDSC for Copolymer $PoEGMA_{Co}(29)$ at Different Concentrations Compared with Those Determined by Fluorescence Method

[PoEGMA] (g/L)	cmt (MTDSC) (°C)	cmt (Nile Red) (°C)
0.0100	19.7 ± 0.5	21.3 ± 1.0
0.0090	23.4 ± 0.5	25.5 ± 1.0
0.0075	28.6 ± 0.5±	26.4 ± 1.0
0.0050	39.5 ± 0.5	36.2 ± 1.0
0.0030	41.0 ± 0.5	---
0.001	40.9 ± 0.5	---

For sake of comparison we measured fluorescence intensity ratio of pyrene as a function of temperature. The I_1/I_3 plots versus temperature did not permit an accurate determination of cmt and this may be related with the partitioning of the pyrene between the two microphases.

The cmt values determined by DSC were compared with those obtained measuring fluorescence intensity of Nile Red as a function of temperature for $POEGMA_{Co}$ solutions of increasing concentration. A sharp increase of fluorescence intensity with temperature occurred over a narrow range of temperature and the cmt was identified as the point at which a tangent drawn to the ascending linear portion of the curve

intersects the extrapolated fluorescence intensity in the absence of aggregation. The data are collected in Table 3.3 together with the MTDSC data. These cmt values calculated from fluorescence spectroscopy are shown to be in good agreement with those calculated from modulated temperature DSC. The small differences reflect the differences in the sensitivity of the methods. The fact that both techniques provides comparable estimates for cmt points out that the process under investigation by MTDSC is the micellization process and shows the self-consistency of the new modulated temperature DSC method supporting its reliability.

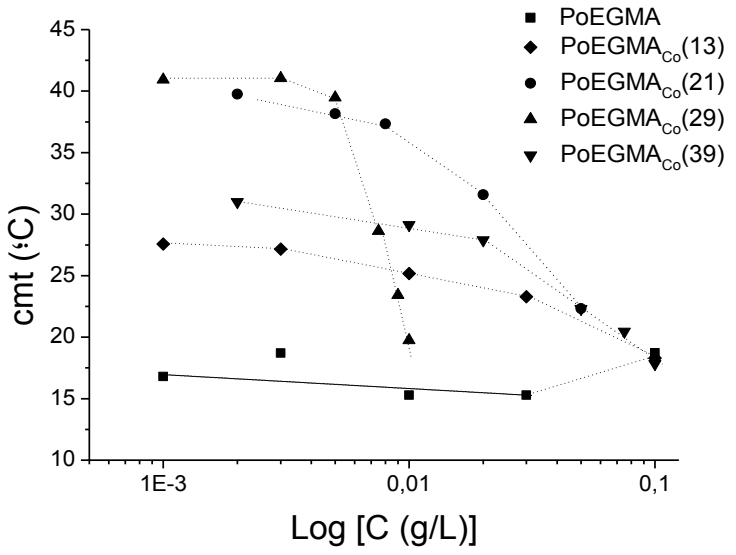

Figure 3.6. Semilogarithmic plot of cmt, determined by TMDSC, against copolymer concentration. Homopolymer POEGMA is included for comparison. Dotted lines are provided to guide the reader.

Figure 3.6 shows the semilogarithmic plot of cmt, determined by MTDSC, as a function of copolymer concentration. It is observed that increasing copolymer concentration reduces the cmt while the cmt value for the homopolymer poly(oligoethylene glycol methacrylate) changes slightly over a wide range of concentration. Another striking feature is that the concentration dependence of cmt becomes more pronounced at higher concentrations.

For further evidence that the POEGMA copolymers did self-aggregate above cmc and cmt, micellar aggregates were studied by Dynamic Light Scattering (DLS) in order to

measure their hydrodynamic diameter and their population distribution in terms of size. The relaxation time distributions obtained by the inverse Laplace transformation of the correlation functions from four different copolymers showed two populations. Additionally, the kurtosis of the distributions were rather broad (polydispersity index > 0.2) which should be ascribed to the polymer polydispersity and/or the presence of micellar clusters. The apparent hydrodynamic diameter of micelles, D_h, determined through the Stokes-Einstein formula, are compiled in Table 3.2 together with molecular mass. As the chain length of the terminal blocks increases dimensions of micelles grow following an almost linear trend.

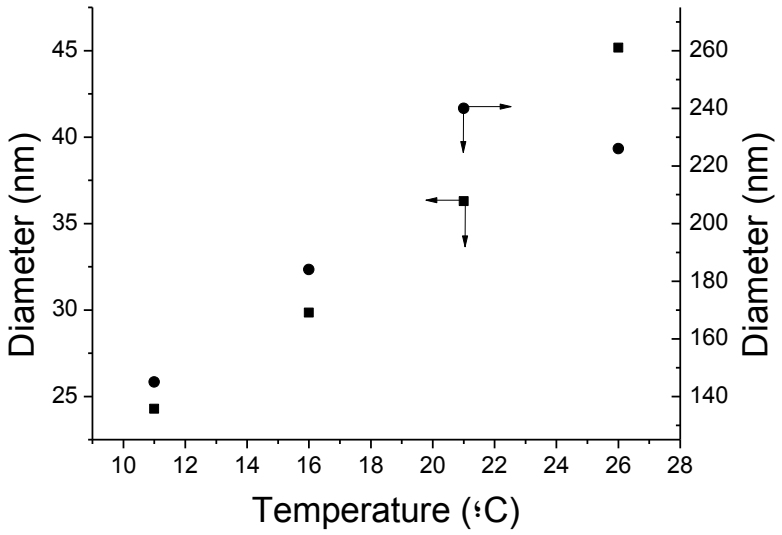

Figure 3.7. Apparent hydrodynamic diameter as a function of temperature for the copolymer $POEGMA_{Co}(29)$ at 0.009 g/L.

In order to address about the state of aggregation of these polymers hydrodynamic diameters as a function of the temperature were determined (figure 3.7). The aim was to decide whether this association leads to well-defined assemblies which remains constant over a wide range of concentration/temperature or to aggregates which vary constantly with conditions changes. The occurrence of two scattering populations of particles was also found. Besides micelles which have a D_h = 25 to 45 nm depending on copolymer composition, one additional population with D_h ≈ 150-250 nm which is attributed to the aggregates.

The morphology of the aggregates was examined by TEM and individual micelles can be distinguished particularly well on the micrograph of $POEGMA_{Co}(21)$ in Figure 3.8.

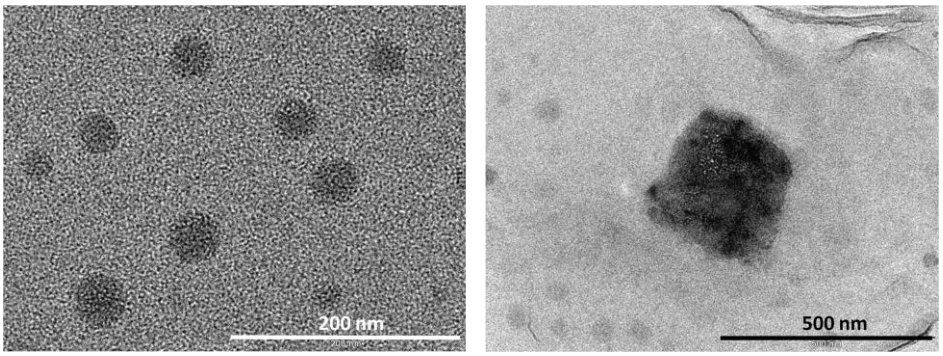

Figure 3.8. (a) TEM micropictures of $POEGMA_{Co}(29)$ micelles and (b) Bright Field TEM of $POEGMA_{Co}(21)$. Scale bar: (a) 200 nm and (b) 500 nm.

The sizes determined from TEM images, circa 34 nm, were in good agreement with those obtained from DLS measurements. This micrograph only just allows the row of micelles to be discerned as circular dark dots, suggesting a spherical shape. Although these results reveal the basic structural elements of micellar arrangement, the imaging and resolution allows a poor characterization of individual micellar size and shape. It has to be pointed out that the morphology of the aggregates depends on copolymer concentration and can be controlled by temperature. Therefore, High-Resolution Transmission Electron Microscopy (HR-TEM) and electron-diffraction pattern simulation by Fast Fourier Transform (FFT) was used to analyze the self-assembly structures. Herein, we report the formation of cubic aggregates from the block copolymer $POEGMA_{Co}(21)$ as concentration increases (Figure 3.8b). Micrographs showed dispersed cubic phases in the aqueous systems of the block copolymers.

Figure 3.9 shows HRTEM image, the image is characterized by two arrays of perpendicular image fringes. From fast Fourier transforms (FFTs) of Figure 3.9 simulated diffraction peaks were observed at ratios of 1:√2; and angles of 90° which can be related with a primitive cubic structure. FFT analysis yielded a mean cubic edge of 4.5 Å.

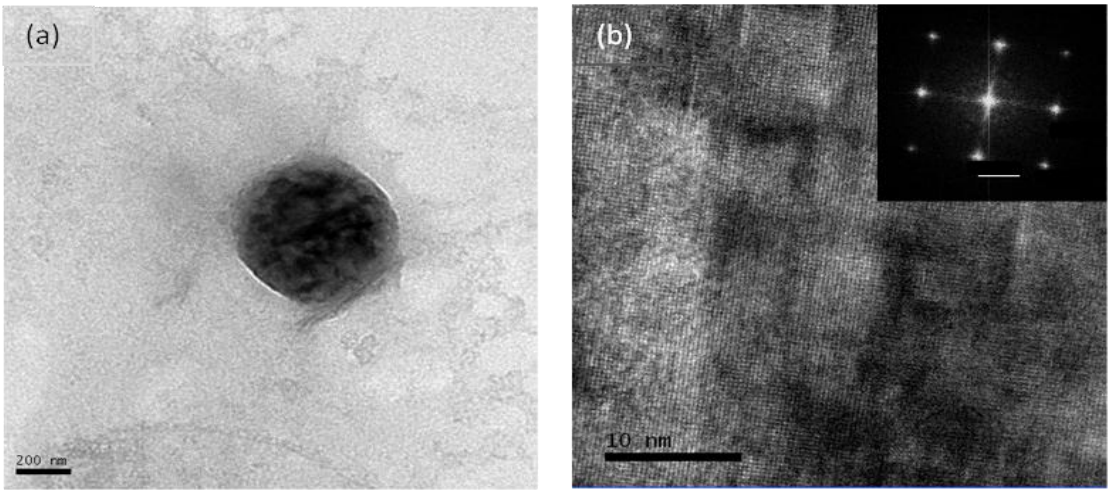

Figure 3.9. HRTEM image of $POEGMA_{Co}(21)$. Inset shows electron diffraction pattern simulation by Fast Fourier Transform of the HRTEM image. FTP pattern can be identified as a cubic plane the distances in the real space are indicated at the spots. Scale bar: (a) 200 nm and (b) 10 nm.

In Figure 3.10, the STEM micrographs allowed to visualize cubic structures and raspberry-like multicomponent micelles/nanosponges which are formed by the interaction of micelles. STEM-HAAD Z-contrast image of a nanosponge shown in Figure 3.10(b).

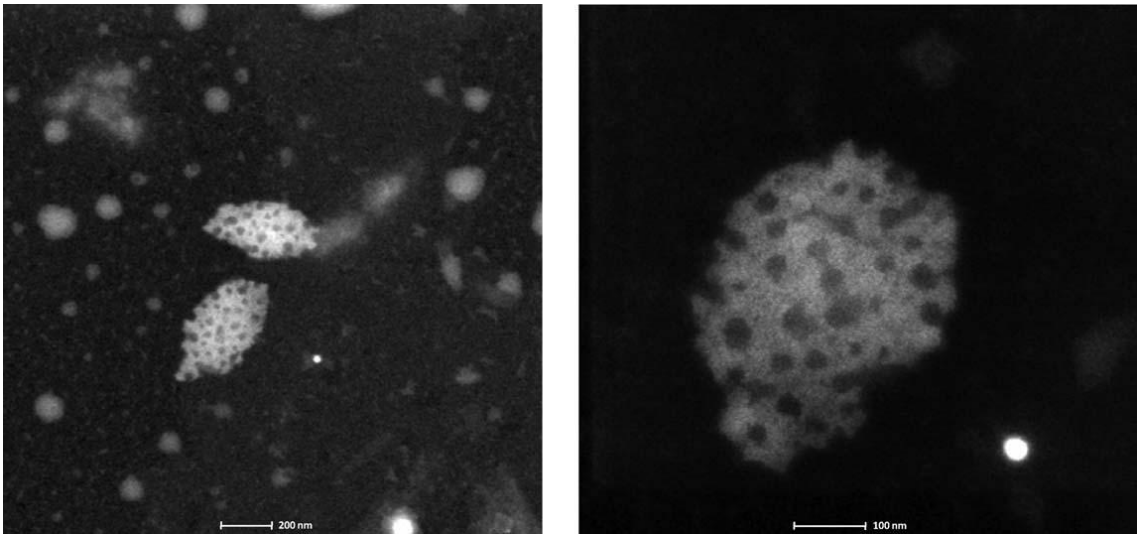

Figure 3.10. (a) STEM-HAAD low resolution Z-contrast image of $POEGMA_{Co}(21)$. Cubic structures and nanosponges are visible. The elements with higher atomic number, or higher density, appear brighter. (b) STEM-HAAD Z-contrast image of a nanosponge. Scale bar: (a) 200 nm and (b) 100 nm.

The transmittance of aqueous polymer solutions was monitored at 550 nm at a heating rate of 1 °C/min for samples $POEGMA_{Co}(29)$ and $POEGMA_{Co}(21)$ in presence and absence of NaCl. These copolymers showed a lower critical solution temperature (LCST) and their aqueous solutions started to become cloudy around 91 °C for $POEGMA_{Co}(21)$, thus, the transmittance rapidly dropped to 0%. In the other hand, the LCST decreased with increasing molecular weight of the copolymer and thus, the LCST value for $POEGMA_{Co}(29)$ was 80 °C. The LCST was concentration dependent and its value for $POEGMA_{Co}(29)$ decreased from 89 to 80 °C as the concentration increases from 0.5 to 1 g/L. These results are consistent with previous reports for well-defined poly(oligo(ethylene oxide) methacrylates) homopolymers.[219] The addition of sodium chloride to $POEGMA_{Co}(29)$ aqueous solution led to a decrease of the LCST from 80 °C (in its absence) to 76 °C for 1 M NaCl.

4. Discussion

It is noteworthy that the ATRP reaction of the methacrylic monomer of oligoethylene glycol proceeds to high conversion degree in spite of the osmotic repulsion that should be experienced by a macromonomer diffusing toward the highly crowded growing chain ends in dilute solution. In the other hand, since OEGMA is a sterically congested monomer, its termination rate constant is several orders of magnitude lower than that of conventional methacrylates, which is expected to lead to improved living character. Therefore, using a bifunctional macroinitiator we open a chemical pathway to obtain a significantly larger main chain than side chain degree of polymerization which has been difficult to reach by living anionic or cationic polymerization.[220]

In this series of copolymers the water solubility diminishes due to the fact that the increase of the ethylene oxide, EO, hydrophilic moieties seems to be counterbalanced by the entropy penalty associated with the increased number of monomer units. Thus, the cmc values diminished as degree of polymerization increased for $POEGMA_{Co}$. In the literature, contradictory behaviours have been observed for micelle formation from copolymers containing poly(ethylene oxide) blocks. Some non-ionic surfactants exhibited an increase of the cmc with the size of EO chain.[221] However, Alexandris et al.[222,223] found the opposite behaviour for a wide series of block copolymers based on ethylene oxide and propylene oxide (Pluronics or Poloxamers). Independently of the

number of EO or PO, larger polymers associated at lower concentrations, even if the increase of size was due to EO units. Also, an increase in the length of the hydrophilic block resulted in a decrease in the cmc when the length of the hydrophobic block was held constant for diblock copolymers, PEG-b-PCL.[224]

It is not only the hydrophilic-lipophilic balance the factor that governs the association of these copolymers into diverse nanostructured particles; rather, it is also that the specific topology of the different blocks significantly influences the micellar morphology. The self assembly behaviour of these rod-coil copolymers was governed by the effect of chain topology on conformational entropy which restricted their ability to stretch, to accommodate packing within self-assembled structures and their ability to gain conformational entropy when dissolved in solution. Therefore, the broad concentration range of the micellization process suggests a large deviation from the phase separation model and low cooperativity of the micellization process.

In a polymeric solution there is a competition between enthalpic interaction and entropic effect, which determine the aggregation behaviour of the copolymers.[225] Under the cmt, the entropic effects play a key role, whereas the enthalpic contribution dominates over entropic effects by increasing temperature, which results in the aggregation of copolymers and microphase separation. A new MTDSC based method has been presented here to provide estimates of cmt. This approach exploits the fact that the chemical potential of the only component (water) in the gaseous phase has to be equal to that of the same component in the more complex phase because the formations of the microphase-separated block copolymer/water. In this way, and because of the entropy of the block copolymer before and after the phase segregation is comparable,[226] the only factor to be considered in this analysis should be the chemical potential, going from a mixture of components where water is interacting with the block copolymer to another where it is not. Thus, the heat transfer, as detected by DSC, after phase transition at temperatures higher than cmt is near zero. The proposed approach is perfectly general and can be applied to any volatile component (e.g. organic solvents, water) in contact with a block copolymer. Here, it has to be pointed out that the success in these measurements was to use non-hermetically sealed aluminum pans allowing water evaporation, and thus working at atmospheric pressure (constant pressure) at cmt. These values were in good agreement with those obtained by fluorescence spectroscopy.

The concentration dependence of temperature at which micellization occurs is readily explained in thermodynamics terms. It is expected that any increase in the amphiphilic copolymer concentration may give rise to a growth of micelle concentration in agreement with the mass action description of the aggregation process. Moreover, the temperature of aggregation should be reduced by increasing copolymer concentration as a consequence of the endothermic nature of the micelle formation. It is therefore observed that increasing copolymer concentration reduces the cmt while the cmt value for the homopolymer poly(oligoethylene glycol methacrylate) changes slightly over a wide range of concentration. Another striking feature is that the concentration dependence of cmt becomes more pronounced at higher concentrations for the copolymers. This behaviour reveals a hierarchically-organized self-assembly where thermally induced premicellization preludes the micellization of these triblock copolymers.

DLS studies indicated that the copolymers form large and loose micellar aggregates due to a low micellar packaging efficiency induced by corona branching. It is expected that a high degree of hydration due to hydrogen bond formation with the ether oxygen contribute to bigger aggregates. Additionally, since the corona of polymeric micelles consists of densely packed chains, entropic repulsion would disfavour any fusion between micelles giving rise to bicontinuous structures. TEM provided evidence of this kind of structures and nanosponges were observed.

The short PCL chain length as long as with T-responsiveness of the densely branched of poly(OEGMA) are responsible of hierarchically self-assembly. The autoassociation model proposed here is based on a premicellization of poly(OEGMA) induced by temperature increase follow up by aggregates formation with concentration increase. Premicelles consisted of the lowest size aggregates where PCL chain was incorporated to the core, polymethacrylate formed the shell and poly(oligoethylene glycol) chains were the corona. It has to be pointed out that even though the polymethacrylate block is not water soluble, it has surface active groups (eg. ester groups) thereby possessing a relatively strong affinity on the water or, at least highest than that of PCL. As copolymer concentration was increased bigger and looser aggregates were formed which were interpreted as soft matter dispersions with ordered inner structure stabilized by poly(oligoethylene glycol)methacrylate chains. The latest feature is explained by the large cross-sectional area of cylindrical shape of poly(OEGMA) result

in little entanglement between the chains. It is assumed that these triblock copolymers provides steric stabilization by having its poly(ε-caprolactone) chains adsorbed on the surface of the stabilized particle, while its more hydrophilic oligo(ethylene glycol) ends extend into the external continuous phase.

In the other hand, sizes increased with temperature indicating the occurrence of aggregates which tend to associate at higher temperature to form more organized structures with a large increase in the micelle aggregation number. This temperature-dependent assembly is attributed to the increasing insolubility of POEGMA side chains with increasing temperatures that favours self-association by enhanced hydrophobic association. Hydration-dehydration processes are responsible for modification in chain packing and modulate supramolecular association modes. For these copolymers, the semibranched topology of the POEGMA segments played a key role in the micellization behaviour enabling a magnification of the size due to an increase of aggregation number as the desolvation of poly(oxyethylene) chains proceeds.

Finally, a hierarchically-organized self-assembly where thermally induced premicellization preludes the aggregation of the triblock copolymers was identified. In these rod-coil copolymers, the thermoresponsive rod chains provide a unique self-organization mechanism that yields morphologies which are truly nanostructured materials, with structure on the molecular, internal mesophase, and nanoparticle length scales. Also, the formation of compartmentalized micelles can be understood by the interplay of several factors and, thus, are the result of equilibrating the different interactions between the three chemically different blocks (two hydrophobic and one thermoresponsive) and the solvent, which competes with the efficiency of rod packing under the geometric constraint of micellar objects. Multiblock copolymers have an extra level of control, introduced by the supra interaction between blocks which give rise to more complex morphologies.[227] We have observed that spherical micelles pack to primitive cubic phases, as the concentration increased, leading to a decrease of the local curvature.

5. Conclusion

The ATRP polymerization of the macromonomer OEGMA (8-9 repeat units) using a bifunctional PCL macroinitiator has led to a series of rod-coil-rod block copolymers

where the rods were formed by densely branched fragments. As the PCL block length was fixed the hydrophilic-hydrophobic balance of the block copolymers was adjusted by varying the degree of polymerization of POEGMA block; this was achieved by changing the monomer-to-macroinitiator ratio from 27:1 to 75:1.

The self-assembly behavior is governed by hydrophilic-lipophilic balance as well as topological effects. Thus, the cmc values were low enough as corresponding to amphiphilic block copolymers and both cmc and partitioning coefficient decreased as the degree of polymerization increased. The latest feature is explained by the inclusion of oligoethylene glycol chains in the interior of the micelle due to the steric repulsion induced by densely branched fragments.

The thermoresponsiveness of these copolymers was studied by MTDSC and turbidimetry. Self-assembly was temperature and concentration dependent for the copolymers $POEGMA_{Co}$, containing a central PCL block, in contrast with the POEGMA homopolymer. As concentration increases the cmt diminished for the copolymers and remained constant for the homopolymer.

Because of the specific architecture (topology, relative block lengths) and the nature of the blocks of the macromolecule, an unprecedented structural diversity and multifunctionality was observed. This has allowed us to identify a range of two-dimensional ordered particles which may be tuned by changing both the temperature and the concentration of polymer solutions. The interplay of the two hydrophobic chains and one thermoresponsive macromolecular chain offers the chance to more complex morphologies with potential applications for lipid-like drug delivery systems.

6. Acknowledgements

The authors are indebted to Francesç Catala, from Mettler-Toledo, for valuable discussions. The authors are grateful to LABMET, TEM Laboratory associated to the Comunidad Autónoma de Madrid network and Mr. J. González-Casablanca for his cooperation with the TEM images.

The authors would like to thank the Plan Nacional I+D+I (Ministerio de Ciencia e Innovación) for financial support (MAT2009-09671) as well as the Comunidad Autónoma de Madrid for the funding through I+D Program (S0505/MAT-0227).

7. References

(173) Peleshanko, S.; Tsukruk, V. V. *Progress in Polymer Science* **2008**, *33*, 523.

(174) Tsukahara, Y.; Tsutsumi, K.; Yamashita, Y.; Shimada, S. *Macromolecules* **1990**, *23*, 5201.

(175) Hadjiantoniou, N. A.; Triftaridou, A. I.; Kafouris, D.; Gradzielski, M.; Patrickios, C. S. *Macromolecules* **2009**, *42*, 5492.

(176) Riess, G. *Progress in Polymer Science* **2003**, *28*, 1107.

(177) Cheng, L.; Cao, D. *Langmuir* **2009**, *25*, 2749.

(178) Durmaz, Y. Y.; Kumbaraci, V.; Demirel, A. L.; Talinli, N.; Yagci, Y. *Macromolecules* **2009**, *42*, 3743.

(179) Borner, H. G.; Duran, D.; Matyjaszewski, K.; da Silva, M.; Sheiko, S. S. *Macromolecules* **2002**, *35*, 3387.

(180) McCullough, L. A.; Dufour, B.; Matyjaszewski, K. *Journal of Polymer Science: Part A: Polymer Chemistry* **2009**, *47*, 5386.

(181) Yin, J.; Ge, Z.; Liu, H.; Liu, S. *Journal of Polymer Science: Part A: Polymer Chemistry* **2009**, *47*, 2608.

(182) Börner, H. G.; Beers, K. L.; Matyjaszewski, K.; Sheiko, S. S.; Möller, M. *Macromolecules* **2001**, *34*, 4375.

(183) Defleux, A.; Schappacher, M. *Macromolecules* **2000**, *33*, 7371.

(184) Edwards, E. W.; Chanana, M.; Wang, D.; Mohwald, H. *Angew. Chem. Int. Ed.* **2008**, *47*, 320

(185) Chanana, M.; Jahn, S.; Georgieva, R.; Lutz, J.-F.; Bäumler, H.; Wang, D. *Chemistry of Materials* **2009**, *21* 1906.

(186) Boyer, C.; Whittaker, M. R.; Luzón, M.; Davis, T. *Macromolecules* **2009**, *42*, 6917.

(187) Lutz, J. F. *J. Polym. Sci. Part A: Polym. Chem.* **2008**, *46*, 3459.

(188) Oyane, A.; Ishizone, T.; Uchida, M.; Furukawa, K.; Ushida, T. *Advanced Material* **2005**, *17*, 2329.

(189) Wischerhoff, E.; Uhlig, K.; Lankenau, A.; Borner, H. G.; Laschewsky, A.; Duschl, C.; Lutz, J. F. *Angew. Chem. Int. Ed.* **2008**, *47*, 5666

(190) Tan, I.; Zarafshani, Z.; Lutz, J. F.; Titirici, M. M. *ACS Applied Materials and Interfaces* **2009**, *1*, 1869.

(191) Wang, X.-S.; Armes, S. P. *Macromolecules* **2000**, *33*, 6640.

(192) Bergenudd, H.; Coullerez, G.; Jonsson, M.; Malmström, E. *Macromolecules* **2009**, *42*, 3302.

(193) Oh, J. K.; Min, K.; Matyjaszewski, K. *Macromolecules* **2006**, *39* 3161.

(194) Oh, J. K.; Perineau, F.; Charleux, B., . ; Matyjaszewski, K. *Journal of Polymer Science: Part A: Polymer Chemistry* **2009**, *47*, 1771.

(195) Lessard, B.; Marić, M. *Macromolecules* **2008**, *41*, 7870.

(196) Li, Z.; Zhang, K.; Ma, J.; Cheng, C.; Wooley, K. L. *Journal of Polymer Science: Part A: Polymer Chemistry* **2009**, *47*, 5557.

(197) Lutz, J.-F.; Börner, H. G.; Weichenhan, K. *Macromolecules* **2006**, *39*, 6376.

(198) Neugebauer, D. *Polymer International* **2007**, *56*, 1469.

(199) Holder, S. J.; Durand, G. G.; Yeoh, C.-T.; Illi, E.; Hardy, N. J.; Richardson, T. H. *J. Polym. Sci. Part A: Polym. Chem.* **2008**, *46*, 7739.

(200) Mertoglu, M.; Garnier, S.; Laschewsky, A.; Skrabania, K.; Storsberg, J. *Polymer* **2005**, *46*, 7726.

(201) San Miguel, V.; Peinado, C.; Catalina, F.; Abrusci, C. *Internat Biodet Biodeg* **2009**, *63*, 217.

(202) Keller, R. N.; Wycoff, H. D. *Inorg. Synth.* **1947**, *2*, 1.

(203) San Miguel, V.; Limer, A. J.; Haddleton, D. M.; Catalina, F.; C., P. *Eur. Polym. J.* **2008**, *44*, 3853.

(204) Liu, X.; Cheng, F.; Liu, H.; Chen, Y. *Soft Matter* **2008**, *4*, 1991.

(205) Leiva, A.; Quina, F. H.; Araneda, E.; Gargallo, L.; Radic, D. *Journal of Colloid and Interface Science* **2007**, *310*, 136.

(206) Kabanov, A.; Nazarova, I.; Astafieva, I.; Batrakova, E. V.; Alakhov, V.; Yaroslavov, A.; Kabanov, V. *Macromolecules* **1995**, *28*, 2303.

(207) Kozlov, M. Y.; Melik-Nubarov, N. S.; Batrakova, E. V.; Kabanov, A. V. *Macromolecules* **2000**, *33*, 3305.

(208) Soo, P. L.; Luo, L.; Maysinger, D.; Eisenberg, A. *Langmuir* **2002**, *18*, 9996.

(209) Fraga, I.; Montserrat, S.; Hutchinson, J. M. *J. Thermal Analysis and Calorimetry* **2007**, *87*, 119.

(210) Wyn, B. *Light Scattering: Principle and Development*; Clarendon Press: Oxford, 1996.

(211) Neugebauer, D.; Zhang, Y.; Pakula, Y., T., ; Sheiko, S. S.; Matyjaszewski, K. *Macromolecules* **2003**, *36*, 6746.

(212) Yamamoto, S. I.; Pietrasik, J.; Matyjaszewski, K. *J. Polym. Sci. Part A: Polym. Chem.* **2008**, *46*, 194.

(213) Gu, L.; Shen, Z.; Lu, G.; Zhang, X.; Huang, X. *Macromolecules* **2007**, *40*, 4486.

(214) Gerle, M.; Fischer, K.; Roos, S.; Müller, A. H. E.; Schmidt, M. *Macromolecules*

(215) Li, Y.; Nakashima, K. *Langmuir* **2003**, *19*, 548.

(216) Kjellander, R.; Florin, E. J. *J. Chem. Soc. Faraday Trans.* **1981**, *77*, 2053.

(217) Linse, P. *Macromolecules* **1993**, *26*, 4437.

(218) Karlström, G. *J. Phys. Chem.* **1985**, *89*, 4962.

(219) Lutz, J. F.; Akdemir O.; Hoth A. *J. Am. Chem. Soc.* **2006**, *128*, 13046.

(220) Neiser, M. W.; Okuda, J.; Schmidt, M. *Macromolecules* **2003**, *36*, 5437.

(221) Atwood, D.; Forence, A. T. *Surfactants systems their chemistry, pharmacy and biology*; Chapman and Hall: London, 1983.

(222) Alexandridis, P.; Holzwarth, J. F.; Hatton, T. A. *J. Am. Oil Chem. Soc.* **1995**, *72*, 823.

(223) Alexandridis, P.; Holzwarth, J. F.; Hatton, T. A. *Macromolecules* **1994**, *27*, 2414.

(224) Allen, C.; Maysinger, D.; Eisenberg, A. *Colloids Surf., B* **1999**, *16*, 3.

(225) Suek, N. W.; Lamm, M. H. *Langmuir* **2008**, *24*, 3030.

(226) Park, M. J.; Balsara, N. P.; Jackson, A. *Macromolecules* **2009**, *42*, 6808.

(227) Berlepsch, H.; Böttcher, C.; Skrabania, K.; Laschewsky, A. *Chem. Commun.* **2009**, *17*, 2290.

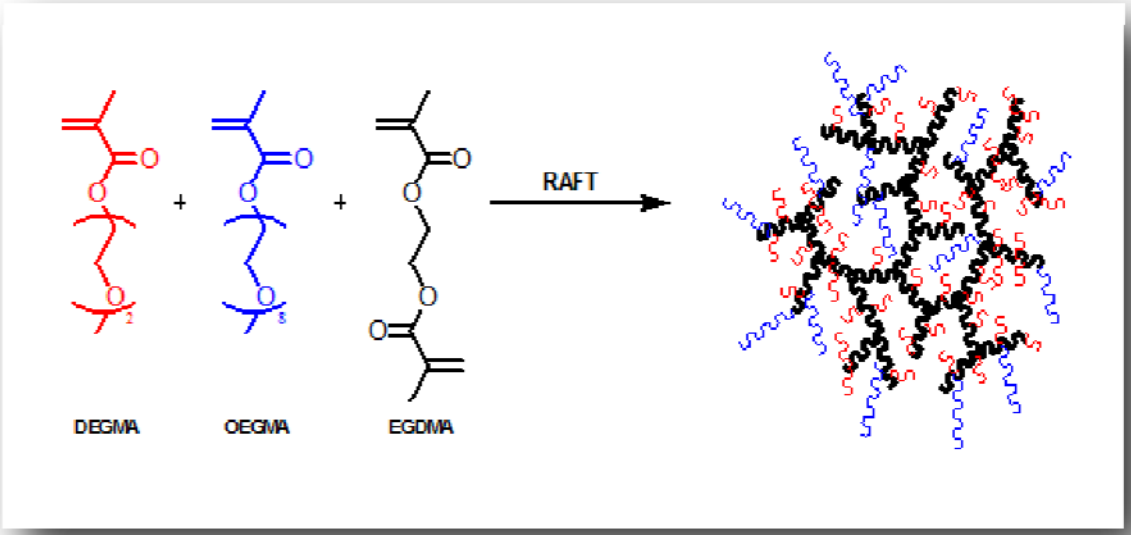

Water-soluble, Thermoresponsive, Hyperbranched Copolymers based on PEG- Methacrylates: Synthesis, Characterization and LCST Behavior

Chapter 4

Published in
Journal of Polymer Science Part A: Polymer Chemistry

Water-soluble, Thermoresponsive, Hyperbranched Copolymers based on PEG- Methacrylates: Synthesis, Characterization and LCST Behavior

Mario Luzon,[1,2] Cyrille Boyer,[2] Carmen Peinado,[1] Teresa Corrales,[1]
Michael Whittaker,[2] Lei Tao[2] and Thomas P. Davis[2]*

Abstract. A series of water-soluble thermoresponsive hyperbranched copoly(oligoethylene glycol)s were synthesized by copolymerization of di(ethylene glycol) methacrylate (DEG-MA) and oligo(ethylene glycol) methacrylate (OEG-MA, M_w = 475 g/mol), with ethylene glycol dimethacrylate (EGD-MA) used as the cross-linker, *via* reversible addition-fragmentation chain transfer polymerization (RAFT). Polymers were characterized by size exclusion chromatography (SEC) and nuclear magnetic resonance (NMR) analyses. According to the monomer composition, i.e. the ratio of OEG-MA: DEG-MA: EGD-MA, the lower critical solution temperature (LCST) could be tuned from 25 ^{o}C to 90 ^{o}C. The thermoresponsive properties of these hyperbranched copolymers were studied carefully and compared to their linear analogues. It was found that molecular architecture influences thermoresponsive behavior, with a decrease of around 5-10 °C in the LCST of the hyperbranched polymers compared to the LCST of linear chains.

***Keywords**: Crosslinked, crosslinking, PEGMA, reversible addition-fragmentation chain transfer polymerization (RAFT), thermoresponsive.*

[1]*Instituto de Ciencia y Tecnología de Polímeros, C.S.I.C.; C/ Juan de la Cierva 3, 28006 Madrid, Spain*
[2]*Centre for Advanced Macromolecular Design (CAMD), School of Chemical Engineering, The University of New South Wales, Sydney, NSW 2052, Australia.*
**Correspondence to: T.P. Davis (t.davis@unsw.edu.au)*

1. Introduction

Hyperbranched polymers are of interest as they demonstrate unique structural properties as imperfect analogues of dendrimers.[228] Dendrimers and hyperbranched polymers are versatile structural platforms for drug/gene delivery applications as they can be fashioned to nanosizes (less than 10 nm), with high solubility and multivalent functionality.[229] The synthesis of dendrimers can be complex and time consuming, with manufacturing on a large scale prohibitively expensive for many applications as numerous repetitive synthetic and purification steps are needed. Hyperbranched polymers with properties similar to those displayed by dendrimers can be synthesized via simple procedures.[230-235] Hyperbranched polymers are irregular macromolecules with high functionality, increased segment density and better solubility than their linear analogues. Because of their imperfect structures, hyperbranched polymers do not exhibit the same dependence of viscosity on molecular weight as dendrimers, and they also exhibit a broader molecular weight distribution.[236,237] Hyperbanched macromolecules have found application in the modification of materials,[238-241] resins,[242,243] gene delivery,[244-248] and drug delivery.[249-253]

Recently, a facile and generic route to branched vinyl polymers employing conventional free radical polymerization was developed by Sherrington and co-workers.[254-256] The strategy, known as “Strathclyde methodology”, involves copolymerizations of a vinyl comonomer with a difunctional (or multifunctional) comonomer in the presence of a free radical transfer agent or catalytic chain transfer species to inhibit cross-linking and gelation. Living radical polymerization has been used recently to prepare hyperbranched polymers and also, has been combined with the strathclyde methodology. In principle, these approaches should allow better control over the branching process because the primary chains are much less polydisperse. Branching behavior has been compared both above and below the coil overlap concentration, c*, in order to assess the effect of the concentration of the linear primary chains in determining the relative probabilities of intramolecular cyclization and intermolecular cross-linking.[257] Gao and Matyjaszewski[258] have recently summarized this area in a comprehensive review on living radical polymerization of monomers in the presence of cross-linkers to yield polymer structures varying from stars to gels. Other strategies have been adopted: Wang *et al*[259] reported on the

synthesis of a RAFT monomer that consists of a dithioester moiety and a double bond, and copolymerized it with styrene to prepare highly branched polystyrene. Inspired by the process used by Yang for nitroxide mediated polymerization[260] and after by Wang for RAFT,[259] Sumerlin and co-workers[261] proposed the synthesis of thermoresponsive hyperbranched polymer by polymerization of (*N*-isopropylacrylamide) using RAFT agent bearing a double bond a similar process described by Wang. Perrier and coworkers reported the synthesis of hyperbranched polymers using EGDMA as cross-linker and RAFT polymerization in the presence of different vinyl monomers.[262] Finally, Armes *et al.*[263] reported on RAFT polymerization of methyl methacrylate and disulfide-based dimethacrylate (DSDMA) to yield hyperbranched polymers. After cleavage of the disulfide bridge, the authors confirm that the polymers chains present similar molecular weight and PDI to linear polymers obtained without addition of cross-linker.

Stimuli-responsive polymers have attracted great interest and several approaches have been attempted for manipulating responsive behavior. The established 'fruitfly" for responsive polymers is poly(*N*-isopropylacrylamide), NIPAAm, which exhibits thermoresponsiveness in aqueous solutions originating from the LCST (lower critical solution temperature).[264-267] The LCST can be mediated by copolymerization with other monomers to adjust the hydrophilic/hydrophobic balance of the polymer chains. This copolymerization strategy can have the disadvantage of reducing the magnitude of the transition. The macromolecular architecture has been shown to be an important parameter for manipulating the temperature of the LCST whilst maintaining the magnitude of the transition.[268,269] An inhibition of the LCST was observed for NIPAAm cyclic polymer chaines, when compared to their linear counterparts.[270]

Poly(ethylene glycol) and derivatives, such as poly(oligoethylene glycol) acrylate or poly(oligoethylene glycol) methacrylate, have desirable chemical properties that make them especially useful in biological and pharmaceutical applications; they are non-toxic, non-immunogenic, low fouling and biocompatible.[271,272] PEG and poly(OEG-MA) derivates can be used to modify a range of biorelevant materials such as nanoparticle surfaces,[273-277] polymer/protein bioconjugates (protein, siRNA, peptide…),[278-280] conferring anti-fouling properties and enhancing blood circulation times. Secondly the hydrophilic polymer layer, facilitates dispersion in aqueous-media and physiological liquids. Polymers based on poly(oligoethylene glycol) methacrylate yield amphiphilic

brush-like polymers with PEG side-chains (hydrophilic) branching from a methacrylate backbone (hydrophobic).

Polymers based on OEG-methacrylates can display thermoresponsive behavior with the LCSTs of the homopolymers critically dependent on the length of the PEG side-chains or, in the case of copolymers, the monomer composition. Lutz *et al.* have studied these dependencies for a range of the different poly(ethylene glycol) methacrylate polymers.[281-284] Increasing the number of ethylene glycol side-chain units results in an increase in the observed LCST (for $PMEO_2MA$ the LCST is 26 °C, $PMEO_3MA$ has a LCST of 52 °C, while the LCST of $PEGMA_{475}$ (8-9 ethylene glycol units) is 90 °C).[281,282] This LCST can be also tuned by the insertion of *ter*-monomers in the polymers.[285] Alexander *et al.* have also reported a salt effect on the LCST behavior for linear PEGMA chains.[286] Finally, several authors have synthesized PEG-based polymers and studied their thermally-induced response.[287-289]

Recently, several authors have proposed a route to nanogels by free radical copolymerization[290] or by atom transfer radical copolymerization[291] of DEG-MA with low ratios of OEG-MA macromonomers in the presence of cross-linker. Paris and Quijada-Garrido[290] show that the swelling behavior of these nanogels is strongly dependent on the length of OEG side chains. These thermoresponsive copolymers based on OEG-macromonomers were also used for the modification of nanoparticles. For example, Lutz et al. proposed the modification of iron oxide nanoparticles by 'grafting from' using OEG-MA and DEG-MA to yield thermoresponsive iron oxide nanoparticles.[292] Boyer and coworkers prepared thermosensitive copoly(oligoethylene oxide) acrylates with narrow polydispersities using RAFT polymerization. These copolymers were then grafted onto gold nanoparticle (GNP) surfaces yielding "smart" thermoresponsive gold nanoparticles.[273]

In this paper, we describe the synthesis of hyperbranched polymers obtained by the copolymerization of OEG-MA and DEG-MA in the presence of ethylene glycol dimethacrylate (EGD-MA) as cross-linker, via reversible addition fragmentation transfer (RAFT). The thermal solution properties (LCST) of the hyperbranched polymers have been studied in different media using turbidity and light scattering techniques.

2. Experimental Section

Materials

Di(ethylene glycol) methyl ether methacrylate (DEG-MA, Aldrich, 99%), oligo(ethylene glycol) methyl ether methacrylate (475 g/mol, OEG-MA, Aldrich, 99%) and ethylene glycol dimethacrylate (EGD-MA, Aldrich, 99%) were passed through a basic aluminum oxide column to remove inhibitors prior to use. 2,2'-Azobisisobutyronitrile (AIBN, Wako Chemicals) was crystallized twice from methanol prior to use. *N,N'*-Dicyclohexylcarbodiimide (DCC, Fluka, 99%), carbon disulfide (Merck, 99%), ethanethiol (Acros, 99+%), 4-(dimethylamino)pyridine (Aldrich, 98%), benzyl alcohol (Aldrich, 99%), potassium hydroxide (SDS), 4,4'-azobis(4-cyanovaleric acid) and *p*-toluenesulfonyl chloride were used as received.

Analytical Techniques

Size Exclusion Chromatography (SEC). Aqueous size exclusion chromatography (SEC) was performed using a Shimadzu modular system comprised of a DGU-12A solvent degasser, a LC-10AT pump, PL aqueous column (2 columns, mixed D) with a guard column and a RID-10A refractive index detector and SPD-10A Shimadzu UV/Vis. detector (flow rate: 1 ml/min). Calibration was performed using PEO standards ranging from 500 to 500,000 g/mol.

SEC analyses of the polymers were also performed in *N,N*-dimethylacetamide [DMAc; 0.03% w/v LiBr, 0.05% 2, 6–di-Butyl-4-methylphenol (BHT)] at 50 °C (flow rate = 1 mL/min) using a Shimadzu modular system comprised of a SIL-10AD auto-injector, a PL 5.0-mm bead-size guard column (50 × 7.8 mm) followed by four linear PL (Styragel) columns (10^5, 10^4, 10^3, and 500Å) and a RID-10A differential refractive-index detector. Polystrene standards (PL) were used for the calibration.

UV-vis Spectroscopy. UV-vis spectra were recorded using a CARY 300 spectrophotometer (Bruker) equipped with a temperature controller. The temperature raise was 1^oC/min.

NMR Spectroscopy. ^1H and ^{13}C NMR spectra were recorded on a Bruker ACF300 (300 MHz for ^1H and 75 MHz for ^{13}C) and ACF500 (500 MHz and 125 MHz for ^1H and ^{13}C NMR) spectrometers, with D_2O or $CDCl_3$ used as solvents. Ethylene Glycol monomer conversion was determined by comparing the vinyl proton signal (~ 5.6-6.1, 2H/mol

Ethylene Glycol monomers) to the total methylene attached to the methacrylate signal (~ 4.2 ppm, 2H/mol Ethylene Glycol).

Dynamic Light Scattering (DLS). Dynamic light scattering studies of the aggregates of the hyperbranched at 1 mg/mL in an aqueous solution were conducted using a Malvern Instruments Zetasizer Nano ZS instrument equipped with a 4 mV He-Ne laser operating at λ = 633 nm, an avalanche photodiode detector with high quantum efficiency, and an ALV/LSE-5003 multiple tau digital correlator electronics system with a measurement angle of 173°.

Transmission Electron Microscopy (TEM). The sizes and morphologies of the aggregates were observed using a transmission electron microscopy JEOL1400 TEM at an accelerating voltage of 100 kV. The particles were dispersed in water (5 mg/mL) and deposited onto 200 mesh, holey film, copper grid (ProSciTech).

For the preparation of samples above the LCST, the solution was heated (to $T > T_{LCST}$.) Concurrently, a copper grid was also equilibrated at this temperature. A few drops of the heated aggregate solution was then, placed on the copper grid and dried in an oven ($T > T_{LCST}$).

Methods

LCST Measurement. The lower critical solution temperature, LCST was determined using a UV-vis spectrophotometer set at 500 nm. The polymer concentrations were maintained at 1 mg/ml in water and a heating rate of 1 °C/min was applied. The temperature at which 90% of the transmittance of the solution was observed was defined as the LCST.

Determination of Particle Size. Hyperbranched copolymer solutions were prepared in distilled water at a polymer concentration of 1 mg/mL. The solutions were filtered through Millipore nylon filters (pore size 0.45 μm) to eliminate dust and large contaminants. The size measurements were carried out in quartz cuvettes and the temperature was allowed to equilibrate for 5 mins. For the determination of size vs. temperature the heating rate was maintained at 1 °C/min.

Synthesis

Synthesis of bis(ethyl hydrogen carbonotrithioate) **(1)**

Ethanethiol(9.3 g, 150 mmnol) , potassium hydroxide (10.3 g, 195 mmol) and carbon disulfide (11.4 g, 150 mmol) were mixed and stirred for 30 minutes at room temperature, followed by cooling to 0 ºC and the slow addition of p-Toluenesulfonyl chloride (14.3 g, 75 mmol). The resulting mixture was stirred at room temperature for 1 h. The resulting crude product was eluted through a silica gel column using hexanes/dichloromethane to yield a yellow oil **(1)**. ^{1}H NMR ($CDCl_3$): δ (ppm): 1.34 (t, 6H $\underline{CH_3}$-CH_2), 3.29 (c, 4H CH_3-$\underline{CH_2}$).

Synthesis of 4-cyano-4-(ethylthiocarbonothioylthio)pentanoic acid **(2)**

Bis(ethyl hydrogen carbonotrithioate) **(1)** (4.57 g, 16.7 mmol) and 4,4'-Azobis(4-cyanovaleric acid) (6.5 g, 23.3 mmol) were dissolved in ethyl acetate and refluxed overnight. The resulting crude product was eluted through a silica gel column using dichloromethane/methanol(10%) to yield a yellow-orange oil **(2)**. ^{1}H NMR ($CDCl_3$): δ (ppm): 1.33 (t, 3H $\underline{CH_3}$-CH_2), 1.85 (s, 3H $\underline{CH_3}$-$C_{4º}$), 2.31 (m, 1H $\underline{CH_a}$-CO), 2.49 (m, 1H $\underline{CH_b}$-CO), 2.66 (m, 2H $\underline{CH_2}$-$C_{4º}$), 3.31 (c, 2H CH_3-$\underline{CH_2}$), 10.99 (s, 1H $\underline{OH}$).

Synthesis of benzyl 4-cyano-4-(ethylthiocarbonothioylthio)pentanoate **(RAFT agent)**

4-cyano-4-(ethylthiocarbonothioylthio)pentanoic acid **(2),** (1 g, 3.8 mmol), benzyl alcohol (4.93 g 4.6mmol), (dimethylamino)pyridine (46 mg, 0.38 mmol) and N,N'-Dicyclohexylcarbodiimide (863 mg, 4.18 mmol) were dissolved in dichloromethane. The reaction was stirred at room temperature for 2 h and the resulting crude product was filtered and purified by a chromatographic column using hexane/dichloromethane as the solvent. The RAFT agent was obtained as an orange oil. ^{1}H NMR ($CDCl_3$):δ (ppm): 1.35 (t, 3H $\underline{CH_3}$-CH_2), 1.86 (s, 3H $\underline{CH_3}$-$C_{4º}$), 2.43 (m, 1H $\underline{CH_a}$-CO), 2.52(m, 1H $\underline{CH_b}$-CO), 2.67 (m, 2H $\underline{CH_2}$-$C_{4º}$), 3.33 (c, 2H CH_3-$\underline{CH_2}$), 5.14 (s, 2H $\underline{CH_2}$-Ar), 7.36 (m, 5H $\underline{Ar}$).

RAFT polymerization.

A typical reaction procedure is described for $[DEGMA]_0/[OEGMA]_0/[EGDMA]_0/[CTA]_0/[AIBN]_0$ = 36/4/3/1/0.2, as follows: A mixture of di(ethylene glycol) methyl ether methacrylate (178 mg, 0.9 mmol), poly(ethylene glycol) methyl ether methacrylate (17.5 mg, 0.1 mmol), ethylene glycol dimethacrylate (14.85 mg, 0.075

mmol), benzyl 4-cyano-4-(ethylthiocarbonothioylthio)pentanoate (8.8 mg, 0.025 mmol) and 2,2'-Azobisisobutyronitrile (0.8 mg, 0.005 mmol) in 1,4-dioxane was purged with nitrogen for 45 minutes. The solution was stirred at 70 °C over 24 h. Different aliquots were taken from the reaction mixture using a purged syringe at predetermined time. Polymer was isolated and purified by repeated precipitation in cold diethyl ether and then dried under vacuum for 24 h, before analysis using ^{1}H NMR and SEC to determine the monomer conversion and molecular weight respectively.

^{1}H NMR ($CDCl_3$): δ (ppm): 0.88, 1.04 (m, 186H $\underline{CH_3}$-$C_{4º}$), 1.53-2.11 (m, 120H $C_{4º}$-$\underline{CH_2}$-$C_{4º}$), 3.39 (s, 186H -O-$\underline{CH_3}$), 3.48-3.81 (m, 354H -O-($\underline{CH_2}$-$\underline{CH_2}$-O)$_n$-), 4.10 (m, 120H –CO-O-$\underline{CH_2}$-), 5.12 (s, 2H -$\underline{CH_2}$-Ar), 7.35 (m, 5H -$\underline{Ar}$).

3. Results and discussion

Synthesis and characterization of polymers

A "one pot" synthesis of hyperbranched polymers using reversible addition-fragmentation chain transfer polymerization (RAFT) was implemented to synthesize soluble hyperbranched amphiphilic copolymers (HBP) as depicted in Scheme 4.1.

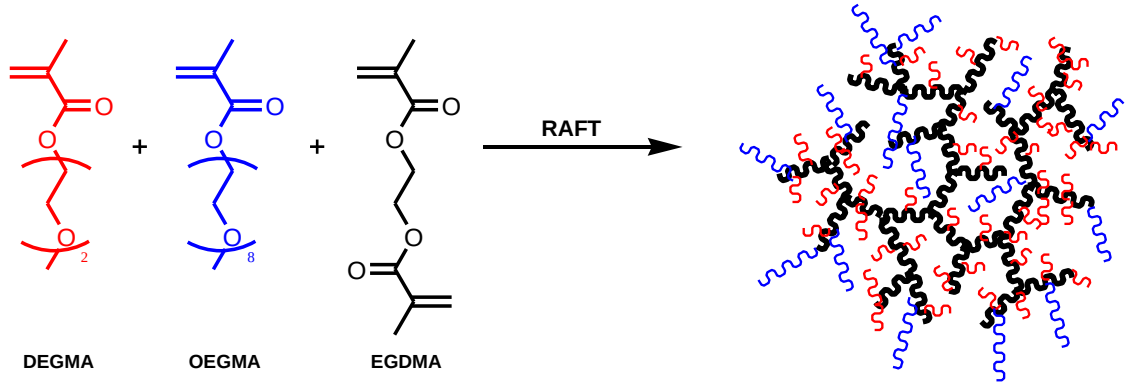

Scheme 4.1. Synthesis of thermoresponsive hyperbranched polymers.

In this synthetic approach, thermoresponsive hyperbranched copolymers of di(ethylene glycol) methacrylate (DEG-MA) and oligo(ethylene glycol) methacrylate (OEG-MA, M_w = 475 g/mol), with ethylene glycol dimethacrylate (EGD-MA) as cross-

linking agent were prepared. Monomer feed ratios ranging from 40/2 to 40/4 ([DEGMA+OEGMA]/[EGDM]) were used to determine the "ideal" ratio that would avoid the formation of insoluble cross-linked polymers (macrogels). Consistently soluble hyperbranched polymers could be obtained using a monomer/ cross-linker ratio equal to 40/3, while 40/4 always gave insoluble polymers (formation of macrogels). A lower monomer composition ratio, that is 40/2, resulted in the production of linear polymer. The RAFT polymerizations were stopped over 90% conversion and no gelation was observed.

We varied the comonomer composition of the feed, to facilitate tuning of the LCST of a range of hyperbranched polymeric structures. In addition linear analogues of the hyperbranched polymers were prepared in the absence of cross-linker (EGDMA); to allow comparison between the properties of hyperbranched and linear polymers. The LCST could be tuned from 17 to 55 ^{o}C. The polymerization conditions and the resultant molecular weight data are given in Table 4.1.

Table 4.1. Summary of the polymers synthesized in this study.

Polymer	DEGMA (%)	OEGMA (%)	M_n $^{theor.}$ (Kg/mol)	M_n (Kg/mol)	PDI	LCST
P1 linear	100	0	9	13	1.1	26
P2 linear	90	10	10	14	1.1	42
P3 linear	80	20	12	15	1.1	55
P4 HBP	100	0	-	34	3.5	17
P5 HBP	90	10	-	21	3.1	35
P6 HBP	80	20	-	43	2.8	46

Experimental condition: [Monomer]: [CTA]: [AIBN] = 100:2.0:0.4, dioxane used as solvent. Determination of the LCST: the copolymer concentration was fixed to 1 mg/mL and the heating rate 1 °C /min.

In the absence of cross-linker, M_n values were consistent with theoretical values (calculated by the following equation, $M_n = ([M]^i \times M_w^i)/ [CTA]+ M_w^{CTA}$, where $[M]^i$ and M_w^i correspond to monomer concentration and molar mass of monomer, respectively), i.e. 13 to 15 Kg/mol, with a low PDI in accord with a living radical polymerization. M_n data for the hyperbranched structures were significantly different, confirming the substantial influence of the EGDMA, introducing branch points. The M_n data ranged between 21-43 Kg/mol and the polydispersity measurements were

consistent with a broadening of the molecular weight distribution with PDIs ranging from 2.8 to 3.5. ^{1}H NMR of the copolymers confirmed the presence of the RAFT end-group (phenyl group at 7.3 ppm) and the incorporation of both OEG-MA and DEG-MA into the polymer (the signals at 3.6 ppm and 4.0 ppm respectively: see Figure 4.1 for one example).

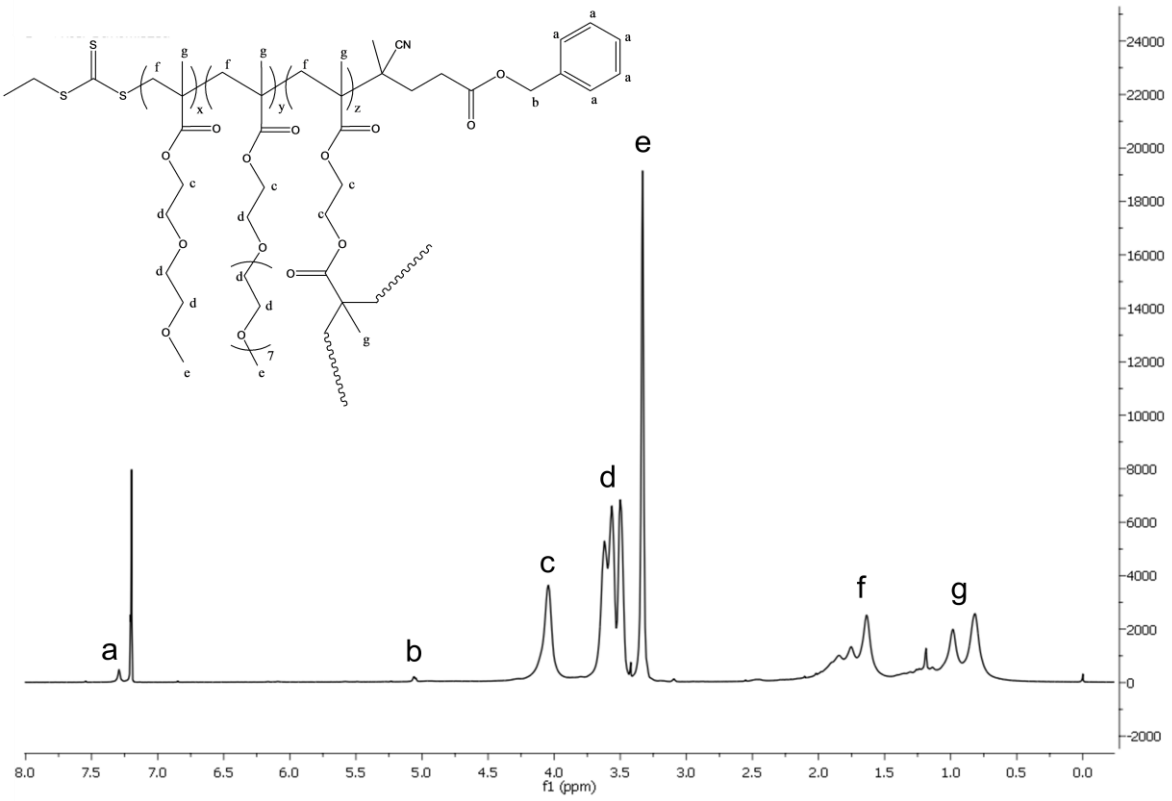

Figure 4.1. ^{1}H NMR of poly(OEG-MA-*co*-DEG-MA) recorded in deuterated chloroform at 298 K.

The monomer conversion versus time profiles was determined by ^{1}H NMR analysis. A kinetic plot for the polymerization of P5 is given in Figure 4.2.A. The HBP syntheses attained 97% conversion after 24 hours of reaction. The rapid increase of molecular weight at high conversions for the synthesis of hyperbranched polymer, i.e. P5 (Figure 4.2.B) is attributed to the onset of gelation (i.e. the cross-linking reaction). The final conversion attained was between 93-97% for both linear and hyperbranched polymers. The addition of chain transfer agents to a polymerization of mono- and difunctional monomers retards gelation as the length of the primary linear-chains can be reduced via the transfer step. Since gelation usually occurs where n+1 chains are

linked (where n is the number of chains) reducing the polymer chain length means that n+1 increases, and so, gelation is delayed to higher conversion. In a living polymerization, termination is reversible so as conversion increases the length of primary linear-chain increases so the probability of more chains including more than 1 cross-link/branch increases.

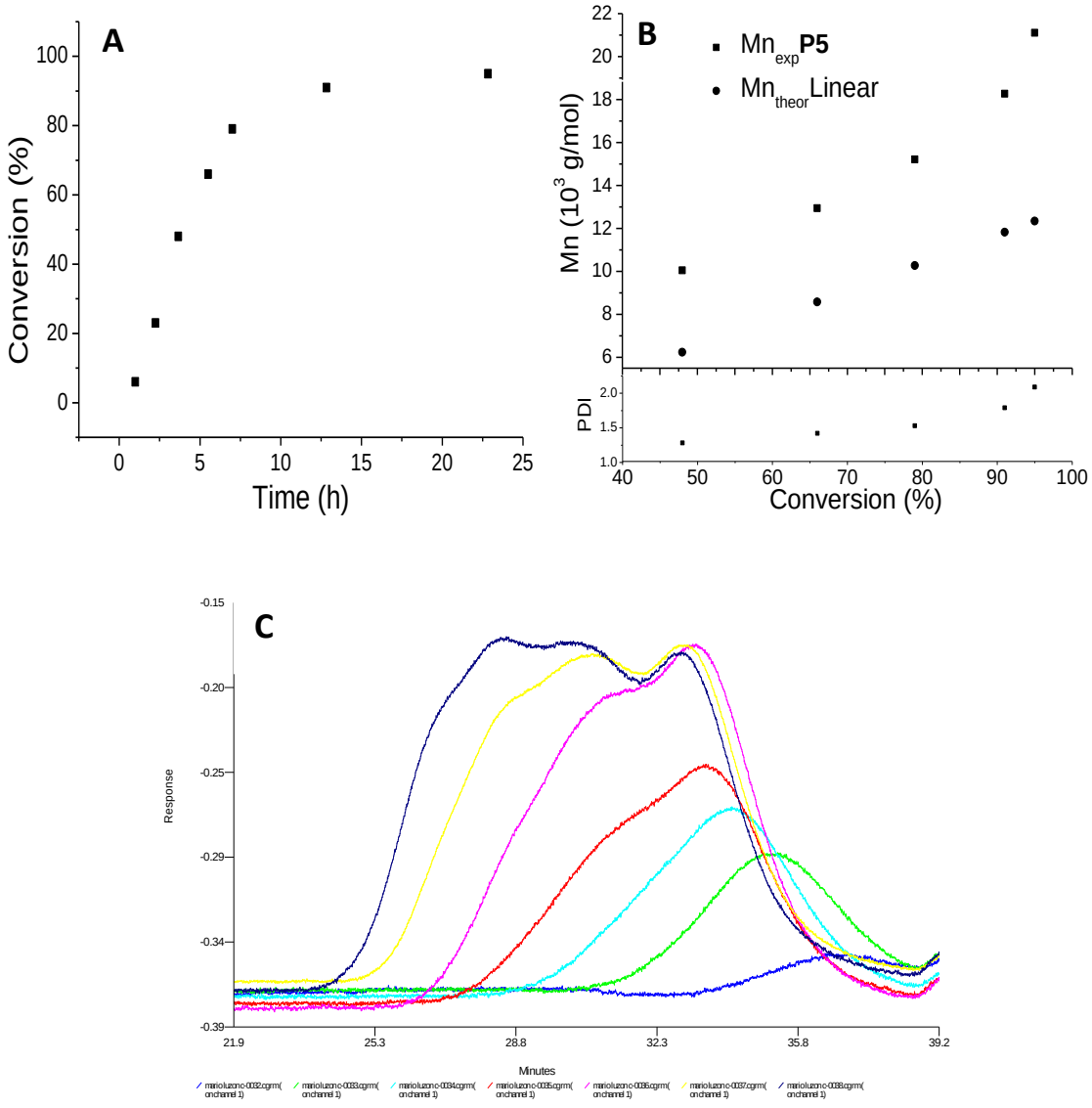

Figure 4.2. RAFT-Polymerization kinetic data for OEGMA and DEGMA. A- The evolution of monomer conversion versus time, B- The evolution of M_n of hyperbranched polymer (P5) compared to theoretical linear polymer and PDI versus time; C- GPC traces of hyperbranched copolymers (P5) taken as the reaction progressed.

The M_n and PDI data obtained from the polymers analyzed at different conversion levels are consistent with branching and an increase in molecular weight (Figure 4.2.B).

The evolution of polydispersity from narrow to broad consistent with the observation of multimodal distributions and the dramatic increase of molecular weight at the end of the polymerization confirms the synthesis of complex hyperbranched structures (Figure 4.2.C).

The lower critical solution temperatures (LCSTs) of aqueous solutions of the hyperbranched polymers were measured and was compared to the LCST obtained for linear copolymers having the same composition (Table 4.1, Figure 4.3.A). The LCST was defined as the temperature corresponding to 90% transmittance.[293] The LCST values of the linear polymers are in very close agreement with the values reported previously in the literature. In contrast, the hyperbranched polymers exhibited a LCST 5-10 ^{o}C lower compared to the equivalent linear chains (Figure 4.3.C). Similar behavior has been reported previously for Poly(NIPAAm) solutions and for Poly(ether amide).[294]

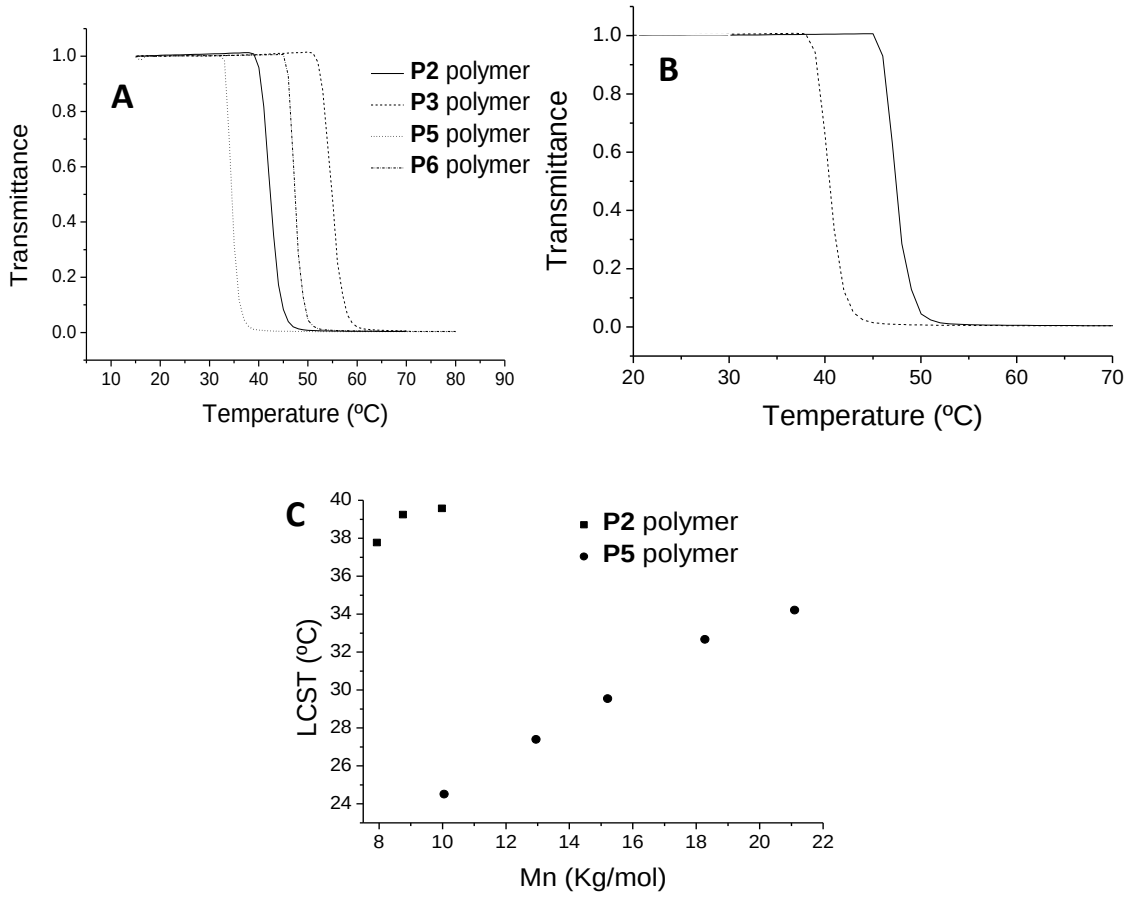

Figure 4.3. LCST measurements of linear and hyperbranched poly(OEG-MA-*co*-DEG-MA) copolymers: A- UV-visible turbidimetric experiment at 500 nm of copolymers in water (1 mg/mL) versus temperature; B- Heating and cooling cycle for hyperbranched copolymers (P5); C- Evolution of the LCST with molecular weight for linear and hyperbranched copolymers.

Lutz and coworkers,[295] noted that higher levels of OEGMA in linear copolymers causes an increase of the LCST (poly(OEG-MA) shows a LCST around 90 ^{o}C). A similar result was observed here for hyperbranched copolymers (Table 4.1). The hysteresis effect observed for the hyperbranched polymers (difference between heating and cooling cycles) is similar to the hysteresis effects observed for linear polymers ≈ 7 ºC under our experimental conditions (Figure 4.3.B). This lack of effect of architecture on LCST hysteresis is quite different to that observed previously for poly(NIPAAM) where a hyperbranched architecture was observed to significantly reduce hysteresis effects (compared to linear polymers).[293]

The evolution of LCST as a function of the molecular weights of both the linear and hyperbranched copolymers is compared in Figure 4.3.C. The LCST of the copolymers is affected by the molecular weight of the chains, with a lower LCST observed at low molecular weights. The LCST is also affected by the structure of the copolymer. At low monomer conversions (50% and below), linear and hyperbranched architectures exhibit a similar trend in LCST behavior. At monomer conversions above 50%, the hyperbranched copolymers show a more rapid increase in LCST than linear copolymers. This is attributed to enhanced branching yielding hyperbranched structures at higher conversions, as revealed by the GPC data (Figure 4.1.C).

The evolution of LCST versus polymerization time (min) for hyperbranched copolymer 5 is shown in Figure 4.4.A, with an increase of the LCST clearly observed during the polymerization. This increase in LCST with conversion contrasts to that observed previously for poly(NIPAAm) and other thermoresponsive polymers,[296,297] where a decrease of LCST occurs with increasing molecular weight. This difference in behavior can be attributed to a change in copolymer composition during the copolymerization reaction (polymer compositional drift). A low incorporation of OEGMA occurs at the outset of polymerization (Figure 4.4.B), as conversion proceeds there is a compositional drift towards an increasing incorporation of OEGMA into the growing polymer chains. The resulting copolymer structure is a gradient copolymer (as the polymerization is performed under living radical conditions). ^{1}H NMR analysis was used to evaluate the copolymer compositions at different conversions and this data combined with the LCST measurements confirms a correlation of LCST with copolymer composition as shown in Figure 4.4.C.

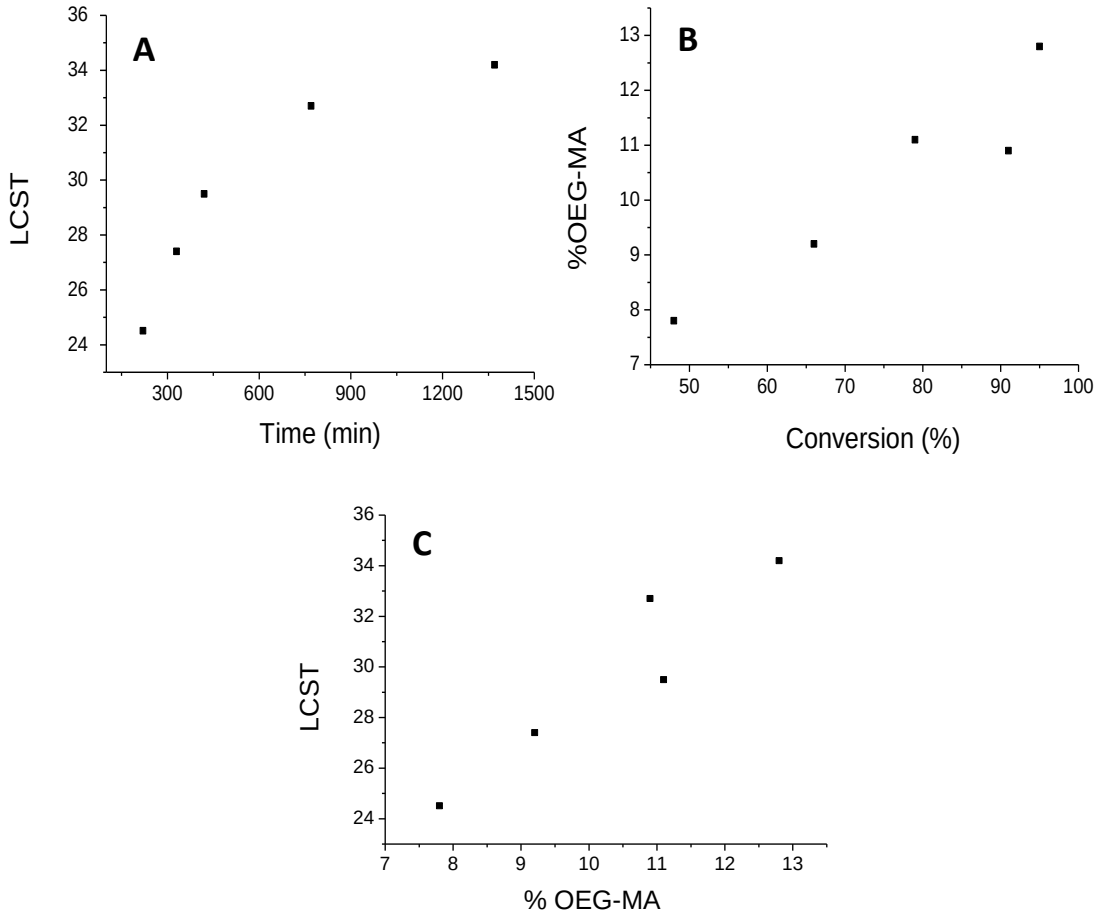

Figure 4.4. Evolution of the LCST for copolymers prepared to different conversions (Polymer #5): A- Evolution of the LCST versus polymerization time; B- Evolution of copolymer composition versus polymerization time; C- Evolution of the LCST versus copolymer composition.

^{1}H NMR spectra were recorded at different temperatures to study the phase transition of P6 in solution (10 mg/mL) in D_2O. The water peak was used as an internal reference. The NMR signals become smaller and broader as temperature increases as expected. The signals at 3.35 ppm and at 3.63 ppm can be attributed to the methyl group at the end of the poly(ethylene glycol) side chain and to the methylene oxide groups of the poly(ethylene glycol) chain, respectively. The integration ratio of the signals at 3.63 ppm and 3.35 ppm for hyperbranched polymer (P6) versus temperature (Figure 4.5) shows little change until a temperature of 37 °C is reached. When the temperature increases from 37 to 44 °C, the signal ratio decreases drastically characteristic of the phase transition associated with the LCST, and the precipitation of polymer. Above 45

°C, the signal ratio remains constant. These results are in accord with the results obtained from UV spectroscopy experiments for the P6 polymer (LCST 45 °C).

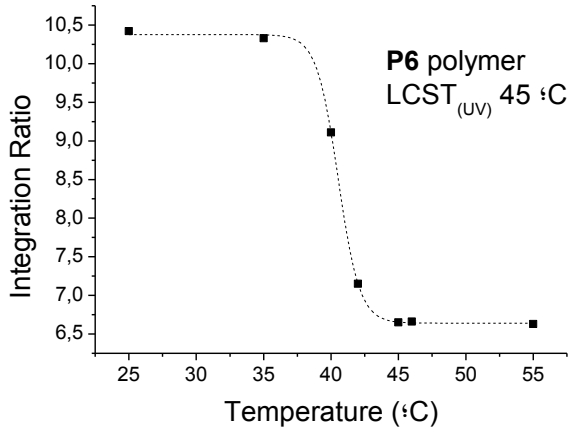

Figure 4.5. Evolution of integration ratio of signal at 3.63 ppm over 3.35 ppm for P6 versus temperature.

Effect of salt concentration on the LCST behavior

The effect of salts, NaCl and Na_2SO_4, on the LCST behavior of these copolymers was also investigated (Figure 4.6). The LCST of poly(NIPAAm) has been previously shown to be affected by the presence of salt in solution. Lutz and coworkers[295] and Alexander and coworkers[286] studied the evolution of LCST in the presence of salt for linear poly(DEGMA-*co*-OEGMA) copolymers, showing that these copolymers are less affected than poly(NIPAAm). The LCSTs of the linear and hyperbranched copolymers were evaluated at different concentrations of NaCl and Na_2SO_4. A strong kosmotrope salt effect was found (i.e., stabilization of hydrophobic aggregates in solution). The "salting out" effect was studied for the polymers P2 and P5 (with a DEGMA/OEGMA molar ratio 90/10) for linear and hyperbranched copolymers, respectively. The LCST values decreased for both types of copolymer structures as the salt concentration was increased. The type of salt also influenced the LCST behavior with the Na_2SO_4 salt exhibiting a stronger effect on the LCST than the NaCl salt. This influence of salt structure is known as the Hofmeister effect,[298] and previous observations on the

influence of Na_2SO_4 on LCST are consistent with our own observations reported herein.[293,299]

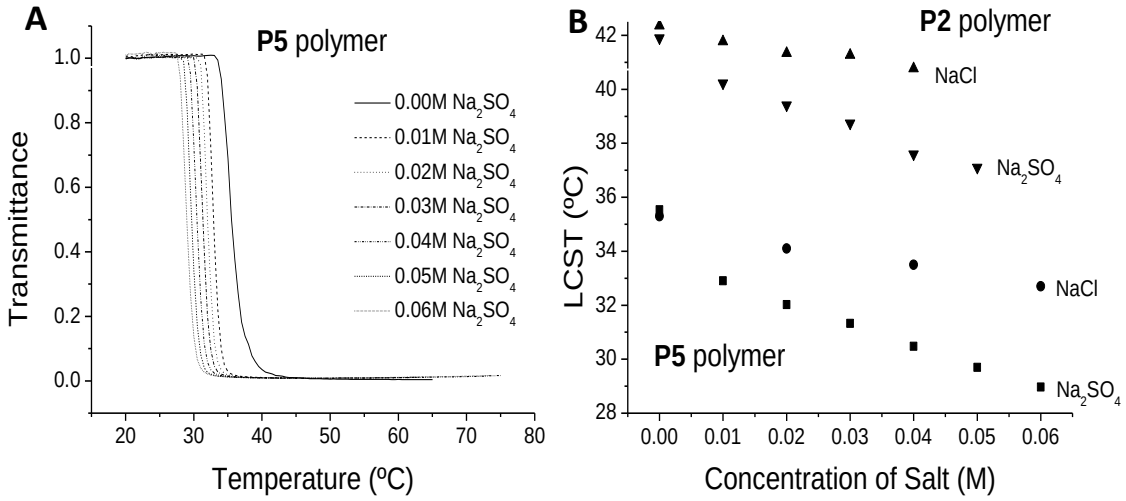

Figure 4.6. Salt effect on LCST behavior. A- Turbidimetry analysis at 500 nm of hyperbranched polymer (P5) at different salt concentrations; B- Change in LCST with salt concentration for hyperbranched and linear copolymers (P5 and P2).

DLS studies of the LCST transition

Aggregate size changes with temperature were studied for aqueous solutions of copolymer P5 by DLS (Figure 4.7). Below the LCST, the aggregates sizes was 10 nm and the PDI was 0.4, above the LCST the aggregates sizes increase to ≈225 nm (with a significant decrease of PDI) and the solution becomes cloudy. The LCST values determined by DLS are consistent with the data from turbidity measurements.

The hyperbranched copolymer sizes were studied versus temperature over a range from 20 to 70 °C. The hyperbranched polymer stayed perfectly dispersed in water, i.e. no precipitation was observed, with a size constant independent of the temperature. In addition, the PDIs of hyperbranched copolymers determined by DLS decreased less than 0.1 with an increase in temperature.

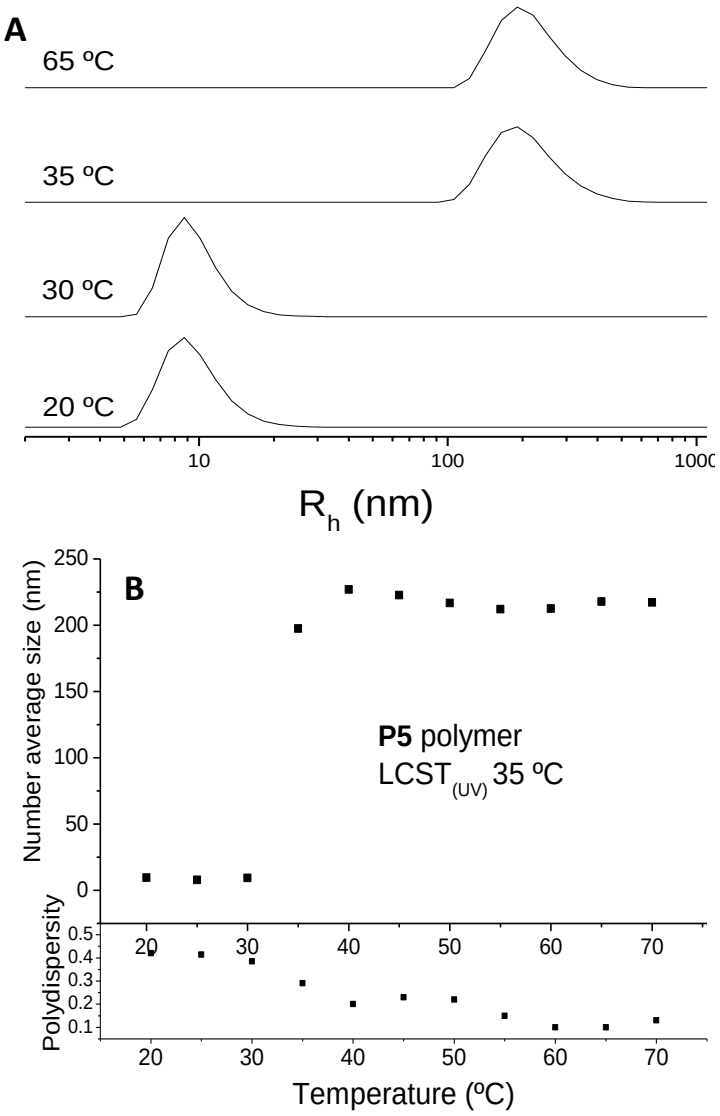

Figure 4.7. DLS characterization of hyperbranched copolymers (P5): A- Number mean sizes versus temperature determined by DLS analysis; B- Evolution of the sizes and PDIs of the aggregates determined by DLS versus temperature.

TEM Characterizations

Samples for TEM were prepared below and above the LCST (from solutions of 5 mg/mL of hyperbranched polymer P5, Figure 4.8). Above the LCST, the images show well-dispersed and well-defined aggregates (with regular shapes and sizes) formed from hyperbranched polymers, while below the LCST, no self-assembled nanoparticles were observed by TEM. The aggregate sizes (around 150-200 nm) found by TEM are slightly smaller than the sizes measured by DLS attributable to differences in the preparation of the samples.

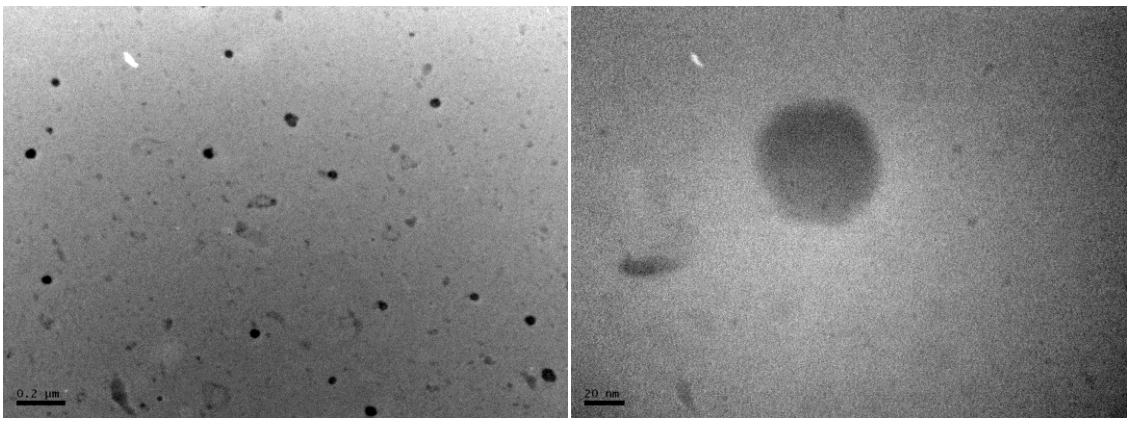

Figure 4.8. TEM pictures of hyperbranched (P5) above the LCST.

4. Conclusion

A series of hyperbranched copolymers made from di(ethylene glycol) methacrylate and oligo(ethylene glycol) methacrylate in the presence of cross-linker (i.e., ethylene glycol dimethacrylate) *via* reversible addition-fragmentation chain transfer polymerization has been synthesized. The copolymers are water soluble, presenting LCST transitions over a range of temperatures. By manipulating the copolymer compositions of DEGMA and POEGMA, the LCST value could be tuned from 25 °C to 90 °C. Changing the monomer ratio, from 10% to 20% of oligo(ethylene glycol) methacrylate, changed the LCST values from 35 to 46 °C, respectively. The addition of salt (i.e., NaCl or Na_2SO_4) causes a decrease in the LCST of hyperbranched polymers. The aggregation of the hyperbranched polymers in water above the LCST was characterized by DLS and TEM.

5. Acknowledgements

ML, TC and CP would like to thank Ministerio de Ciencia e Innovación of Spain for financial support Plan National I+D+I (MAT2006-05979) and ML is also thankful for his travelling scholarship. CB and TPD are thankful for a APD fellowship and the federation fellowship, respectively, from the Australian Research Council.

6. References

(228) Voit, B. I.; Lederer, A. *Chem. Rev.* **2009**, *109*, 5924.

(229) Peleshanko, S.; Tsukruk, V. V. *Prog. Polym. Sci.* **2008**, *33*, 523.

(230) Xu, J.; Tao, L.; Boyer, C.; Lowe, A. B.; Davis, T. P. *Macromolecules* **ASAP**.

(231) Santra, S.; Kaittanis, C.; Perez, J. M. *Langmuir*, *DOI: 10.1021/la9037843*.

(232) Konkolewicz, D.; Gray-Weale, A.; Perrier, S. *J. Am. Chem. Soc.* **2009**, *131*, 18075.

(233) Iha, R. K.; Wooley, K. L.; Nystrm, A. M.; Burke, D. J.; Kade, M. J.; Hawker, C. J. *Chem. Rev.* **2009**, *109*, 5620.

(234) Xu, J.; Tao, L.; Liu, J.; Bulmus, V.; Davis, T. P. *Macromolecules* **2009**, *42* 6893.

(235) Liu, B.; Kazlauciunas, A.; Guthrie, J. T.; Perrier, S. *Macromolecules* **2005**, *38*, 2131.

(236) Maier, G.; Zech, C.; Voit, B.; Komber, H. *Macromol. Chem. Phys.* **1998**, *199*, 2655.

(237) Klajnert, B.; Bryszewska, M. *Acta Biochimica Polonica* **2001**, *48*, 199.

(238) Wang, P.; Wang, X.; Meng, K.; Hong, S.; Liu, X.; Cheng, H.; Han, C. C. *J. Polym. Sci. PartA: Polym. Chem.* **2008**, *46*, 3424.

(239) Liu, H.; Chen, Y.; Shen, Z. *J. Polym. Sci. PartA: Polym. Chem.* **2007**, *45*, 1177.

(240) Saha, A.; Ramakrishnan, S. *Macromolecules* **2008**, *41*, 5658.

(241) Shen, Y.; Kuang, M.; Shen, Z.; Nieberle, J.; Duan, H.; Frey, H. *Angew. Chem., Inter. Ed.* **2008**, *47*, 2227.

(242) Wang, X.-Y.; Luo, Y.-J.; Xia, M.; Li, X.-M.; Gao, R.-Z. *Polymeric Materials Science and Engineering* **2009**, *25*, 158.

(243) Drisko, G. L.; Cao, L.; Kimling, M. C.; Harrisson, S.; Luca, V.; Caruso, R. A. *ACS Appl. Mater. Interfaces* **2009**, *1*, 2893.

(244) Paleos, C. M.; Tziveleka, L.-A.; Sideratou, Z.; Tsiourvas, D. *Expert Opinion on Drug Delivery* **2009**, *6*, 27.

(245) Paleos, C. M.; Tsiourvas, D.; Sideratou, Z. *Molecular Pharmaceutics* **2007**, *4* 169.

(246) Arote, R. B.; Lee, E.-S.; Jiang, H.-L.; Kim, Y.-K.; Choi, Y.-J.; Cho, M.-H.; Cho, C.-S. *Bioconjugate Chem.* **2009**, *20*, 2231.

(247) Chen, J.; Wu, C.; Oupick, D. *Biomacromolecules* **2009**, *10*, 2921.

(248) Tao, L.; Liu, J.; Tan, B. H.; Davis, T. P. *Macromolecules* **2009**, *42*, 4960.

(249) Paleos, C. M.; Tsiourvas, D.; Sideratou, Z.; Tziveleka, L. *Current Topics in Medicinal Chemistry* **2008**, *8*, 1204.

(250) Jiang, G.; Chen, W.; Xia, W. *Designed Monomers and Polymers* **2008**, *11*, 105.

(251) Stover, T. C.; Kim, Y. S.; Lowe, T. L.; Kester, M. *Biomaterials* **2007**, *29*, 359.

(252) Kojima, C.; Yoshimura, K.; Harada, A.; Sakanishi, Y.; Kono, K. *Bioconjugate Chem.* **2009**, *20*, 1054.

(253) Cao, X.; Li, Z.; Song, X.; Cui, X.; Cao, P.; Liu, H.; Cheng, F.; Chen, Y. *Europ. Polym. J.* **2008**, *44*, 1060.

(254) O'Brien, N.; McKee, A.; Sherrington, D. C.; Slark, A. T.; Titterton, A. *Polymer* **2000**, *41*.

(255) Slark, A. T.; Sherrington, D. C.; Titterton, A.; Martin, I. K. *J. Mater. Chem.* **2003**, *13*, 2711−2720.

(256) Isaure, F.; Cormack, P. A. G.; Sherrington, D. C. *J. Mater. Chem.* **2003**, *13*, 2701−2710.

(257) Rosselgong, J.; Armes, S. P.; Barton, W. R. S.; Price, D. *Macromolecules* **2010**, *43*, 2145.

(258) Gao, H.; Matyjaszewski, K. *Progress in Polymer Science* **2009**, *34*.

(259) Wang, Z.; He, J.; Tao, Y.; Yang, L.; Jiang, H.; Yang, Y. *Macromolecules* **2003**, *36*, 7446.

(260) Li, C.; He, J.; Li, L.; Cao, J.; Yang, Y. *Macromolecules* **1999**, *32*, 7012.

(261) Vogt, A. P.; Sumerlin, B. S. *Macromolecules* **2008**, *41*, 7368.

(262) Liu, B.; Kazlauciunas, A.; Guthrie, J. T.; Perrier, S. *Macromolecules* **2005**, *38*, 2131.

(263) Rosselgong, J.; Armes, S. P.; Barton, W.; Price, D. *Macromolecules* **2009**, *42*, 5919.

(264) C. K. Chee, S. R., D. A. Shaw, I. Soutar, L. Swanson *Macromolecules* **2001**, *34*.

(265) Y. Maeda, H. Y. a. I. I. *Langmuir* **2001**, *17*.

(266) Kesim, H.; Rzaev, Z. M. O.; Dincer, S.; Piskin, E. *Polymer* **2003**, *44*.

(267) Barker, I. C.; Cowie, J. M. G.; Huckerby, T. N.; Shaw, D. A.; Soutar, I.; Swanson, L. *Macromolecules* **2003**, *36*.

(268) Chee, C.-K.; Hunt, B. J.; Rimmer, S.; Rutkaite, R.; Soutar, I.; Swanson, L. *Soft Matter* **2009**, *5*, 3701.

(269) Qiu, X.-P.; Winnik, F. M. *Macromol. Symp.* **2009**, *278* 10.

(270) Qiu, X.-P.; Tanaka, F.; Winnik, F. M. *Macromolecules* **2007**, *40*, 7069.

(271) York, A. W.; Kirkland, S. E.; McCormick, C. L. *Adv Drug Deliver Rev* **2008**, *60*, 1018.

(272) Stadler, V.; Kirmse, R.; Beyer, M.; Breitling, F.; Ludwig, T.; Bischoff, F. R. *Langmuir* **2008**, *24*, 8151.

(273) Boyer, C.; Whittaker, M.; Luzon, M.; Davis, T. P. *Macromolecules* **2009**, *42*, 6917.

(274) Boyer, C.; Bulmus, V.; Priyanto, P.; Teoh, W. Y.; Amal, R.; Davis, T. P. *J. Mat. Chem.* **2009**, *19*, 111.

(275) Kim, D.; Park, S.; Lee, J. H.; Jeong, Y. Y.; Jon, S. *J. Am. Chem. Soc.* **2007**, *129*, 7661.

(276) Lee, H.; Lee, E.; Kim, D. K.; Jang, N. K.; Jeong, Y. Y.; Jon, S. *J. Am. Chem. Soc.* **2006**, *128*, 7383.

(277) Liu, H.; Li, J. *Iranian Polymer Journal* **2008**, *17*, 721.

(278) Boyer, C.; Bulmus, V.; Davis Thomas, P.; Ladmiral, V.; Liu, J.; Perrier, S. *Chem. Rev.* **2009**, *109*, 5402.

(279) Boyer, C.; Liu, J.; Bulmus, V.; Davis Thomas, P. *Aust. J. Chem.* **2009**, *62*, 830.

(280) Boyer, C.; Liu, J.; Wong, L.; Tippett, M.; Bulmus, V.; Davis, T. P. *Journal of Polymer Science, Part A: Polymer Chemistry* **2008**, *46*, 7207.

(281) Lutz, J.-F.; Hoth, A. *Macromolecules* **2006**, *39*, 893.

(282) Lutz, J.-F. *J. Polym. Sci. PartA: Polym. Chem.* **2008**, *46*, 3459.

(283) Lutz, J.-F.; Akdemir, O.; Hoth, A. *J. Am. Chem. Soc.* **2006**, *128*, 13046.

(284) Lutz, J.-F.; Andrieu, J.; Üzgün, S.; Rudolph, C.; Agarwal, S. *Macromolecules* **2007**, *40*, 8540.

(285) Becer, C. R.; Hahn, S.; Fijten, M. W. M.; Thijs, H. M. L.; Hoogenboom, R.; Schubert, U. S. *J. Polym. Sci., A, Polym. Chem.* **2008**, *46*, 7138.

(286) Magnusson, J. P.; Khan, A.; Paasparakis, G.; Saeed, A. O.; Wang, W.; Alexander, C. *J. Am. Chem. Soc.* **2008**, *130*, 10852.

(287) Li, W.; Wu, D.; Schlüter, A. D.; Zhang, A. *J. Polym. Sci. Part A: Polym. Chem.* **2009**, *47* 6630.

(288) Gupta, N.; Lin, B. F.; Campos, L.; Dimitriou, M. D.; Hikita, S. T. T., N.D.; ; Tirrell, M. V.; Clegg, D. O.; Kramer, E. J.; Hawker, C. J. *Nature Chemistry* **2010**, *2*, 138.

(289) Rieger, J.; Grazon, C.; Charleux, B.; Alaimo, D.; Jérôme, C. *J. Polym. Sci. Part A: Polym. Chem.* **2009**, *47*, 2373.

(290) Paris, R.; Quijada-Garrido, I. *Eur. Polym. J.* **2009**, *45*, 3418.

(291) Badia, N.; Lutz, J.-F. *Journal of Controlled Release* **2009**, *140* 224.

(292) Chanana, M.; Jahn, S.; Georgieva, R.; Lutz, J.-F.; Bäumler, H.; D. Wang *Chem. Mater.* **2009**, *21*, 1906.

(293) Liu, X.; Cheng, F.; Liu, H.; Chen, Y. *Soft Matter* **2008**, *4*, 1991.

(294) Lin, Y.; Gao, J.-W.; Liu, H.-W.; Li, Y.-S. *Macromolecules* **2009**, *42*, 3237.

(295) Lutz, J. F.; Akdemir O.; Hoth A. *J. Am. Chem. Soc.* **2006**, *128*, 13046.

(296) Ramkissoon-Ganorkar, C.; Gutowska, A.; Liu, F.; Baudys, M.; Kim, S. W. *Pharmaceutical Research* **1999**, *16*, 819.

(297) Ramkissoon-Ganorkar, C.; Liu, F.; Baudys, M.; Kim, S. W. *Journal of biomaterials science* **1999**, *10*, 1149.

(298) Hofmeister, F. *Arch. Exp. Pathol. Pharmakol.* **1888**, *24*, 247−260.

(299) Pegram, L. M.; Record, M. T. *J. Phys. Chem. B* **2007**, *111*, 5411.

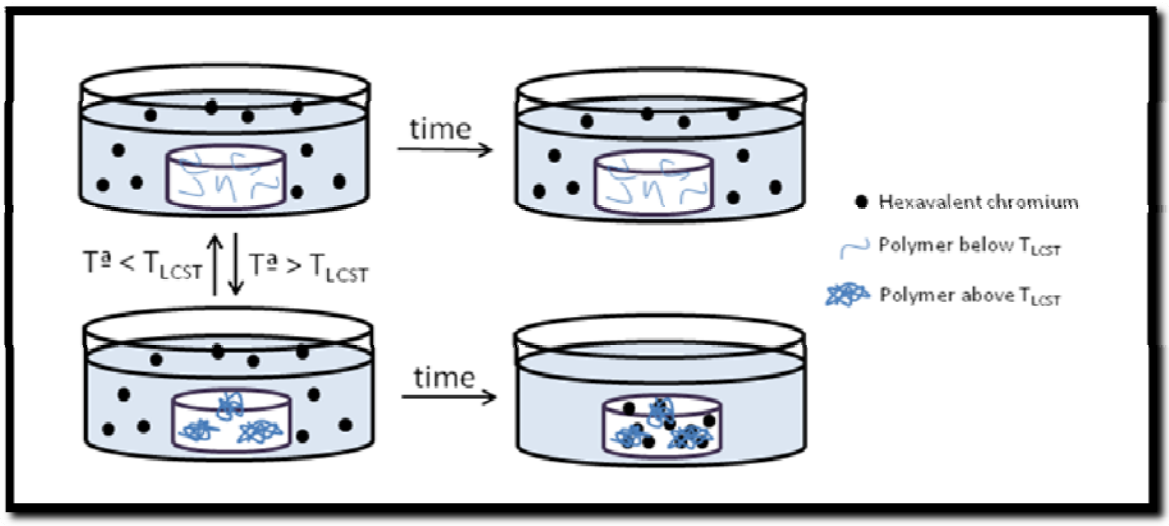

Thermal studies and chromium removal efficiency of thermoresponsive hyperbranched copolymers based on PEG-methacrylates

Chapter 5

Published in
Journal of Thermal Analysis and Calorimetry

Thermal studies and chromium removal efficiency of thermoresponsive hyperbranched copolymers based on PEG-methacrylates

Mario Luzon[1], Teresa Corrales[1]*

Abstract. This study deals with the removal of chromium species from aqueous dilute solutions using thermoresponsive linear and hyperbranched copolymers based on PEG-methacrylates. The thermal stability of polymers was studied by thermogravimetric analysis (TGA) and chemiluminescence emission (CL), which evidenced a slightly enhanced stability for hyperbranched polymers respect to linear structures. Their lower critical solution temperature (LCST) was successfully determined by TOPEM (temperature modulated d.s.c.), and similar values to those obtained by UV spectroscopy were obtained. The adsorption capacities for chromium hexavalent of the polymers have been investigated as function of LCST. The results showed highest retention capacity of Cr(VI) for all polymers above LCST. Hyperbranched polymers were more efficient than linear polymers, because of the structure of the polymers. Hyperbranched polymers when precipitate form a network with more nanocavities where the chromium can be adsorbed. The efficiency increased with ratio of OEGMA/DEGMA, reaching a maximum retention capacity value of 40 mg Cr(VI)/g polymer).

Keywords: thermoresponsive, hyperbranched, chromium removal, TMDSC, chemiluminescence

[1]*Polymer Photochemistry Group, Instituto de Ciencia y Tecnología de Polímeros, C.S.I.C. Juan de la Cierva 3, 28006-Madrid, SPAIN*

* Corresponding author: Tel: 34 912587484, fax: 34 915644853, e-mail: tcorrales@ictp.csic.es

1. Introduction

Heavy metals are highly toxic pollutant therefore they are a very great environment concern.[300-302] Chromium is one of those heavy metals usually generated from various industrial activities such as textile dyeing,[303] leather tanning process,[304] electroplating,[305] wood treatment and water treatment. Hexavalent chromium produces a general toxic effect on the human organism,[306,307] because of its high water solubility and mobility, as well as its easy reduction. The toxicological effects of Cr(VI) is originated from the action of its form itself as an oxidizing agent, as well as the formation of free radicals during the reduction of Cr(VI) to Cr(III) that occurs inside the cell. Another reason of the higher toxicity of Cr(VI) is that chromate ions pass quicker through cellular and nuclear membranes than trivalent species.

Different technologies have been employed for the removal of chromium (VI) ions from aqueous solutions, including electrochemical precipitation,[308] phytoextraction,[309] reverse osmosis,[310] ultrafiltration[311] and evaporative recovery.[312] It has been proved that the most effective and economical technique to remove chromium from water is adsorption and there are many kinds of adsorbents such as bacteria, fungal biomass, alga biomass or chemicals components from agricultural products, that have been studied for this purpose.[313-317] There are two types of adsorbents, the specific sorbents which have a ligand (e.g., ion exchanger or chelating agent) and an inorganic (aluminum oxide, activated carbon, silica, etc.)[318] or a polymeric (styrene-divinylbenzene copolymer, etc.) carrier matrix,[319] and the non-specific adsorbents such as activated carbon, metal oxides, silica or ion exchanger resins.[320] By using traditional separation techniques, the adsorbents are difficult to be separated from the solution. In the past few years, magnetic sorbents[321-323] have emerged as a new generation of materials for environmental decontamination, which can be separated by application of an external magnetic field.[324] Iron and iron oxide nanostructures have been proved to be highly efficient materials.[325] Recently, hybrid materials consisting on MMT sheets as support of magnetite nanoparticles coated with hyperbranched PEI were prepared by using a cationic exchange strategy.[326] Hyperbranched polymers based on polyethylenimine possess primary and secondary amine groups in a molecule, which exhibit good sorption ability of heavy metals.[327] The combination of the three components resulted in a new magnetic material with a number of advantages: high

removal efficiency in a wide pH range, chemical stability at any pH, solved co-aggregation and easy magnetic separation.

In recent years, new organic adsorbents in forms of resins or polymers have become under attention as exciting new absorbing materials because of its higher removal capacities, versatility and more overall efficiency.[328,329] Polymers have high adsorption capacity and they are easy handling and especially useful because they can be reused, recovering the heavy metals. Otherwise, polymer are versatile, can be produced in a wide range of size, size distribution, porosity, hydrophilicity, etc. and they can be modified easily inserting different ligands into the structure making them specific sorbents for each contaminant.

In the present paper, the adsorption capacities for chromium hexavalent of polymers based on ethylene glycol methacrylates synthesized via RAFT polymerization have been evaluated as function of the structure and the lower critical solution temperature (LCST). The polymers based in ethylene glycol methacrylate monomer are stimuli-responsive polymers which have attracted great interest and several approaches have been attempted for manipulating responsive behavior. Polymers based on OEG methacrylates can display thermoresponsive behavior with the LCSTs of the homopolymers critically dependent on the length of the PEG side chains or in the case of copolymers dependent on the monomer composition.[330-332] Above the LCST, polymer becomes dehydrated and hence insoluble in water thereby it precipitates and form porous structures making them promising as viable absorbents. Modulated differential scanning calorimetry called TOPEM has been successfully used to determine the lower critical solution temperature (LCST) and the results were compared with those obtained by UV spectroscopy. The thermal stability of the polymer was studied by thermogravimetric analysis (TGA) and chemiluminescence emission (CL), which has been proven to be a sensitive tool for this purpose.[333] The CL in polymers is due to the light emission that accompanies the thermal decomposition of the thermooxidative degradation products (hydroperoxides) which are formed during processing or in-service life of the material under ambient conditions. Then, the CL emission can be used to evaluate the degree of degradation or stability of polymers.

2. Experimental

Materials

Di(ethylene glycol) methyl ether methacrylate (DEG-MA, Aldrich, 99 %), oligo(ethylene glycol) methyl ether methacrylate (OEG-MA, 475 g/mol, Aldrich, 99 %) and ethylene glycol methacrylate (EG-DMA, Aldrich, 99 %) were passed through a basic aluminum oxide column to remove inhibitors before use. 2,2'-Azobisisobutyronitrile (AIBN, Wako Chemicals) was crystallized twice from methanol prior to use. Benzyl 4-cyano-4-(ethylthiocarbonothioylthio)-pentanoate (RAFT Agent) was synthesized as described elsewhere.[334] Diphenylcarbazide (Sigma Aldrich). Potassium Chromate (Productos Químicos Reactivos). Deionized water used for these experiments were purified by MILIQ system with a resistivity of 17.9 mΩ/cm. Hyperbranched polymers were synthesized as published elsewhere.[334]

Analytical Techniques

Nuclear Magnetic Resonance. ^{1}H and ^{13}C NMR spectra were recorded on a Varian INOVA-400 instrument operated at 400 MHz with $CDCl_3$ used as solvent.

Gel Permeation Chromatography. Molecular weights and polydispersity measurements were carried out using a Waters 1515 Isocratic HPLC Pump system equipped with a Waters 2414 Refractive Index Detectors. Calibration was carried out using linear poly(ethylene oxide) standards (Polymer Standards Service Gmbh), ranging from 2.4x104 to 5.7x105 $g \cdot mol^{-1}$. The mobile phase was ACN/Water (15 % v/v) at a flow rate of 0.5 $mL \cdot min^{-1}$. The system was equipped with a guard column Ultrahydrogel 6x40 mm and two Ultrahydrogel 7.8x300 mm mixed columns in series, thermostated at 25 ºC.

Thermo Gravimetrical Analysis. A TA Instruments Q500 Thermogravimetric Analyzer employing the Hi-ResTM,[335] was used to determine the onset temperature of weight loss, Td, and the char yield at 900 °C. Hi-Res scans were run at 50 °C/min with resolution and sensitivity parameters of 4.0 and 1.0, respectively, in the temperature range of 100–850 °C. The purge gas was nitrogen (60 mL/min) and the sample mass was ca. 10 mg.

Chemiluminescence. CL spectra were obtained with a CL400 Chemi-LUME analyzer developed by Atlas Electric Devices Co. Samples were placed in temperature controlled

cells with specimen holders consisting of disposable aluminum dishes. The cells were closed by optical lenses that focused the corresponding emission light of each sample in a photon-counting photomultiplier (Hamamatsu R1527 P), which was water-cooled at 17 °C. The photomultiplier was previously calibrated with a radioactive standard provided by Atlas. Dynamic tests were performed, the samples were heated at a heating rate of (10 °C/min) under a constant flow (50 mL/min) of nitrogen or oxygen. Samples for CL measurements were prepared by casting of dichloromethane solution in a circular crucible of 1.8 cm in diameter, therefore the emission area was kept constant for all determinations.

Optical Transmittance measurements. Optical transmittance of block copolymer in aqueous solution was measured at 550 nm with a Lambda 35 UV–Vis spectrometer (Perkin-Elmer). The sample cell was thermostatized in a refrigerated circulator bath Thermomix 1441 (B.BRAUN) at different temperatures from 10 to 90 °C prior to measurements. The lower critical solution temperature (LCST) of the polymer solution was defined as the temperature at the onset of the decrease in optical transmittance. This method seems to be accurately utilized only when two prerequisites are satisfied. The first prerequisite is that all the initial transmittance values of the curves are the same, and the second is that the phase-transition ranges of all the curves are similar.[336]

Calorimetry measurements. Differential Scanning Calorimetry (DSC) measurements were performed by using a DSC 823-Mettler Toledo equipped with sample robot and cooled by Julabo FT400 intracooler and controlled with a STARe software 9.10 version. Aluminium standard crucibles with 20 µl of sample were used for analyses that were carried out under a nitrogen atmosphere. Indium and water were used for temperature and enthalpy calibration.

TOPEM mode was chosen as temperature modulated DSC method. Instead of being based upon a periodic modulation of the heating rate, as is the situation with temperature modulated DSC (MTDSC) techniques, TOPEM uses a stochastic modulation of the heating or cooling rate by means of random pulses of temperature. This feature has the advantage that a set of experiments require only scan of the samples but not for the blank as in other MTDSC techniques.[337] The parameters selected were: temperature range for the scan was from 10 to 50 °C in order to cover the LCST; the underlying heating rate was 0.25 K min^{-1}; the amplitude of the

temperature pulse took values of 0.0005 K; and the switching time range, which limits the duration of the pulses, had a minimum of 30 s and a maximum of 60 s. Data analysis was carried out using TOPEM software. To calculate the response function for the system, the evaluation window was selected covering a region of the data in which there is no transition. The TOPEM evaluation yields the curve of *c*p0, the 'quasi-static' specific heat capacity and the separation of correlated and non-correlated components of the heat flow with respect to the heating rate, which are related to the reversing and non-reversing heat flows in the usual MTDSC terminology.

Adsorption experiments

To determine the adsorption capacity dialysis experiments were performed. A dialysis bag (MWCO = 6000-8000 Da) containing 6 mL of the polymer solution was sealed and immersed in ultra pure water solution (70 mL, pH 7) at 45 ºC in a thermostatically controlled oven. The copolymer concentration was 5 g/l for all the polymers, lineal and hyperbranched. Aliquots of 1 mL were withdrawn from the solution periodically. The volume of the solution was held constant by adding 1 mL fresh ultra pure water solution after each sampling to ensure sink conditions. The amount of chromium adsorbed by polymers was determined by a normalized method for chromium (VI) determination.[338]

The colorimetric method to determine chromium hexavalent was used to know the concentration of chromium in solution. A calibration curve was done before the determination. Dissolved hexavalent chromium may be determined colorimetrically by reaction with diphenylcarbazide in acid solution. Addition of an excess of diphenylcarbazide yields the red-violet product, and its absorbance is measured photometrically at 540nm.

3. Results and discussion

A series of water-soluble thermoresponsive linear and hyperbranched copoly(oligoethylene glycol)s have been synthesized by copolymerization of di(ethylene glycol) methacrylate (DEGMA) and oligo(ethylene glycol) methacrylate (OEG-MA, Mw ¼ 475 g/mol), with ethylene glycol dimethacrylate (EGD-MA) used as the crosslinker, via reversible addition fragmentation chain transfer polymerization.

Polymers have been characterized by size exclusion chromatography and nuclear magnetic resonance analyses and the results are shown in Table 5.1.

Table 5.1. Summary of the Polymers Synthesized in this Study

Polymer	DEGMA (%)	OEGMA (%)	M_n^{Theor} (Kg/mol)	M_n (Kg/ mol)	PDI
L1 linear	92	8	20	21	1.09
L2 linear	80	20	20	23	1.14
H1 HBP	87	13	-	32	1.90
H2 HBP	76	24	-	37	2.27

Thermal stability of polymers

The thermal behavior of the polymers was evaluated by Thermo gravimetric analysis (TGA) and Chemiluminescence emission analysis (QL). The TGA of the copolymers is plotted in Figure 5.1, and the derived data are shown in Table 5.2. All polymers undergo a three-step degradation process. The onset of the first weight loss, which occurs at about 180-190 °C, corresponds to the water physically adsorbed, the experimental weight loss was slightly higher for hyperbranched compared to linear polymer, and could be attributed to the formation of porous structures. At temperatures above 200 °C, where decomposition of PEGMA homopolymer has been reported,[339] two decomposition steps were observed, the second degradation step take place at about 270 °C, and can be ascribed to the loss of PEG side chains, since the experimental weight loss was higher for L2 and H2 (29 and 25 % repectively) compared to L1 and H1 (22 and 21 % respectively) with lower content of OEGMA. The third major decomposition step, which is the most important with experimental weight loss around 57 %, was observed at 315 °C for linear polymers and 324-336 °C for hyperbranched, and could be attributed to the random main chain scission of the poly(methacrylate). From these results, the conclusion can be drawn that thermal stability of hyperbranched slightly increased when compared with the linear structures.

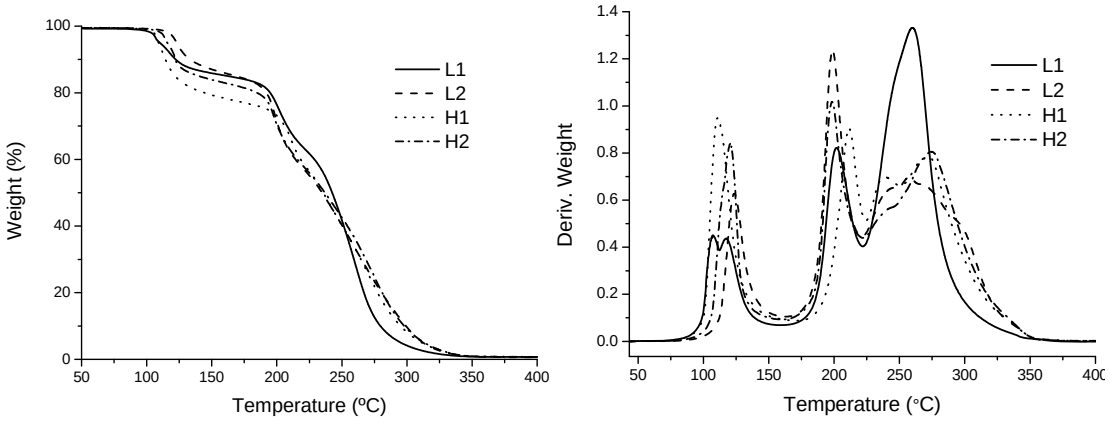

Figure 5.1. TGA curves of the linear and hyperbranched polymers.

It has been proposed that random scission occurs by peroxide degradation at sites which has been preoxidised.[340] While thermogravimetric analysis provides information on the degradation stages at which volatiles are lost, chemiluminescence emission analysis allows to obtain information on the hydroperoxides decomposition. The chemiluminescence in polymers is due to the light emission that accompanies the thermal decomposition of the thermooxidative degradation products (hydroperoxides), which are formed during processing or service life of the material under ambient conditions. This bimolecular reaction promotes ketone products to its lowest triplet state and the radiative deactivation gives chemiluminescence emission in the visible region.[341] Figure 5.2 shows the degradation of polymers under nitrogen and oxygen as measured by temperature-ramping CL. On hyperbranched polymers, no emission of CL was detected at temperatures below 175 °C on inert atmosphere, and enhanced CL intensity was observed for polymer with higher density of grafting points (H2) in the whole range of temperatures. A slight decrease in stability was detected for linear polymers which exhibited lower onset of temperature. For all samples two distinct processes could be detected which may be assigned to formation of hydroperoxides with different stability.

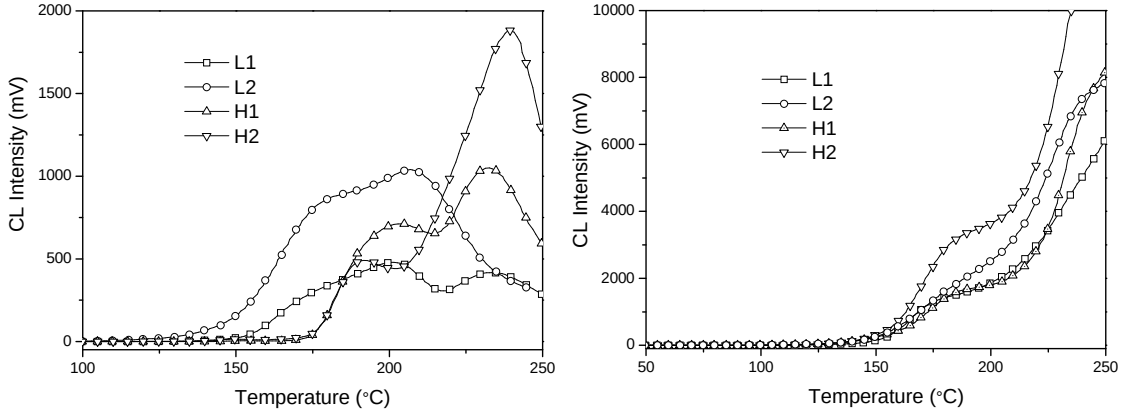

Figure 5.2. Chemiluminescence curves of the polymers; (A) in nitrogen; (B) in oxygen.

Under oxygen the behavior was similar, although a higher intensity of chemiluminescence was observed and the onset of temperature was seen to decrease to lower values, since in such conditions, the samples are highly oxidised in a diffusion-controlled reaction simultaneously to the emission. Macroradicals react with the oxygen to give peroxy radicals and its concentration will be large and the bimolecular termination reaction of two peroxy radicals to give ketone products will be enhanced. Both, TGA and CL analysis, showed the stability of the polymers at temperatures closed to practical use.

Table 5.2. TGA parameters: the onset and the maximum temperature peak of the first, second and third degradation steps, (T_{1max}, T_{2max}, and T_{3max} respectively).

Polymer	T_{onset}	T_{1max} (°C)	T_{2max} (°C)	T_{3max} (°C)
L1	100	117	202	260
L2	112	124	198	258
H1	101	111	212	273
H2	106	120	198	270

LCST study

In this work, the thermoresponsive character of the linear and hyperbranched copolymer has been studied by temperature modulated DSC using TOPEM, which has

been proposed as a new technique to determine the LCST values. In PEGMA polymers, the LCST increase when the number of the ethylene glycol in the side chains increase, also it has been seen that the LCST of the hyperbranched polymers decrease compared with linear polymers with same structure.[334]

In temperature modulated DSC using TOPEM, stochastic temperature modulations are superimposed on the underlying rate of a conventional DSC scan. These modulations consist of temperature pulses, of fixed magnitude and alternating sign, with random durations within limits specified in the experimental conditions, whereas periodic modulation of the heating rate is used in other modulated DSC techniques. The modulation creates high instantaneous heating rates which increases sensitivity. The low underlying constant heating rate is used to get better resolution. Similar experiments using conventional DSC were unsuccessful to determine LCST.

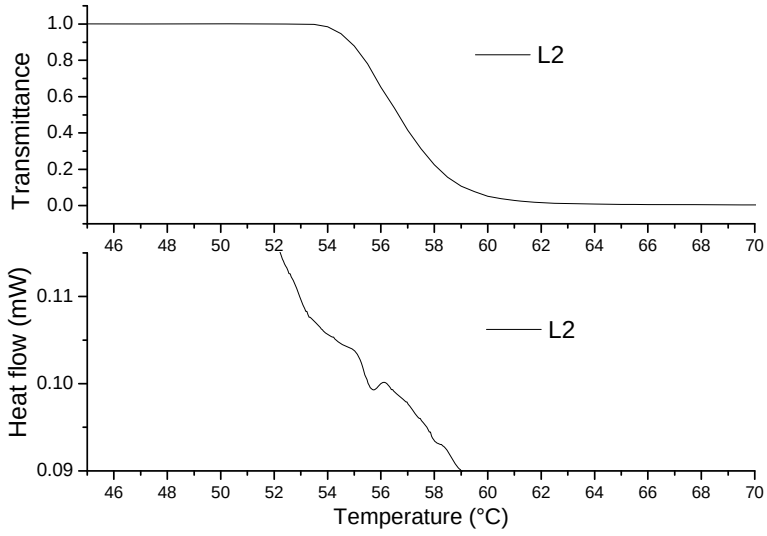

Figure 5.3. LCST measurements of linear and hyperbranched poly(OEGMA-*co*-DEGMA) copolymers: (A) UV-visible turbidimetric experiment at 500 nm of copolymer L2 in water (1 mg/mL) versus temperature; (B) temperature modulated DSC experiment of copolymer L2 versus temperature.

Total heat flow variation curve versus temperature is represented in Figure 5.3 for linear polymer with 20 % content of PEGMA. The temperature at the maxima of the DSC total heatflow curve was identified as the LCST of the polymer. Since the LCST transition is a very quick and low energy process, the parameters for the experiment as well as the parameters for data evaluation were carefully selected. The temperature

underlying rate was 0.25 K min^{-1} which is sufficiently slow to observe the phase transition. The amplitude of temperature pulse was ±0.005 K, small enough so that the sample response remains linear. Another important parameter to take in to account is the calculation window width. In previous works,[337] it is recommend that the window width should be less than one third of the transition interval. As the LCST transition is estimated to occur in 3 minutes the calculation window width used in the evaluation was 30 seconds, which is in concordance with Fraga's et al works.

The LCST values determined by mDSC were on very good agreement with those compared with those obtained by UV-vis. The LCST values obtained by UV-vis were defined as the temperature at which 90 % of the transmittance of the solution was observed. The data are collected together in Table 5.3. The fact that both techniques provide comparable LCST values, point out the reliability of the technique to measure the lower critical solubility temperature of the polymers.

Table 5.3. The LCST values determined by MTDSC for the different copolymers compared with those determined by UV-vis method

Polymer	LCST (MTDSC) (°C)	LCST (UV) (°C)
L1	38.1	38.7
L2	55.7	54.9
H1	38.9	38.4
H2	53.3	51.1

Chromium adsorption

The adsorption of Cr (VI) ions onto the copolymers synthesized have been investigated and the effect of the initial heavy metal ion concentration and temperature of the medium and capacity were analyzed. The effect of initial chromium (VI) ion concentration over the Cr (VI) adsorption by hyperbranched polymer at two different temperatures, below and above LCST, is shown in Figure 5.4. Six different concentration for Cr(VI), 10, 50, 100, 200, 500, 1000 ppm, while maintaining the adsorbent dosage at 5 g/l, were tested in order to determine the amount of chromium adsorbed at equilibrium. The study was done at two different temperatures and it was

observed that adsorption of metal ions onto the polymers below LCST temperature was negligible. It has been described, that the polymers based in ethylene glycol methacrylates adsorb almost no Cr (VI) because there is no reactive functional group in their structure for complexation with this metal ion. The low adsorption of metal ions by copolymers based on polyethylene glycol has been observed[342]. The small adsorption value was explained in terms of weak interaction produced between those ions and the hydroxyl groups on the surface of the beads as result of the diffusion of the small metal ions into the few pores of the beads formed.

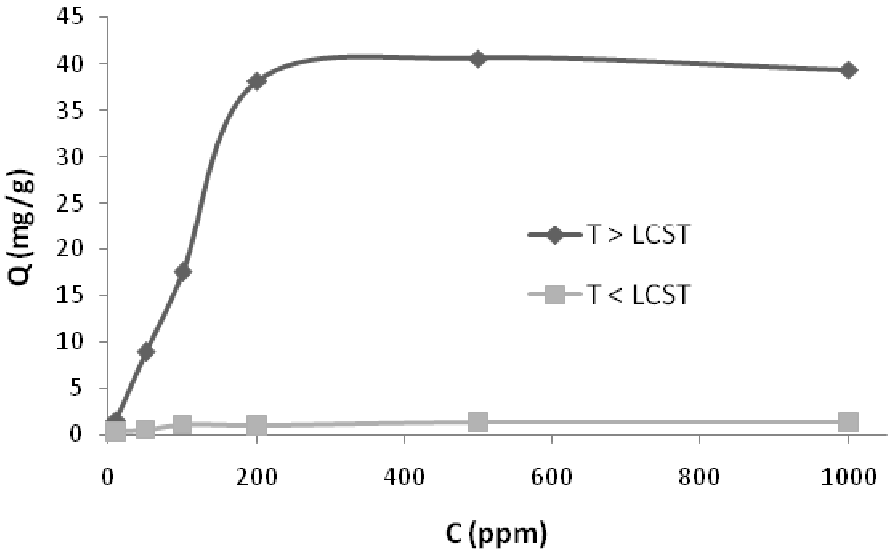

Figure 5.4. Effect of initial Cr(VI) concentration onto polymer H2 at two different temperatures: 35 °C (below LCST) and 60 °C (above LCST).

When the temperature is higher than the LCST it was observed that amount of Cr(VI) adsorbed increase from 1.2 to 40.4 mg/g for copolymer H2. At temperature above the lower critical solution temperature the polymers form aggregates and porous structures may be formed with nanocavities where the metal ions can get into them. Samples for TEM were prepared below and above the LCST (from solutions of 5 mg/mL of hyperbranched). Above the LCST, the TEM images showed well-dispersed and well-defined aggregates (with regular shapes and sizes around 150–200 nm) formed from hyperbranched polymers, while below the LCST, no self-assembled nanoparticles were observed by TEM.

Increasing the initial ion concentration, the system reached the maximum of the adsorption capacity at 200 ppm of metal ion. Above that value, the adsorption capacity remained stable where a saturation value was achieved, and the removal efficiency of chromium (VI) decreased when the adsorbent concentration increased. This reduction of the removal efficiency might be attributed to the fact that the number of ions exceeds the number of accommodation sites, therefore the material become saturated with analytes.

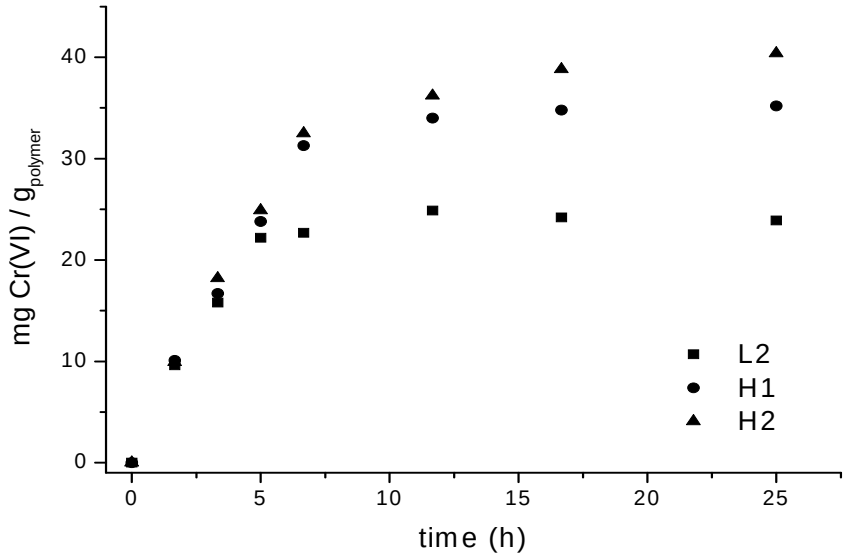

Figure 5.5. Effect of contact time on the removal of hexavalent chromium. Conditions are shown in table 5.4.

Figure 5.5 shows the effect of the contact time, at a temperature above LCST, for the adsorption of chromium (VI) on the polymers. The removal of chromium (VI) increases from the beginning until the seventh hour, showing maximum efficiency achieved at that point. The parameters and adsorption capacities for polymers are shown in Table 5.4. Hyperbranched polymers adsorbed more chromium (VI) than the linear polymer because of the structure of the polymers. Hyperbranched polymers when precipitate form a network with more nanocavities where the chromium can be adsorbed. Also, it is observed that hyperbranched polymer with higher ratio of OEGMA/DEGMA is more efficient as adsorbent and it would be related to the number of long ethylene glycol side chains which may form porous aggregates.

Table 5.4. Parameters and adsorption capacity of hexavalent chromium for samples

Polymer	OEGMA (%)	Concentration Cr(VI) (ppm)	Temperature (°C)	Q (mg/g)
L2	20	200	60	23.9
H1	13	200	45	35.2
H2	24	200	60	40.4

The results obtained showed that these polymers could be used as an effective adsorbent, and have great potential applications in environmental protection. The adsorption capacity of the copolymers is comparable with those obtained by other authors using different systems, 95 mg g^{-1} by *Pseudomonas;*[343] 284 mg g^{-1} by *Aeromonas caviae;*[344] 117 mg g^{-1} with dead biomass of marine Aspergillus niger;[345] 22 mg g^{-1} with almond shell;[346] 77 mg g^{-1} by chitosan beads.[347] Otherwise, at temperatures above the LCST polymer becomes dehydrated and hence insoluble in water thereby it precipitates and form pore structures making them promising as viable absorbents which can be separated from the medium. These copolymers are a new approach for the preparation of metal-chelating matrix, and showed some advantages over conventional preparation techniques, which needed the activation of the matrix for metal-chelating ligand immobilization.

4. Conclusions

In this study, a series of linear and hyperbranched copolymers based in ethylene glycol methacrylate has been synthesized. It was successfully determined its lower critical solution temperature by MTDSC, obtaining similar values than those obtained by UV spectroscopy. The thermal stability of hyperbranched polymers was slightly enhanced respect to linear structures, as it was evidenced by thermogravimetric analysis and chemiluminescence emission. The effect of the LCST transition for linear and hyperbranched polymers on the hexavalent chromium removal from aqueous solution have been investigated. The results show that these polymers at temperature below LCST are useless, and above LCST hyperbranched polymer are more efficient than

linear polymers and the efficiency increase with ratio of OEGMA/DEGMA. The values of chromium captured for hyperbranched are close to 40 mg per gram of polymer, which means that these polymers could be used as an effective adsorbent, which can be separated from the medium.

5. Acknowledgements

The authors would like to thank the Plan Nacional I+D+I (Ministerio de Ciencia e Innovación) for financial support (MAT2009-09671). M. Luzon would like to thank the fellowship to MICINN.

6. References

(300) Park, D.; Yun, Y.-S.; Yim, K. H.; Park, J. M. *Bioresource Technology* **2006**, *97* 1592.

(301) Murphy, V.; Hughes, H.; McLoughlin, P. *Chemosphere* **2008**, *70* 1128.

(302) Prabhakaran, S. K.; Vijayaraghavan, K.; Balasubramanian, R. *Ind. Eng. Chem. Res.* **2009**, *48*, 2113.

(303) *Chromium(VI) Handbook, CRC Press, New York*; Jacobs, J. A.; Testa, S. M.; in: J. Guertin, J. A. J., C.P.Avakian (Eds), Eds., 2004.

(304) *Prevention and Determination of Cr(VI) in Leather, United Nations Industrial Development Organization*; Hauber, C., Ed., 2000.

(305) *Materials and Process in Manufacturing 9th Ed., Wiley, New York*; Paul, D. E.; Black, J. T.; Kohser, A. R., Eds., 2003.

(306) Costa, M. *Toxicology and Applied Pharmacology* **2003**, *188*, 1.

(307) Tsapakos, M. J.; Hampton, T. H.; Wetterhahn, K. E. *Cancer Res.* **1983**, *43*, 5662.

(308) Kongsricharoern, N.; Polprasert, C. *Water Science and Technology* **1996**, *34*, 109.

(309) Garbisu, C.; Alkorta, I. *Bioresource Technology* **2001**, *77*, 229.

(310) Mousavi Rad, S. A.; Mirbagheri, S. A.; Mohammadi, T. *World Academy of Science, Engineering and Technology* **2009**, *57* 348.

(311) Ghosh, G.; Bhattacharya, P. K. *Chemical Engineering Journal* **2006**, *119* 45.

(312) Aksu, Z.; Özer, D.; Ekiz, H. I.; Kutsal, T.; Çaglar, A. *Environ. Technol.* **1996**, *17*, 215.

(313) Levankumar, L.; Muthukumaran, V.; Gobinath, M. B. *Journal of Hazardous Materials* **2009**, *161*, 709.

(314) Garg, U. K.; Kaur, M. P.; Sud, D.; Garg, V. K. *Desalination* **2009**, *249*, 475.

(315) Gupta, V. K.; Rastogi, A.; Nayak, A. *Journal of Colloid and Interface Science* **2010**, *342*, 135.

(316) Narayanan, N. V.; Ganesan, M. *Journal of Hazardous Materials* **2009**, *161*, 575.

(317) Neagu, V.; Mikhalovsky, S. *Journal of Hazardous Materials* **2010**, *183*, 533.

(318) Hu, J.; Zhong, L.; Song, W.; L., W. *Advanced Material* **2008**, *20*, 2977.

(319) Salih, B.; Denizli, A.; Kavakli, C.; Say, R.; E., P. *Talanta* **1998**, *46*, 1205.

(320) Mohan, D.; Pittman, C. U. *Journal of Hazardous Materials* **2006**, *137*, 762.

(321) Oliveira, L. C. A.; Petkowicz, D. I.; Smaniotto, A.; Pergher, S. B. C. *Water Research* **2004**, *38*, 3699.

(322) Booker, N. A.; Keir, D.; Priestley, A. J.; Sudarmana, D. L.; Woods, M. A. *Water Science and Technology* **1991**, *23*, 1703.

(323) Orbell, J. D.; Godhino, L.; Bigger, S.; Nguyen, T. M.; Ngeh, L. N. *J. Chem. Educ.* **1997**, *74*, 1446.

(324) Hua, X.; Wangc, J.; Liu, Y.; Li, X.; Zenga, G.; Bao, Z.; Zeng, X.; Chen, A.; Long, F. *J. Hazard. Mater.* **2011**, *185*, 306.

(325) Zhang, W. *J. Nanopart. Res.* **2003**, *5*, 323.

(326) Larraza I; López-Gónzalez M; Corrales T; G., M. *J. Colloid. Interf. Sci.* **2012**, *385*, 24.

(327) Ghoul, M.; Bacquet, M.; Morcellet, M. *Water Research* **2003**, *37*, 729.

(328) Liu, M.; Zhang, H.; Zhang, X.; Deng, U.; Liu, W.; Zhan, H. *Water Research* **2001**, *73*, 322.

(329) Kobya, M. *Bioresource Technology* **2004**, *91*, 317.

(330) Lutz, J. F.; Akdemir O.; Hoth A. *J. Am. Chem. Soc.* **2006**, *128*, 13046.

(331) Lutz, J.-F.; Andrieu, J.; Uzgun, S.; Rudolph, C.; Agarwal, S. *Macromolecules* **2007**, *40*, 8540.

(332) Lutz, J. F. *J. Polym. Sci. Part A: Polym. Chem.* **2008**, *46*, 3459.

(333) Corrales, T.; Catalina, F.; Peinado, C.; Allen, N. S.; Fontan, E. *Journal of Photochemistry and Photobiology A: Chemistry* **2002**, *147*, 213.

(334) Luzon, M.; Boyer, C.; Peinado, C.; Corrales, T.; Whittaker, M.; Tao, L.; Davis, T. P. *Journal of Polymer Science: Part A: Polymer Chemistry* **2010**, *48*, 2783.

(335) Gill, P. S.; Sauerbrunn, S. R.; Crowe, B. S. *J. Thermal Analysis and Calorimetry* **1992**, *38*, 255.

(336) Liu, X.; Cheng, F.; Liu, H.; Chen, Y. *Soft Matter* **2008**, *4*, 1991.

(337) Fraga, I.; Montserrat, S.; Hutchinson, J. M. *J. Thermal Analysis and Calorimetry* **2007**, *87*, 119.

(338) APHA, A., WPCF **1989**, 3.

(339) Chen, Y.; Chen, L.; Wang, X.; He, X. *Macromolecular Chemistry and Physics* **2005**, *206*, 2483.

(340) García, N.; Corrales, T.; Guzmán, J.; Tiemblo, P. *Polymer Degradation and Stability* **2007**, *92*, 635.

(341) Billingham, N. C.; Then, E. T. H.; Gijsman, P. J. *Polymer Degradation and Stability* **1991**, *34*, 263.

(342) Duran, A.; Soylak, M.; Tuncel, S. A. *Journal of Hazardous Materials* **2008**, *155* 114.

(343) Ziagova, M.; Dimitriadis, G.; Aslanidou, D.; Papaioannou, X.; Tzannetaki, E. L.; Liakopoulou-Kyriakides, M. *Bioresource Technology* **2007**, *98* 2859.

(344) Loukidou, M. X.; Karapantsios, T. D.; Zouboulis, A. I.; Matis, K. A. *Ind. Eng. Chem. Res.* **2004**, *43*, 1748.

(345) Khambhaty, Y.; Mody, K.; Basha, S.; Jha, B. *Chemical Engineering Journal* **2009**, *145* 489.

(346) Agarwal, G. S.; Bhuptawat, H. K.; Chaudhari, S. *Bioresource Technology* **2006**, *97* 949.

(347) Wan Ngah, W. S.; Kamari, A.; Fatinathan, S.; Ng, P. W. *Adsorption* **2006**, *12*, 249.

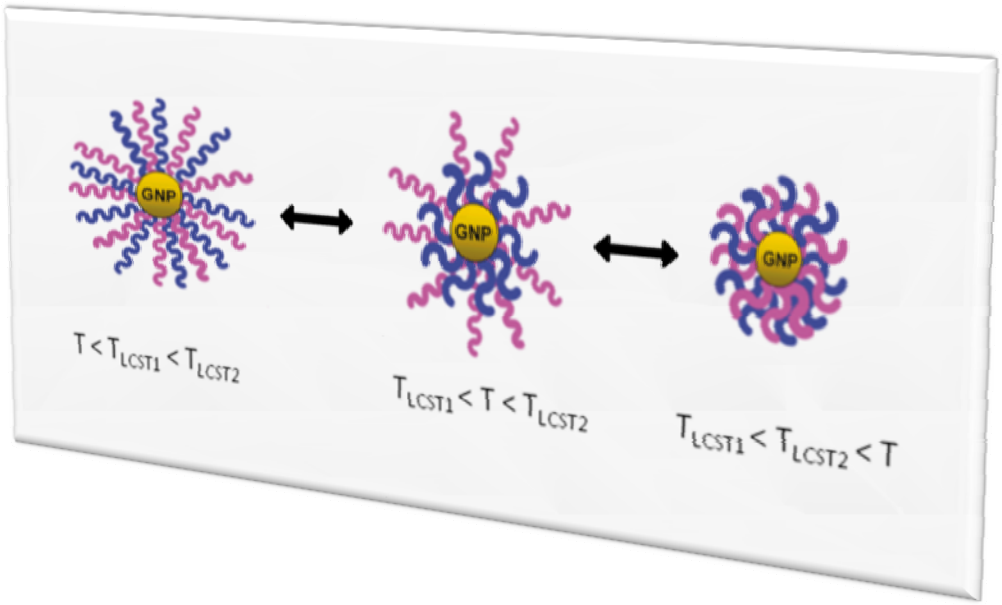

Design and Synthesis of Dual Thermo-Responsive and Anti- Fouling Hybrid Polymer/Gold Nanoparticles

Chapter 6

Published in
Macromolecules

Design and Synthesis of Dual Thermo-Responsive and Anti- Fouling Hybrid Polymer/Gold Nanoparticles

Cyrille Boyer[a], Michael R Whittaker[a], Mario Luzon[b], Thomas P. Davis[a]

Abstract. A new class of thermosensitive copoly(oligoethylene oxide) acrylates with narrow polydispersities were prepared by the copolymerization of oligo(ethylene oxide) acrylate and di(ethylene oxide) ethyl ether acrylate using reversible addition-fragmentation chain transfer polymerization (RAFT). These copolymers exhibit tunable LCST behavior over the range of 15 °C to 90 °C dependent on their compositions. Subsequently, these copolymers were grafted onto gold nanoparticle (GNP) surfaces yielding "smart" thermosensitive gold nanoparticles. The thermoresponsive properties of these hybrid GNPs/poly(OEG-A-*co*-DEG-A) nanoparticles were evaluated in solution using dynamic light scattering and UV-visible spectroscopy. In addition, the susceptibility of these GNPs to protein fouling was assessed by a Bradford's assay, and found to be significantly reduced by the copolymer stabilizing layer. We also demonstrate, in a unique one-pot assembly process, the synthesis of a hybrid nanoparticle that shows dual temperature responsiveness. These hybrid nanoparticles open new applications in biotechnology and medicine.

[a]Centre for Advanced Macromolecular Design (CAMD), School of Chemical Sciences and Engineering, The University of New South Wales, Sydney, NSW 2052, Australia. E-mail: t.davis@unsw.edu.au
[b]Instituto de Ciencia y Tecnología de Polímeros, C.S.I.C. ; C/ Juan de la Cierva 3, 28006 Madrid, Spain

1. Introduction

Thermoresponsive and functional gold nanoparticles[348] (GNP) have received considerable interest for applications in a diverse range of areas embracing biotechnology,[349-362] nanotechnology,[363-366] and catalysis.[367-371] Their unique optical and scattering properties combined with a pre-engineered ability to respond predictably to their environment in solution confers interesting attributes for use as targeted vectors for drug/gene delivery[359,372-375] and contrast agents.[349,352,376-379] To impart desirable thermoresponsive properties and to improve their stabilities in solution, an appropriate functional/responsive polymer layer can be grafted to these GNPs using either the grafting "from"[380-385] or "to"[386-388] approaches. The "pros" and "cons" of both these methods have been widely discussed.[389,390] Recent work has shown that well-defined polymers synthesized via RAFT polymerization can bind inherently to gold making the 'grafting to' method particularly attractive and versatile. This was demonstrated for the first time by McCormick, Lowe and Sumerlin et al.[386,391-394], and later by other teams.[395-398] These RAFT derived polymers have inherent gold binding abilities originating from the RAFT end-groups (typically di- and tri- thio compounds) (Figure 6.1).[399-402] In addition, RAFT end-group functionality can be transformed easily to the established gold-binding functionality of thiol. (Figure 6.1).[403-406]

In such applications as targeted drug/gene delivery and imaging agents, these nanoparticles must not only show targeted or "smart" behavior, but it is also important that they evade the reticuloendothiel system (RES).[407] It is this system that is responsible for the rapid clearance of these particles from the body. In the above applications the blood circulation time is critical for their success. However, the incorporation of a smart polymer layer often enhances protein absorption and specific biomolecular tagging processes, leading to faster clearance times of nanoparticles from the body. To circumvent this problem PEGylation, has been a common strategy employed to increase the blood residence time of not only nanoparticles,[408-411] but a diverse range of therapeutic molecules.[412-415] PEGylation while providing "stealth" characteristics fails to impart any "smart" behavior to the nanoparticles and hence limits their application in these newer technologies.

Previously, several authors have coated GNPs with thermosensitive polymers, [416-420] thereby conferring new properties. Conventionally, the favored thermosensitive polymer has been poly(N-isopropylacrylamide) (PNIPAAm). [416-420] PNIPAAm has a lower critical solution temperature (LCST) of 31-32 °C in water. [421-423] However, the grafting of PNIPAAm on GNPs suffers from some limitations: (i) PNIPAAm presents only one fixed LCST; (ii) the presence of amide groups on the GNP surface can induce protein adsorption leading to fast clearance rates from the body. To improve the potential of PNIPAAm, different authors have attempted to tune the thermoresponsive behaviour of PNIPAAm by copolymerization with a pH-sensitive monomer[424-426] or by the addition of hydrophilic/hydrophobic monomers such acrylamide[427] during the polymerization. In addition, the use of block copolymers of PNIPAAm with PEG has been explored, with the block lengths used as a design tool for tuning the LCST behavior.[428,429] Moreover, antifouling properties can be controlled using the LCST of the PNIPAAm block.[430,431]

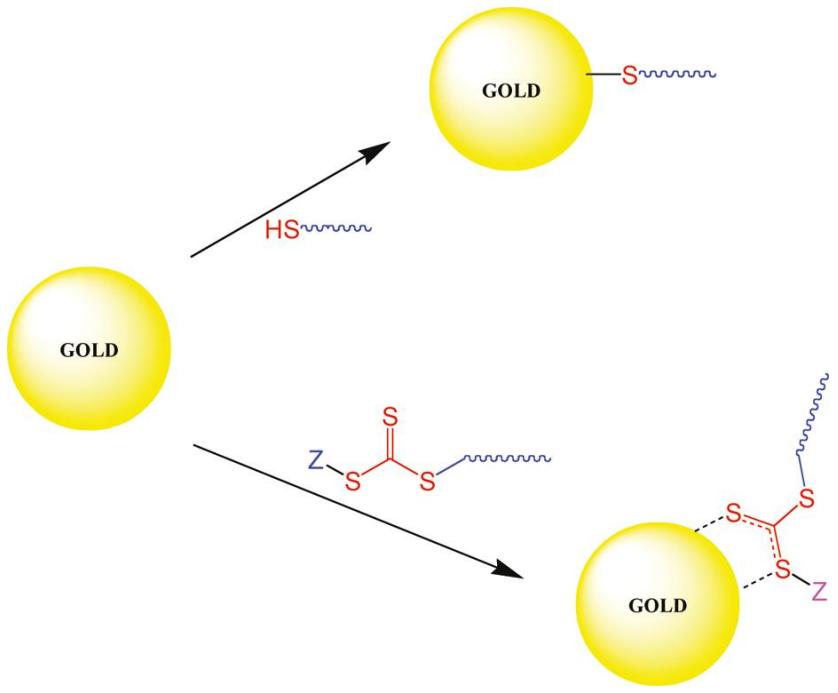

Figure 6.1. Schematic Representation of the Interaction Gold-Thiol Polymers and Gold-Trithiocarbonate Polymers

Recently, a new class of polymers combining temperature responsiveness and anti-fouling/stealth behavior has been reported. These macromolecules, based on

copolymers of di(ethylene glycol) ethyl ether acrylate (DEG-A) and oligoethylene glycol acrylate (OEG-A) are analogues of PEG.[432-434] These copolymers present tunable thermo-responsive behavior and additional properties such as biocompatibility, protein adsorption resistance and stealth-like behavior (analogous with PEG).[411,435]

Herein, we report the RAFT synthesis of this new class of thermosensitive PEG based polymers and their novel use in the "grafting-to" formation of GNP/polymer hybrid nanoparticles. Using this technique, copolymers of poly(OEG-acrylate) and di(ethylene glycol) ethyl ether acrylate were prepared having LCST values ranging from 15 to 90 °C. These copolymers were grafted onto GNP surfaces yielding thermosensitive gold nanoparticles. The hybrid GNPs/copolymer nanoparticles possess similar temperature responsive properties to established gold/PNIPAAm particles, but more importantly have additional properties that make them more suitable for use in bio-applications. The presence of a poly(OEG-A-*co*-DEG-A) layer confers an anti-fouling surface on the GNPs, resistant to protein adsorption, thereby imparting stealth-like abilities to the nanoparticles. To our knowledge, it is the first time GNPs have been coated with a polymer coating imbuing thermoresponsive behavior, anti-fouling and stealth properties.

2. Experimental Part

Materials

Oligoethylene glycol acrylate (OEG-A) (1, number average molecular weight M_n = 450 g/mol, PDI = 1.02) and di(ethylene glycol) ethyl ether acrylate (2) were purified via an alumina column to remove the inhibitor prior to use. N-isopropylacrylamide (NIPAAm) (Aldrich, 99%) was crystallized twice from hexane prior to use. 2,2'-Azobisisobutyronitrile (AIBN) was purchased from Wako Chemicals and was crystallized twice from methanol prior to use. Hydrogenotetrachloroaurate (III) hydrate ($HAuCl_4$, 99.9%, Aldrich), trisodium citrate dehydrate (99%, Aldrich), bovine serum albumin (BSA, 99%, Aldrich) and pyrene (99.9%, Fluka) were used as received. Deionized water used for these experiments were purified by MILIQ system with a resitivity of 17.9 mΩ/cm.

Analytical Techniques

Size Exclusion Chromatography (SEC). Aqueous size exclusion chromatography (SEC) was implemented using a Shimadzu modular system comprising a DGU-12A solvent degasser, a LC-10AT pump, a CTO-10 A column oven, and a RID-10A refractive index detector and SPD-10A Shimadzu U.V. Vis. detector (flow rate: 1 ml/min). The column was equipped with a PL 5.0 mm bead-size guard column (50 × 7.8 mm^2) followed by three PL aquagel-OH columns (50, 40, 30; 8μm). Calibration was performed with PEO standards ranging from 500 to 500,000 g/mol. SEC analyses of the polymers were also performed in N,N-dimethylacetamide [DMAc; 0.03% w/v LiBr, 0.05% 2, 6–di-Butyl-4-methylphenol (BHT)] at 50 °C (flow rate = 1 mL/min) using a Shimadzu modular system comprising an SIL-10AD auto-injector, a PL 5.0-mm bead-size guard column (50 × 7.8 mm) followed by four linear PL (Styragel) columns (105, 104, 103, and 500Å) and an RID-10A differential refractive-index detector and in tetrahydrofuran (THF) at 40 °C (flow rate = 1 mL/min) using a Shimadzu modular system comprising an SIL-10AD auto-injector, a PL 5.0-mm bead-size guard column (50 × 7.8 mm) followed by four linear PL (Styragel) columns (105, 104, 103, and 100 Å). Calibration was achieved with commercial polystyrene standards ranging from 500 to 106 g/mol.

UV-vis Spectroscopy. UV-vis spectra were recorded using a CARY 300 spectrophotometer (Bruker) equipped with a temperature controller.

NMR Spectroscopy. ^{1}H and ^{13}C NMR spectra were recorded on a Bruker ACF300 (300 MHz) or ACF500 (500 MHz) spectrometer, with D_2O or $CDCl_3$ used as solvents. NIPAAm monomer conversion was determined by comparing the vinyl proton signal (δ ≈ 5.4-6.3, 3H/mol NIPAAm monomer) to the total isopropyl methylene signal (δ ≈ 3.6- 3.85 1H/mol NIPAAm).

Infrared Spectroscopy. FT-IR spectra were obtained using a Bruker Spectrum BX FT-IR system using diffuse reflectance sampling accessories and a resolution of 2 cm^{-1}. Each sample was analyzed using 128 scans.

Dynamic light scattering (DLS) and zeta-potential. Dynamic light scattering studies of the GNPs at 5 mg/mL in an aqueous were conducted using a Malvern Instruments Zetasizer Nano ZS instrument equipped with a 4 mV He-Ne laser operating at λ = 633 nm, an avalanche photodiode detector with high quantum efficiency, and an ALV/LSE-5003 multiple tau digital correlator electronics system.

Microscopies. TEM and AFM. The sizes and morphologies of the nanoparticles were observed using a transmission electron microscopy JEOL1400 TEM at an accelerating voltage of 100 kV. The particles were dispersed in water (1 mg/mL) and deposited onto 200 mesh, holey film, copper grid (ProSciTech).

For the preparation of samples above the LCST, the solution was heated to $T > T_{LCST}$ and at the same time, a copper grid was also equilibrated at this temperature. A few drops of the heated nanoparticles solution were then, placed on the copper grid and dried in the oven ($T > T_{LCST}$).

For atomic force microscopy (AFM), GNP solutions (200 µL) were deposited on a mica surface and dried at temperatures below or above the LCST. The sample was characterized by AFM (Digital Instruments 3000 AFM) in tapping mode.

Methods

LCST Measurement. The lower critical solution temperature, LCST was determined by a UV-vis spectrophotometer at 500 nm. The polymer concentrations were 0.2 mg/ml (0.2 % wt) in water with a heating rate of 1 °C/min. The temperature at which 10 % of the maximum absorbance of the solution was observed was defined as the LCST.

Determination of particle size. GNPs (or GNPs/polymer) solutions were prepared in distilled water with GNPs concentration of 5 mg/mL. The solution was filtered trough Millipore nylon filters (pore size 0.45 µm) to eliminate dust and large contaminants. The size measurements were carried out in quartz cuvette and the temperature was allowed to equilibrate for 5 mins. For the determination of size vs. temperature the heating rate was 1 °C/min.

Syntheses

Synthesis of gold nanoparticles. Citrate-stabilized gold nanoparticles (20 nm) were prepared using published procedures.[436] Briefly, all glassware was first washed with an aqua-regia solution (25 % nitric acid and 75 % of concentrated hydrochloric acid), then rinsed with MilliQ water several times and dried. MilliQ water (100 mL) and 1 % solution trisodium citrtate dehydrate (5 mL, 1.053 g of trisodium citrtate) were mixed. The solution was heated up to boiling point with vigorous stirring and then hydrogenotetrachloroaurate (III) hydrate stock solution (0.01 M) (2.54 mL) was introduced rapidly using a syringe. The solution was boiled for a further 30 minutes

with vigorous stirring. A progressive change of color was observed from yellow to wine-red. The solution was cooled down and stored in a fridge at 5 °C until required. The particles were characterized by TEM and DLS.

Synthesis of RAFT agents. The syntheses of 3-(benzylsulfanylthiocarbonylsulfanyl)-propionic acid (3, BSPA) is described elsewhere.[406]

RAFT polymerizations

RAFT polymerization of N-isopropyl acrylamide (NIPAAm) in the presence of 3-(benzylsulfanylthiocarbonylsulfanyl)-propionic acid (BSPA). An example of polymerization of NIPAAm is given for $[NIPAAm]_0/[CTA]0/[AIBN]_0 = 250/1/0.2$. NIPAAm (1.13 g, 0.01 mol), 3- (benzylsulfanylthiocarbonylsulfanyl)-propionic acid (10 mg, 3.64×10^{-5} mol), AIBN (1.2 mg. 7.3×10^{-6} mol) and acetonitrile (10 mL) were mixed. The solution was cooled in an ice bath and purged nitrogen for 30 min before heating to 65 °C. After 5 hours, the solution was partially evaporated under vacuum, and the polymer was precipitated in cold diethyl ether (at 0 °C). The precipitation was repeated twice more to remove any unreacted monomer or residual RAFT agent. The product was dried in vacuo to yield a yellow powder.

RAFT polymerization of di(ethylene glycol) ethyl ether (DEG-A) in the presence of 3-(benzylsulfanylthiocarbonylsulfanyl)-propionic acid (BSPA). An example of polymerization of DEG-A is given for $[DEG\text{-}A]_0/[CTA]0/[AIBN]_0 = 150.0/1.0/0.2$. DEG-A (1.88 g, 0.01 mol), 3- (benzylsulfanylthiocarbonylsulfanyl)-propionic acid (30 mg, 3.64×10^{-5} mol), AIBN (2.0 mg. 1.22×10^{-5} mol) and acetonitrile (10 mL) were mixed. The solution was cooled in an ice bath and purged with nitrogen for 30 min before heating to 60 °C. After 5 hours, the solution was partially evaporated under vacuum, and the polymer was precipitated in cold diethyl ether (at 0 °C) yielding a viscous yellow product. The precipitation was repeated twice more to remove any unreacted monomer or residual RAFT agent. The product was dried in vacuo to yield a yellow viscous product. A similar process was repeated for all the polymerizations with OEG-A and the copolymerization with OEG-A and DEG-A.

Grafting of polymer "to" GNPs.

A stirred GNP solution (10 mL of 1 mg/mL previously obtained) was placed in an ice bath under for 30 mins. Cooled polymer solution (1 mL concentration: 30 mg/L) was

added to the GNP solution, followed by stirring for 30 mins. Then, the GNPs were purified by centrifugation at 20 000 rpm, for 30 mins at 5 °C followed by re-suspension in cooled water. This process was repeated 3 times.

GNPs/polymer nanoparticles were stored in solution (10 mg/mL) or freeze dried. After freeze drying the hybrid GNP/polymer nanoparticles could be redispersed easily in water (in contrast to GNPs with no polymer coating).

Protein adsorption

GNP/polymer nanoparticles (1.0 mg/mL) prepared above were suspended in aqueous solution with bovine serum albumin (BSA) at an initial concentration of 1 mg/mL (pH = 6.5). The samples were shaken at room temperature for 3 h to reach adsorption equilibrium. GNPs were removed by centrifugation and the supernatant was analyzed for BSA. The supernatant BSA concentrations were determined via the Bradford method[437] using a UV-Visible spectrometer (Varian Cary 300 scan). An aliquot of the supernatant (10 µL) was then added to Bradford's reactant (3 mL), and mixed for 2 minutes at room temperature (the solution becomes blue). The concentration of BSA was measured by absorption at 595 nm. The test was repeated three times for each sample. The average of the replicate measurements was taken to determine the BSA concentration at equilibrium. The amount of BSA adsorbed was calculated by difference from a reference solution (solution treated using the same method but without gold nanoparticles).

$$\%\text{-BSA}_{\text{adsor}} = 100 - (([\text{BSA}]_{\text{eq}}./[\text{BSA}]_0) \times 100)$$

Where $[\text{BSA}]_0$ and $[\text{BSA}]_{\text{eq}}$. correspond to BSA concentrations measured by Bradford's assay without GNPs and BSA concentrations in the presence of GNPs at equilibrium, respectively.

Fluorescence measurements

GNPs/[poly(DEG-A)/poly(OEG-A-*co*-DEG-A) = 50/50 wt %] (5 mL, 1 mg/mL) were mixed with pyrene/acetone solution (50 µL) (10^{-4} M) overnight at 5 °C. GNP solution (2 mL) was charged to a 1.0 cm square quartz cell. The solution was carefully heated from 5 to 40 °C (at a heating rate of 0.5 °C/min) under analysis using a fluorescence spectrophotometer (Varian Fluorescence Spectrophotometer) at an excitation wavelength of 335 nm.

3. Results and Discussion

The synthesis of different poly(OEG-A-*co*-DEG-A) compositions was achieved by RAFT polymerization using 3-(benzylsulfanylthiocarbonylsulfanyl)-propionic acid (BSPA, 3) as the RAFT agent and AIBN as the initiator (scheme 6.1). A summary of the different copolymers obtained and their characteristics are given in Table 6.1. Copolymer compositions were determined via ^{1}H NMR using the characteristic peak at 1.1 ppm from CH_3 of DEG-A and at 3.6 ppm from $–OCH_2$- of the OEG chain. The feed ratios and the compositions of the copolymers were found to be close, indicating that these two monomers have similar reactivity in the RAFT mediated copolymerization reaction. Moreover, accord between the targeted and experimental molecular weights, and the attainment of narrow polydispersities (PDIs below 1.2) for all the copolymers indicates effective RAFT control.

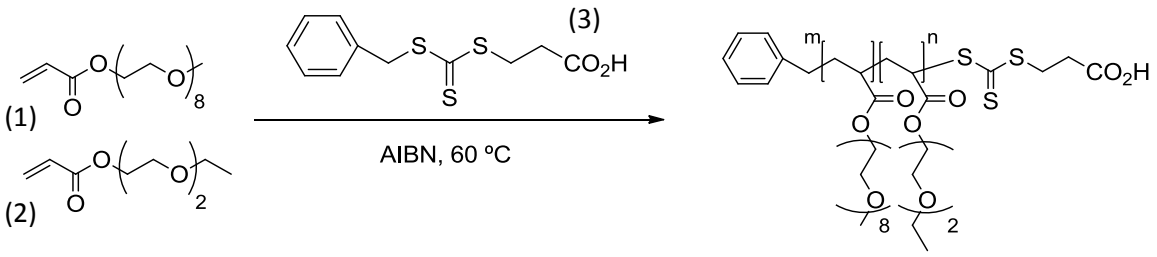

Scheme 6.1. Copolymerization of Oligo(ethylene glycol) Acrylate (1) and Di(ethylene glycol) Acrylate (2) Using 3- Benzylsulfanylthiocarbonylsulfanyl) propionic Acid (BSPA, 3)

The maintenance of the RAFT end-groups (after purification), an essential factor for the subsequent modification of the GNPs, was confirmed by UV-visible spectroscopy using the characteristic absorbance peak at 305 nm of the trithiocarbonate end-group and the following equation: $f^{RAFT} = 100 \times [Abs^{305\ nm} / \varepsilon^{RAFT}]/[polymer]_0$, where $Abs^{305\ nm}$, ε^{RAFT} and $[polymer]_0$ corresponding to the absorbance of RAFT agent , extinction coefficient and polymer concentration, respectively. All the characterized copolymers had RAFT end-group functionality greater than 85%.

Table 6.1. A summary of polymers and copolymers used in this study.

	feed ratio (mol %)		composition[a] (mol %)				
entry	OEG-A	DEG-A	OEG-A	DEG-A	M_n[b] (g/mol)	PDI[b]	T(LCST)[c] (°C)
1	0	100	0	100	21 500	1.23	1
2	5	95	6	94	22 200	1.26	22
3	10	90	10	90	20 300	1.22	33
4	15	85	16	84	18 600	1.24	45
5	20	80	20	80	22 300	1.22	50
6	25	75	26	74	21 400	1.25	58
7	30	70	29	61	18 500	1.24	65
8	50	50	45	55	20 500	1.26	72
9	100	0	0	100	21 200	1.24	92

[a]Determined by ^1H NMR. [b]Assessed by DMAc GPC (poly(styrene) calibration). [c]LCST assessed by turbidity measurement at 500 nm assessed by UV-vis measurement.

The water LCST behavior of these different copolymers (1 mg/mL) was determined by turbidity measurements (at λ = 500 nm) as a function of temperature. Poly(DEG-A) was found to have a LCST of 15 °C, while poly(OEG-A) has an LCST close to 90 °C (Figure 6.2.A). These LCST values are consistent with previously published work.[438] Increasing the concentration of the DEG-A monomer in the copolymer chain decreases the LCST and allows the synthesis of copolymers with LCST ranging from 15 to 90 °C (Table 6.1). A small hysteresis (≈ 5 °C) effect was observed between the heating and cooling cycles (Figure 6.2.B). When the heating-cooling cycles were repeated several times there was no significant shift in either the LCST or the measured absorbance during these cycles (Figure 6.2.C). It is noteworthy, that the polymer chain-length control exerted by RAFT polymerization results in an improved thermo-sensitivity response of these copolymers when compared to chains synthesized by conventional free radical polymerization. Indeed, the presence of a broad distribution of chain lengths in the case of free radical polymerization results in a broader LCST transition when heated and a larger hysteresis effect on cooling. This result is in accord with the ATRP results given by Lutz and coworker[433] for similar copolymers.

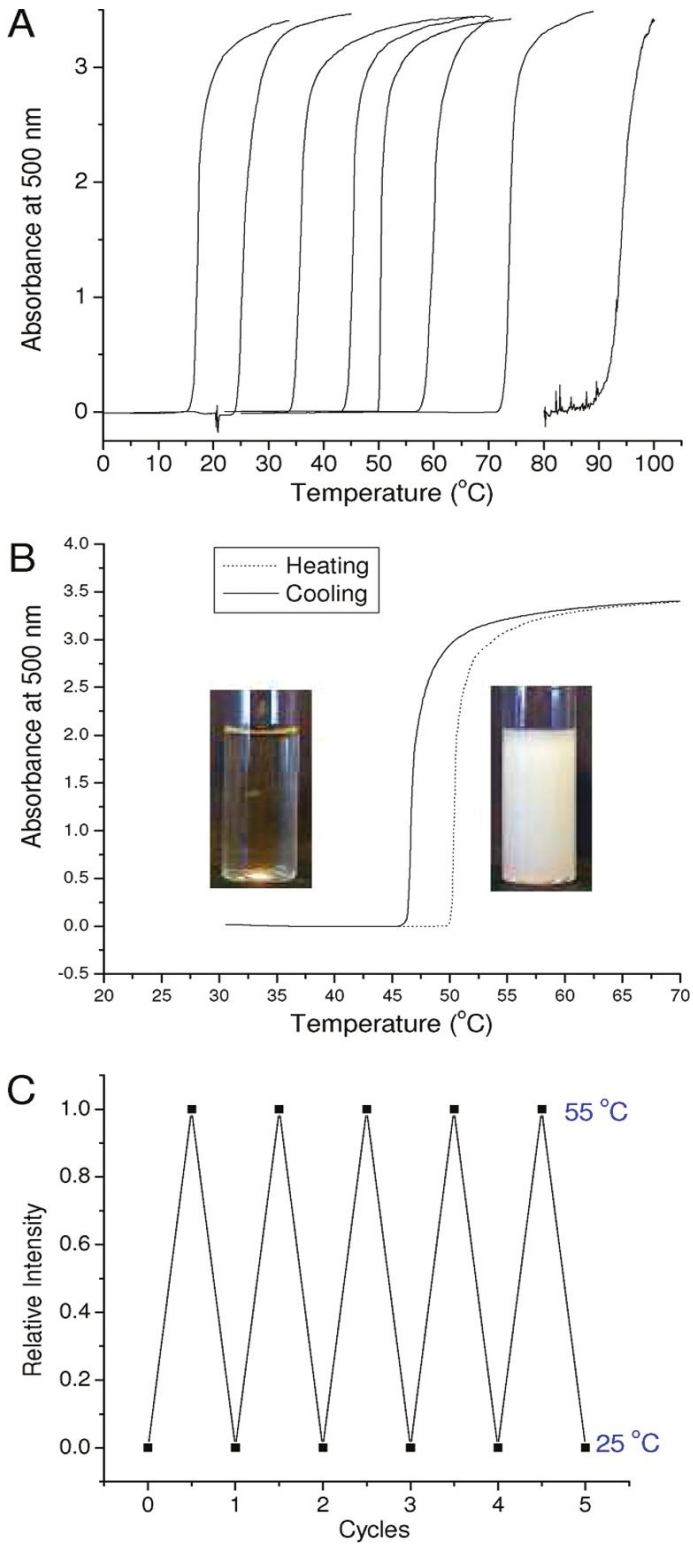

Figure 6.2. Thermal properties for the copolymers obtained by RAFT polymerizations. A- UV-visible turbidity measurement of copoly[(OEG-A)-*co*-(DEG-A)] (left to right: entry 1 to 9 of Table 6.1) for the heating cycle, B- UV-visible turbidity measurement of copoly[(OEG-A)-*co*-(DEG-A)] (run 4 of Table 6.1) for the heating and cooling cycle, inset: picture of solution below and above the LCST, C- Relative intensity of copoly[(OEG-A)-*co*-(DEG-A)] for several cycles.

Highly uniform gold nanoparticles (GNP) were synthesized via the established citrate reduction method[436] (reduction of $HAuCl_4$ by boiling with sodium citrate) to yield spherical gold nanoparticles with a diameter close to 20 nm as observed by transmittance electronic microscope (TEM) and by dynamic light scattering (DLS). GNP size can be tuned from 10 to 150 nm using our approach; smaller sizes can obtained using other techniques.[439] In the present case, we selected a size around 20nmasmodel (commonly used in the literature), [440-442] as these GNPs can be purified easily using centrifugation techniques. Indeed, smaller GNPs can be difficult to purify by centrifugation, while bigger GNPs typically show broader size distributions. However, the approach described in this paper for the coating of 20 nm nanoparticles could be applied easily to both larger and smaller GNP sizes.

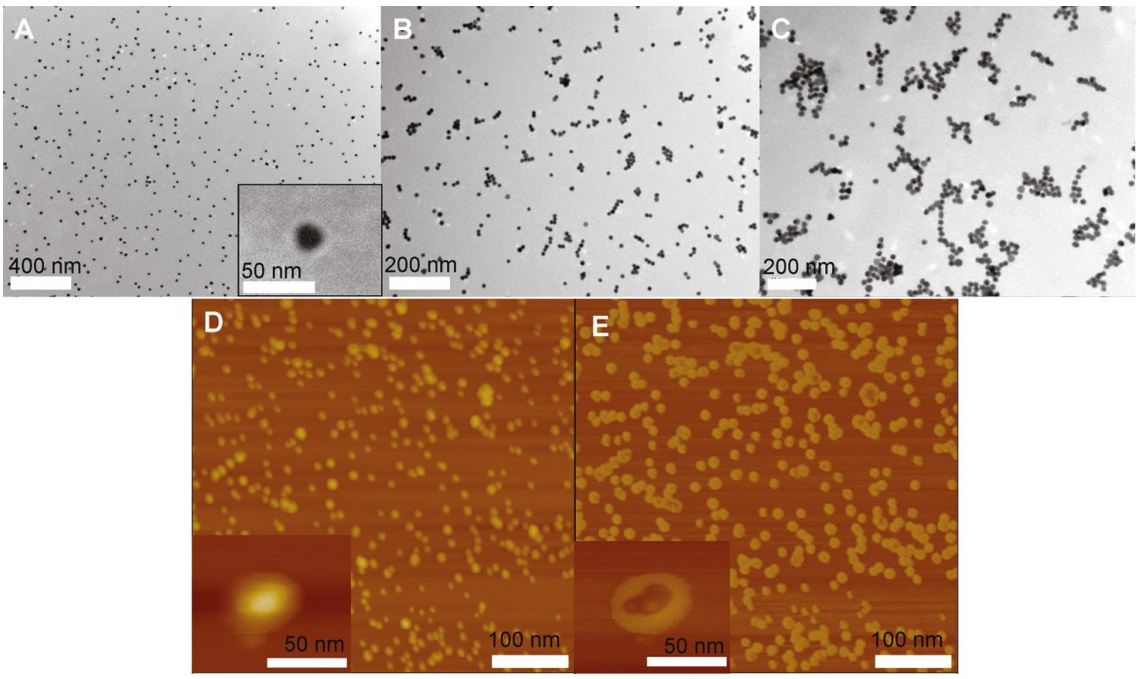

Figure 6.3. TEM and AFM pictures of GNPs/poly(DEG-*co*-OEG-A) (entry 3). (A) at 25 °C, inset: particle with phosphotungsten acid as contrast agent, (B) at 30 °C and (C) at 35 °C; (D,E) AFM pictures of GNPs/poly(DEG-*co*-OEG-A), (D) contact and (E) phase.

RAFT functionalized copoly(DEG-*co*-OEG) in aqueous solution was mixed with the GNPs and the strong affinity of the trithiocarbonate functionality for the gold surface resulted in the assembly of polymers onto the gold surface.[401] After polymer attachment, the solution undergoes a slight color change, accompanied by a blue-shift

(typically, 5-10 nm) of the characteristic Plasmon resonance absorption peak at 525 nm. Extraneous non-grafted copolymer chains were removed by repeated washing/centrifugation cycles with ultrapure water. The purified gold/polymer hybrid nanoparticles were finally re-dispersed in water. It was found that the attached polymer shell was imperative for GNP re-dispersal in water after centrifugation. DLS measurements confirmed that coating GNPs with copoly(DEG-*co*-PEG) results in an increase in the hydrodynamic diameter of the nanoparticles. In addition, TEM images of the polymercoated GNPs show well-dispersed particles with minimal aggregation (Figure 6.3). Further TEM characterization using phosphotungsten acid as a negative stain, confirmed the presence of a grafted polymer layer as shown by contrasting white halos around the GNPs (Inset of picture A, Figure 6.3). AFM measurements confirmed the presence of monodispersed hybrid GNPs with sizes ranging from 20 to 30 nm. The phase contrast image (inset of picture E, Figure 6.3) of the same hybrid particles confirms the presence of a soft shell (polymer) around a hard gold core.

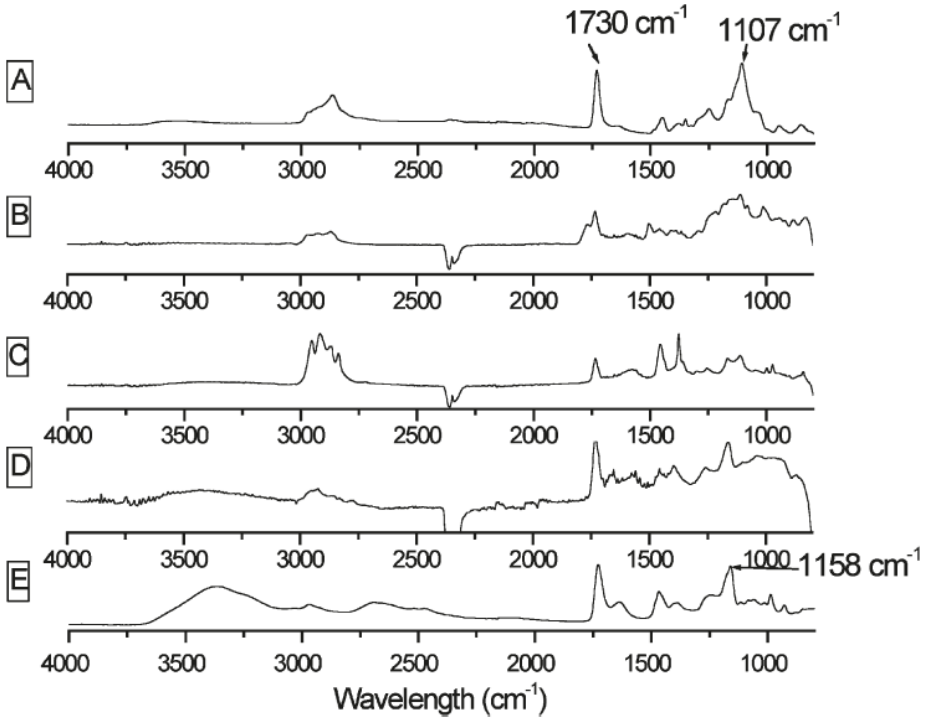

Figure 6.4. ATR analyses purified GNPs/poly(OEG-*co*-DEG-A): (A) GNPs/poly(OEG-A), (B) GNPs/poly(OEG-*co*-DEG-A) [entry 2 of Table 6.1]; (C) GNPs/poly(OEG-*co*-DEG-A) [entry 6 of Table 6.1]; (D) GNPs/poly(OEG-*co*-DEG-A) [entry 8 of Table 6.1]; (E) GNPs/poly(OEG-*co*-DEG-A) [entry 9 of Table 6.1].

The zeta potentials of the GNPs both before and after grafting were measured, recording an increase from ≈ - 40 mV to ≈ 0 mV (+/- 5 mV). This result is consistent with an exchange of the negative citrate ions on the GNP surface (originating from the GNP synthetic method) with the uncharged polymer stabilizing layer.

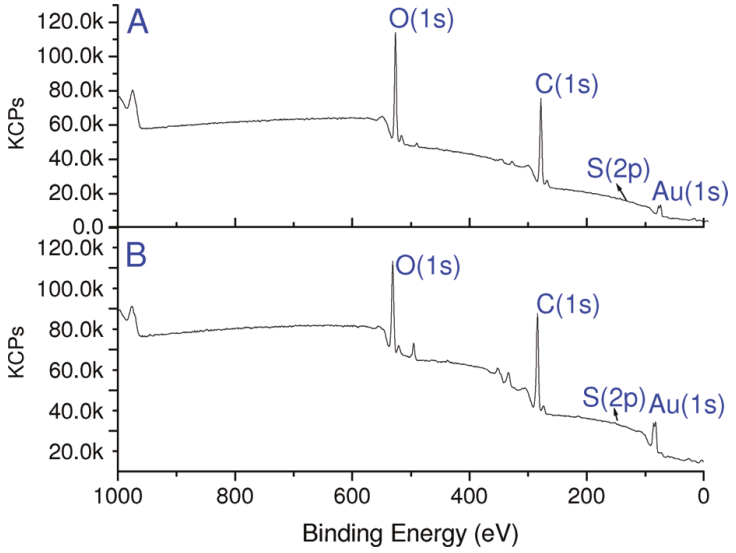

Figure 6.5. XPS analyses: (A) GNPs/poly(OEG-*co*-DEG-A) [entry 6 of Table 6.1]; (B) GNPs/poly(OEG-*co*-DEG-A) [entry 2 of Table 6.1].

The presence of a grafted copolymer layer on the GNPs was accrued using ATR (Figure 6.4) and X-ray photoelectron spectroscopy (XPS) (Figure 6.5). As expected, the ATR of the hybrid GNPs reveal characteristic PEG absorption signals: the C-O ether bond at 1480 cm^{-1} and the C=O carbonyl bond at 1730 cm^{-1}. In addition, as the copolymer composition of the polymer shell changes, (with increased DEG), a concomitant increase in the absorption of the carbonyl bond, relative to the ether bond, is observed. XPS measurements indicate different elemental signals attributable to the carbon, oxygen and sulfur atoms at the surface of the hybrid GNPs. High resolution XPS confirms the presence of C(1s) from the C-O ether bond (at 286.45 eV)[443] and the presence of an intense signal associated with oxygen (1s) at 532.38 eV.[444] In addition, XPS detected sulfur bonds S(2p) at 162.0 and at 163.4 eV originating from the gold-sulfur bond, suggesting that the gold-polymer bonding is in fact not through the trithiocarbonate functionality, but via a thiol-gold interaction. It is possible to hypothesize that the trithiocarbonate is reduced to thiol in the presence of the GNP

surface, explaining the results from XPS. Recently, Theato and coworker55 reported surface plasma resonance (SPR) experiments confirming that the dithiocabonate moiety (the RAFT end-group here) can bind directly with gold surfaces. However, the gold-thiocarbonate interaction is known to be weaker than the gold-thiol interaction.[400,401]

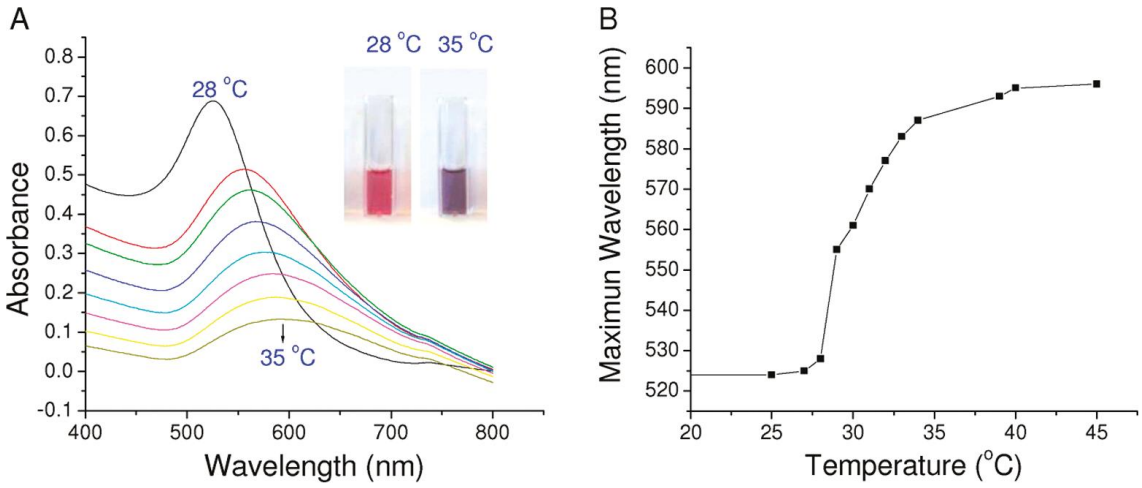

Figure 6.6. (A) UV-visible spectra of GNPs/poly(OEG-A-*co*-DEG-A) (entry 3 of Table 6.1) versus temperature. Each spectrum was taken after increasing of 1 °C (from 28 °C to 35 °C), inset: picture of gold/poly(OEG-A-*co*-DEG-A) dispersed in water at 25 and 35 °C, respectively; (B) Evolution of maximum wavelength versus temperature.

The thermoresponsive character of the gold/polymer hybrid nanoparticles in aqueous solutions was demonstrated by non-isothermal turbidity measurements. On heating to the vicinity of the LCST transitions, the GNP- aqueous solution changes its colour from red to purple (a shift of the wavelength from 520 nm to 600 nm) as shown in Figure 6.6. The colour of GNPs is known to depend on both their dimensions and their environment. On GNP aggregation, the characteristic GNP plasmon resonance of 520 nm (red solution) shifts towards longer wavelengths (blue solution) characteristic of an increased electronic dipole-dipole interaction among near-neighbour GNPs. In addition, as the absorbance wavelength shifts there is also a decrease in the measured absorbance intensities. Maintaining the GNP solution above the LCST for several hours results in a purple precipitate, however, this can be redispersed rapidly by cooling the mixture below the LCST with gentle shaking. UV-visible spectroscopy measurements were used to confirm the reversible nature of the LCST transition. The aggregates formed above the LCST were characterized using DLS measurements, confirming the presence of aggregates with sizes of 200 nm, as shown in Figure 6.7. TEM was also

applied to characterize the aggregates, revealing the formation of GNP chains consisting of 8-12 nanoparticles (Pictures B and C, Figure 6.3). On cooling, below the LCST, the aggregates observed by both DLS and TEM disappeared. However, the temperature of dissociation and re-dispersion of these aggregates was always found to be slightly lower (≈ 5-8 °C) than the temperature observed for their aggregation. DLS data show that the particles returned to their original sizes (measured below the LCST) after a complete heating-cooling cycle. No change in their spectroscopic properties (such as λ_{max} and average size) could be detected after several heating-cooling cycles (Figure 6.7.D)

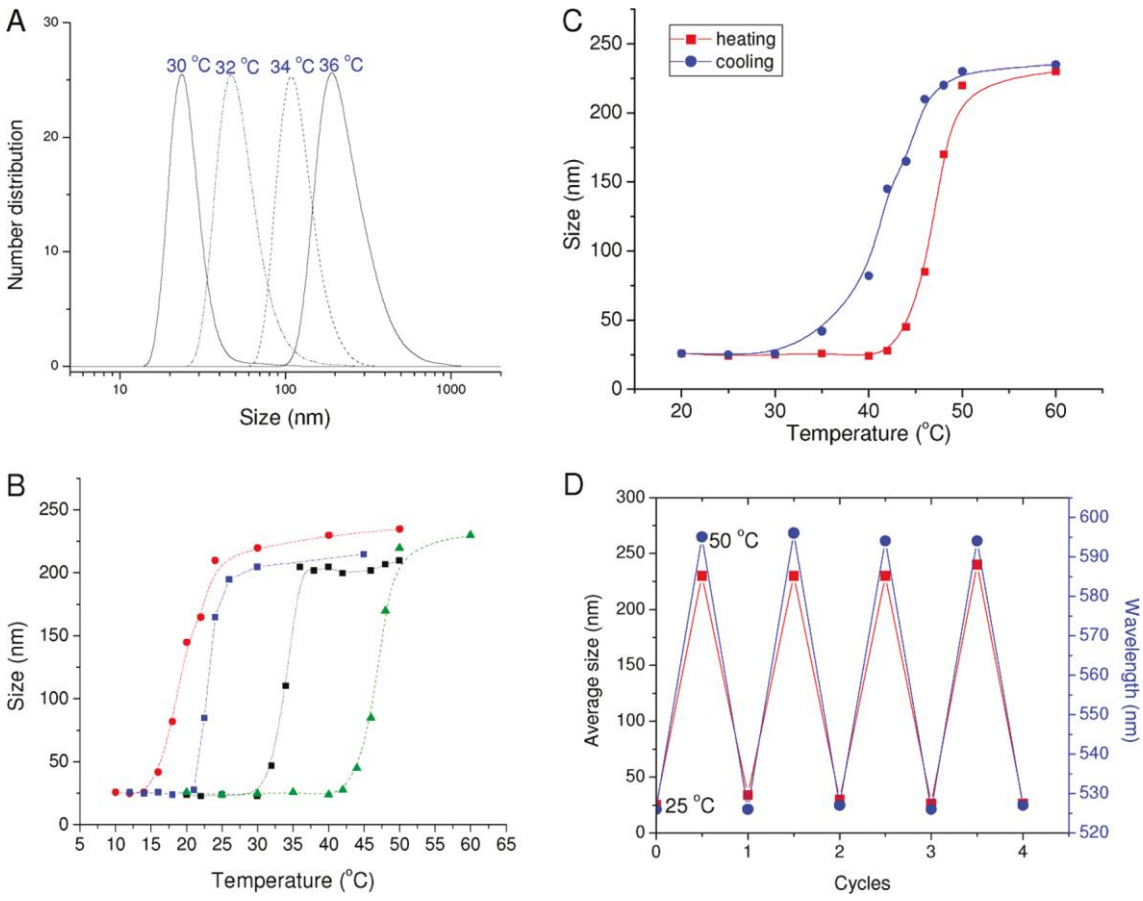

Figure 6.7. Number distribution versus size (nm) for GNPs coated with poly(DEG-*co*-OEG-A): (A) evolution of size at different temperatures for poly(DEG-*co*-OEG-A): entry 3 of Table 6.1; (B) evolution of size versus temperature for four different GNPs/poly(DEG-*co*-OEG-A) (red curve: entry 1 of Table 6.1, blue curve: entry 2 of Table 5, black curve: entry 3 of Table 6.1 and green curve: entry 4 of Table 6.1). (C) Evolution of average size (determined for the number distributions) versus temperature for GNPs/poly(DEG-*co*-OEG-A) (entry 4 of Table 6.1) (heating and cooling cycle). (D) Variation of the average sizes and λ_{max}(assessed by UV-vis spectroscopy) for different cooling/heating cycles of GNPs/poly(DEG-co.OEG-A) (entry 4 of Table 6.1)

Attached PEG copolymers are known to imbue favorable characteristics to metal nanoparticles[378,445] including anti-fouling and stealth characteristics, as demonstrated by both in-vitro and in-vivo testing.[358,378,446-453] To investigate these properties further, the nanoparticles prepared in this study were subjected to Bradford assays, using BSA as a model protein. The Bradford assay,[437] evaluates the amount of unbound BSA after 3 hours of incubation with the GNP dispersion. After incubation, the GNPs were removed from solution by centrifugation and the supernatant was analyzed for the presence of "free" BSA. Two control assays were also conducted to afford comparisons with 'naked' GNPs (stabilized by citrate) and GNPs stabilized with PNIPAAm. The results from the Bradford assays are given in Figure 6.8 which shows the proportion of BSA adsorbed onto each of the nanoparticles, are given in Figure 6.8. In the presence of a poly(OEG-A-*co*-DEG-A) stabilizing layer below the LCST, less than 0.10 (± 0.07) mg/m^2 (± 1014 molecules/m^2) of BSA was adsorbed. This low adsorption yield is close to the experimental error and can be interpreted as effectively zero adsorption. When the level of DEG-A in the copolymer is increased, the BSA adsorption (below the LCST) slightly increased (from 0.10 to 0.15 (± 0.07) mg/m^2) (Figure 6.8). A hypothesis can be tendered that the length of ethylene glycol is insufficient to confer perfect antifouling behavior as the number of ethylene glycol units is an important parameter for controlling the adsorption of protein on surfaces.[454] In contrast, 0.44 mg of BSA /m^2 (± 0.10) in solution was adsorbed onto nanoparticles stabilized with PNIPAAm at 25 °C; a result strongly favoring the use of these thermoresponsive PEGs where GNPs are used in bioapplications. Finally, in the absence of any polymer coating, 2.8 mg/m^2 (or 2.5 x 10^{16} BSA/m^2) was adsorbed from solution onto the gold surface, consistent with strong charge interactions between the citrate stabilizing groups and the protein. This measured adsorption corresponds (assuming BSA dimensions of 5.5 x 5.5 x 9.0 nm) to the formation of a BSA monolayer on the GNPs obtained for an end-on binding mechanism (theoretical values are 3.3 and 2.0 mg/m^2 for an end-on and a side binding, respectively). This result is consistent with previous results reported for GNPs/citrate systems.[455,456]

A similar experiment was conducted above the LCST of the GNPs. A slight increase in the adsorption of BSA was observed for the PEG stabilized GNPs from 0.10 to 0.15 (± 0.07) to 0.20-0.35 (± 0.07) mg/m^2 and for GNPs/PNIPAAm from 0.44 (± 0.14) to 1.3 mg/m^2, consistent with an increase in hydrophobic interactions between the protein and the polymers. BSA has a defined tertiary structure displaying surfaces with both

positively and negatively charged domains with a distinct hydrophobic region.[457] In the case of P(OEG-*co*-DEG-A) even above the LCST, the BSA adsorption was still relatively low, suggesting that the hydrophobic interactions are fairly weak. After BSA incubation, the GNP/poly(OEG-A-*co*-DEG-A) nanoparticles could be isolated and redispersed in water. Subsequent DLS and zeta potential measurements reveal that the nanoparticles exhibit similar sizes and surface charges to measurements made prior to the Bradford assay.

The stability of GNPs/poly(OEG-A-*co*-DEG-A) was also studied in 50 vol % of fetal bovine serum (FBS), used as a model system for a biological fluid,[430] below and above the LCST of the grafted polymer layer. The size and zeta potential of these nanoparticles were monitored with time using DLS. Encouragingly, it was found that these nanoparticles stayed perfectly dispersed after 3 days, at temperatures below the LCST.

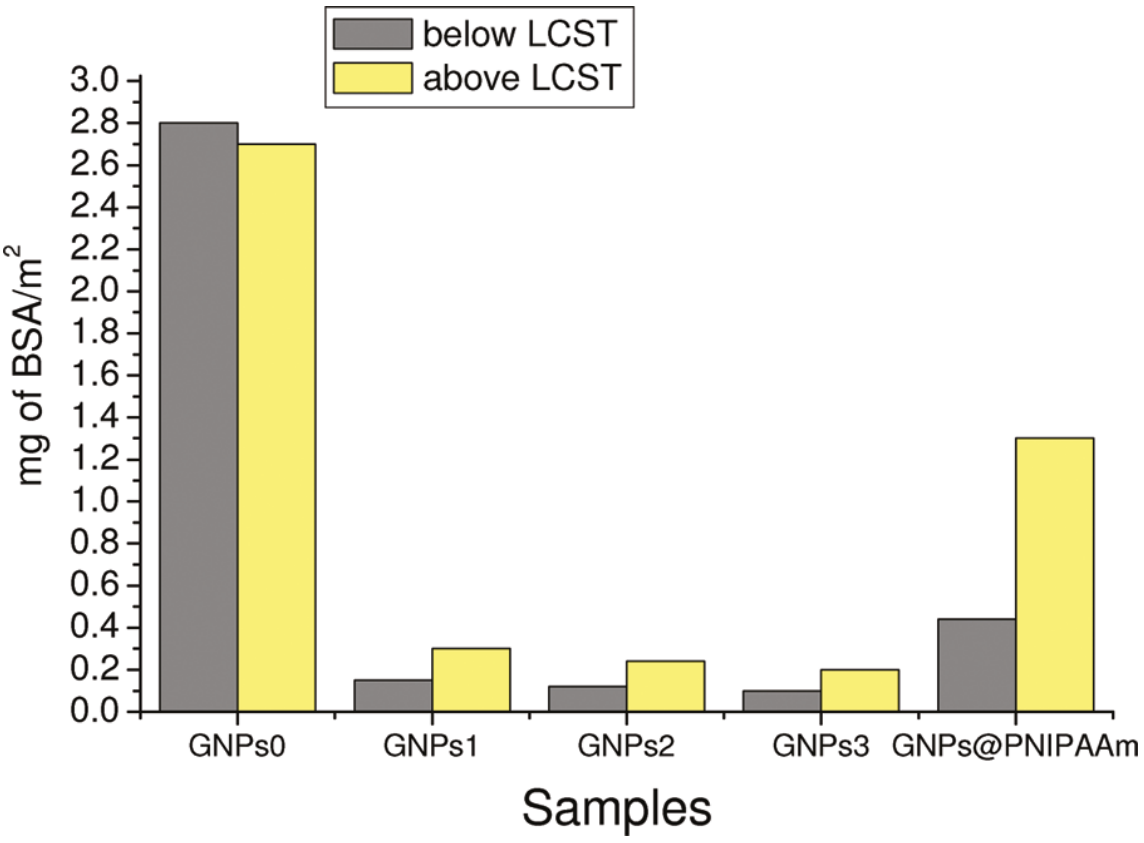

Figure 6.8. BSA absorption on different GNPs: "naked" GNPs (0), GNPs (1): GNPs/poly(OEG-*co*-DEGA) [entry 2 of Table 6.1]; GNPs (2): GNPs/poly(OEG-*co*-DEG-A) [entry 3 of Table 6.1]; GNPs (3): GNPs/poly(OEG-*co*-DEG-A) [entry 4 of Table 6.1]; GNPs/PNIPAAm, M_n = 20 000 g/mol, PDI =1.08.

Note: BSA absorbed calculated by 100 × (1- (Ab_{GNP}595 nm / $Ab_{(0)}$ 595 nm)), where Ab_{GNP} 595 nm and $Ab_{(0)}$ 595 nm correspond to absorbance of Bradford reactant after incubation with and without GNPs, respectively.

Two different copolymers, having different LCST behaviour (one close to 15 °C, i.e. poly(DEG-A) and one close to 33 °C, i.e. poly(DEG-A-*co*-OEG-A), entry 3 of Table 6.1) were assembled onto GNPs to form mixed-layer GNP hybrids. These two copolymers (of similar molecular weight, both 20 kg/mol) were mixed together in different proportions (25/75, 50/50 and 75/25 wt %) with GNPs yielding hybrid nanoparticles with mixed polymer layer compositions. After purification, the surface layer composition was characterized using XPS, revealing the presence of signals characteristic of C and O bonds, attributable to both OEG-A and DEG-A moieties. Quantification of the polymers grafted onto the gold surface was achieved via elemental composition analysis by XPS. Accordingly, the O/C ratio of poly(DEG-A) and copoly(DEG-A-*co*-OEG-A)) (pure non-adsorbed polymer samples) was 44 % and 54 %, respectively. In the case of hybrid GNPs coated with two different copolymers (50/50 wt %), the ratio O/C was measured to be 48 %. Similarly, the O/C ratios were measured to be 46 % and 51 % for poly(DEG-A)/copoly(DEG-A-*co*-OEG-A) = 75/25 and 25/75 wt %, respectively. The XPS results show that the polymer compositions assembled onto the GNPs correlates strongly with the corresponding compositions of the polymer solutions used for their preparation. All three different stabilizing polymer compositions yielded 30 nm nanoparticles with low polydispersities in solution (determined at 5 °C by DLS).

The effect of temperature on the particle size changes of these GNP dispersions was then assessed using DLS (Figure 6.9). As the temperature increased slowly up from 5 °C to 25 °C, no significant change to the characteristic colour (i.e. the plasmon absorbance determined by UV-visible spectroscopy) or to the particle size as determined by DLS (a slight decrease) was observed. However as the temperature was further increased to 28-30 °C, slightly lower than the second higher LCST, the properties of the mixed hybrid nanoparticles changed (both colour and size). The aggregate sizes increased quickly from 35 nm to 250 nm and the solutions underwent a colour change to purple indicating aggregation was occurring. It is also evident from the results presented in Figure 6.9 that the LCST exhibited by these mixed layered systems is sensitive to the composition of the polymer surface layer. The GNPs coated with 75 wt % of poly(DEG-A) and 25 wt % of poly(OEG-A-*co*-DEGA) showed a thermoresponsive transition shifted to a lower temperature when compared to the 50/50 mixed polymer hybrid system; i.e., there is a slight decrease in the LCST (about 5 °C) as the amount of poly(DEG-A) on the surface layer increased from 50 % to 75 %. Moreover, the LCST transition of the

hybrid nanoparticles with a mixed polymer layer was broader than those found for the GNPs coated with only one type of polymer. This result can be attributed to the fact that these nanoparticles are stabilized by a distribution of surface layer compositions, displaying slightly different LCSTs.

This outcome demonstrates that the properties of the GNPs in solution are dictated by the bound copolymer with the higher LCST. We speculate that as the temperature is raised there is a hydrophilic to hydrophobic transition of the copolymer chains with the lower LCST. This transition causes the formation of an internal hydrophobic layer through the collapse of these extended chains to a globular form, but as a whole, the nanoparticles are still stabilized by those copolymer chains with the higher LCST. These chains are still extended from the surface and remain hydrophilic. On further heating the second LCST is reached inducing a hydrophilic- hydrophobic transition. This causes a destabilization of the mixed hybrid nanoparticles in solution resulting in aggregation.

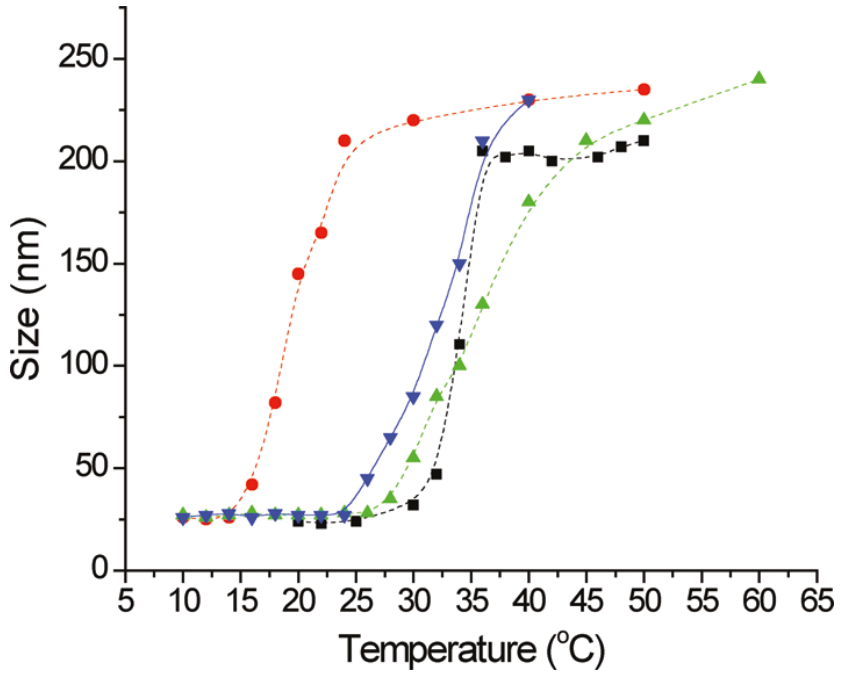

Figure 6.9. Evolution of size vs. temperature for different GNPs: (•) GNPs/poly(DEG-A) [entry 1 of Table 6.1], (■) GNPs/poly(DEG-A-*co*-OEG-A) [entry 3, Table 6.1], (▲) GNPs/ Mixed polymers [poly(OEG-A)/ poly(DEG-A-*co*-OEG-A)] = 50/50 wt-%], (▼) GNPs/ Mixed polymers [poly(DEG-A)/poly(DEG-A-*co*-OEG-A)] = 75/25 wt %].

To confirm this, an experiment was designed to probe the formation of a hydrophobic layer within the mixed hybrid nanoparticles using pyrene.[458] The change in the fluorescent spectrum of pyrene has commonly been used as a hydrophobic probe to evaluate the polarity of the environment surrounding the pyrene molecules. When a hydrophobic domain is present in the water solution, pyrene tends to partition into the hydrophobic domain. On entering these domains, there is a red shift in the emission spectrum, viz. a decrease in the intensity ratio of the first I_1 to the third I_3 vibration bands.[459] GNP/[poly(DEG-A) /poly(OEG-A-*co*-DEG-A) = 50/50 wt %] (1 mg/mL) was mixed with a pyrene solution (10^{-6} mol/L) overnight at 5 °C. The change of I_1 /I_3 values versus temperature is shown in Figure 6.10. Two majors transitions were observed: first (at 8-10 °C), the values dropped from 1.9 to 1.7, followed by a second decrease in the ratio values (from 1.7 to 1.5) around 25-28 °C. This result is totally reversible, if the temperature decreases the ratio values increase. These LCST values are slightly lower than those determined independently for the two copolymers in aqueous solution, however, it has been shown previously in similar GNP/PNIPAAm hybrid systems that the LCST of the grafted polymer layer is affected by the confinement of the PNIPAAm chains at a surface.[420] The outcome of this experiment demonstrates the systematic formation of a hydrophobic zone in the mixed layer hybrid nanoparticles consistent with two different polymers self-assembled onto the GNP surface. As a control experiment, GNP/[poly(DEG-A)] and GNP/[poly(OEG-A-*co*-DEG-A) were separately analyzed using pyrene. In the case of these two different GNPs, we observed only one change for I_1/I_3 ratio when the temperature was increased. The changes for GNP/[poly(DEG-A)] and GNP/[poly(OEG-A-*co*-DEG-A) were close to 8-10 and 25-28 °C, respectively.

The antifouling properties of these mixed polymer layer GNPs were evaluated as before; below the first LCST, between the two LCSTs, and above the second LCST. A low protein adsorption ($\sim 0.10 \pm 0.05$ mg/m^2) was observed below the first LCST and also between the LCSTs in accord with previous results. The absence significant protein adsorption at the temperature between the two LCSTs confirms the maintenance of a nonfouling layer. A slight increase in BSA adsorption ($\sim 0.20 \pm 0.10$ mg/m^2) was found above the second LCST, in accord with our earlier results.

Clearly the presence of poly(DEG-A) chains in the layer is affecting the LCST transition of the copoly(DEG-A-*co*-OEG-A) chains. Further experiments to investigate this are underway. Clearly, the composition of the polymer surface layer provides another

variable allowing for the precise tuning of the LCST behaviour of these hybrid nanoparticles.

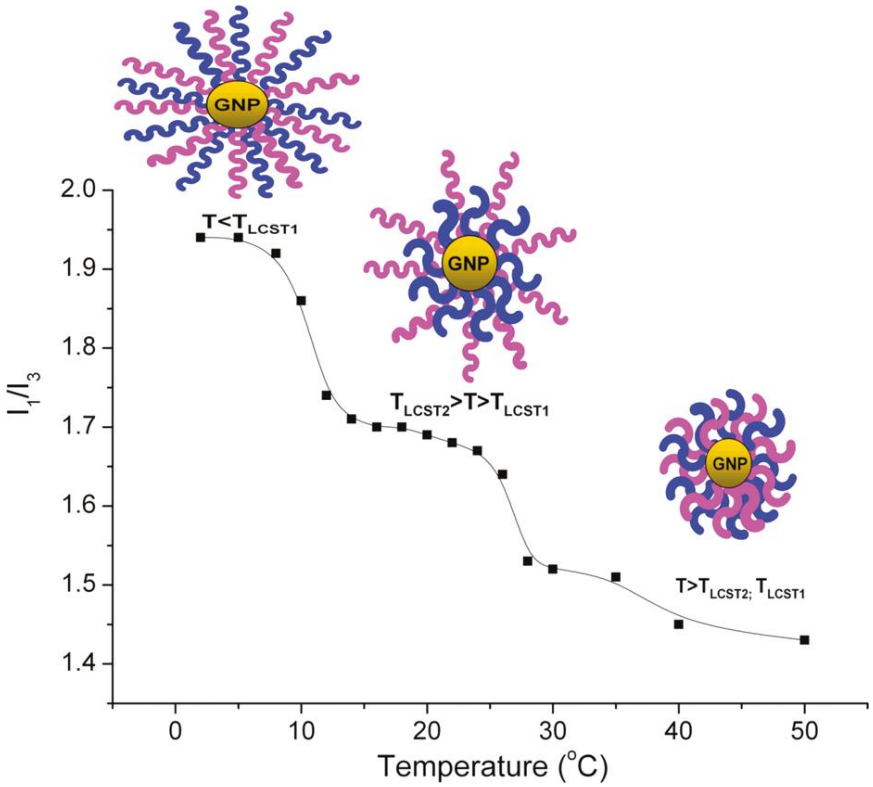

Figure 6.10. Evolution of I_1/I_3 versus the temperature for GNPs/Mixed polymers [poly(OEG-A)/ poly(DEG-A-*co*-OEG-A)] = 50/50 wt %].

4. Conclusions

In this work, we have demonstrated for the first time the formation of a new class of hybrid polymer/GNP nanoparticles using novel PEG based thermosensitive polymers displaying a broad range of LCST values (from 15 to 90 °C). These new hybrid nanoparticles have not only been shown to have tunable thermosensitive behavior but also anti-fouling/protein resistant surfaces and stealth characteristics. By judicious choice of the copolymers used in the assembly of these hybrid nanoparticles, it is possible to form hybrid nanoparticles with uniquely nanostructured hydrophilic/hydrophobic polymer surface layers as demonstrated here from the one PEG based polymer system.

5. Acknowledgment.

TPD acknowledge the Australian Research Council for the award of Discovery Grants and Federation Fellowship (TPD).

6. References

(348) Chen, P. C.; Mwakwari, S. C.; Oyelere, A. K. *Nanotechnol. Sci. Appl.* **2008**, *1*, 45.

(349) Huang, X.; El-Sayed, I. H.; Qian, W.; El-Sayed, M. A. *J. Am. Chem. Soc.* **2006**, *128*, 2115.

(350) Kim, S.; Lim, Y. T.; Soltesz, E. G.; De Grand, A. M.; Lee, J.; Nakayama, A.; Parker, J. A.; Mihaljevic, T.; Laurence, R. G.; Dor, D. M.; Cohn, L. H.; Bawendi, M. G.; Frangioni, J. V. *Nature Biotechnology* **2004**, *22*, 93.

(351) Krause, W. *Advanced Drug Delivery Reviews* **1999**, *37*, 159.

(352) Weissleder, R. *Science* **2006**, *312*, 1168.

(353) De, M.; Ghosh, P. S.; Rotello, V. M. *Advanced Material* **2008**, *20*, 4225.

(354) Ghosh, P. S.; Kim, C.-K.; Han, G.; Forbes, N. S.; Rotello, V. M. *ACS Nano 2008*, *2*, 2213.

(355) Cho, E. C.; Xie, J.; Wurm, P. A.; Xia, Y. *Nano Letters* **2009**, *9*, 1080.

(356) Javakhishvili, I.; Hvilsted, S. *Biomacromolecules* **2009**, *10*, 74.

(357) Aqil, A.; Qiu, H.; Greisch, J.-F.; Jerome, R.; De Pauw, E.; Jerome, C. *Polymer* **2008**, *49*, 1145.

(358) Bergen, J. M.; von Recum, H. A.; Goodman, T. T.; Massey, A. P.; Pun, S. H. *Macromol. Biosci.* **2006**, *6*, 506.

(359) Giljohann, D. A.; Seferos, D. S.; Prigodich, A. E.; Patel, P. C.; Mirkin, C. A. *J. Am. Chem. Soc.* **2009**, *130*, 2073.

(360) Zhao, W.; Chiuman, W.; Lam, J. C. F.; McManus, S. A.; Chen, W.; Cui, Y.; Pelton, R.; Brook, M. A.; Li, Y. *J. Am. Chem. Soc.* **2008**, *130*, 3610.

(361) Durocher, S.; Rezaee, A.; Hamm, C.; Rangan, C.; Mittler, S.; Mutus, B. *J. Am. Chem. Soc.* **2009**, *131*, 2475.

(362) Tessier, P. M.; Jinkoji, J.; Cheng, Y.-C.; Prentice, J. L.; Lenhoff, A. M. *J. Am. Chem. Soc.* **2008**, *130*, 3106.

(363) Michalet, X.; Pinaud, F. F.; Bentolila, L. A.; Tsay, J. M.; Doose, S.; Li, J. J.; Sundaresan, G.; Wu, A. M.; Gambhir, S. S.; Weiss, S. *Science* **2005**, *307*, 538.

(364) Shan, J.; Tenhu, H. *Chem. Commun.* **2007**, 4580.

(365) Storhoff, J. J.; Lazarides, A. A.; Mucic, R. C.; Mirkin, C. A.; Letsinger, R. L.; Schatz, G. C. *J. Am. Chem. Soc.* **2000**, *122*, 4640.

(366) Daniel, W. L.; Han, M. S.; Lee, J.-S.; Mirkin, C. A. *J. Am. Chem. Soc.* **2009**, *131*, 6362.

(367) Park, J. B.; Graciani, J.; Evans, J.; Stacchiola, D.; Ma, S.; Liu, P.; Nambu, A.; Sanz, J. F.; Hrbek, J.; Rodrigue, J. A. *Proceedings of the National Academy of Sciences U.S.A.* **2009**, *106*, 4975.

(368) Della Pina, C.; Falletta, E.; Rossi, M.; Sacco, A. *J. Catal.* **2009**, *263*, 92.

(369) Huang, X.; Guo, C.; Zuo, J.; Zheng, N.; Stucky, G. D. *Small* **2009**, *5*, 361.

(370) Chen, L.; Hu, J.; Richards, R. *J. Am. Chem. Soc.* **2009**, *131*, 914.

(371) Han, J.; Liu, Y.; Guo, R. *J. Am. Chem. Soc.* **2009**, *131*, 2060.

(372) Agasti, S. S.; Chompoosor, A.; You, C.-C.; Ghosh, P.; Kim, C. K.; Rotello, V. M. *J. Am. Chem. Soc.* **2009**, *131*, 5728.

(373) Cheng, Y.; Samia, A. C.; Meyers, J. D.; Panagopoulos, I.; Fei, B.; Burda, C. *J. Am. Chem. Soc.* **2008**, *130*, 10643.

(374) Kim, C. K.; Ghosh, P.; Pagliuca, C.; Zhu, Z.-J.; Menichetti, S.; Rotello, V. M. *J. Am. Chem. Soc.* **2009**, *131*, 1360.

(375) Thomas, M.; Klibanov, A. M. *Proceedings of the National Academy of Sciences U.S.A.* **2003**, *100*, 9138.

(376) Alric, C.; Serduc, R.; Mandon, C.; Taleb, J.; Le Duc, G.; Le Meur-Herland, A.; Billotey, C.; Perriat, P.; Roux, S.; Tillement, O. *Gold Bull.* **2008**, *41*, 90.

(377) Alric, C.; Taleb, J.; Le Duc, G.; Mandon, C.; Billotey, C.; Le Meur-Herland, A.; Brochard, T.; Vocanson, F.; Janier, M.; Perriat, P.; Roux, S.; Tillement, O. *J. Am. Chem. Soc.* **2008**, *130*, 5908.

(378) Kim, D.; Park, S.; Lee, J. H.; Jeong, Y. Y.; Jon, S. *J. Am. Chem. Soc.* **2007**, *129*, 7661.

(379) Qian, X.; Peng, X.-H.; Ansari, D. O.; Yin-Goen, Q.; Chen, G. Z.; Shin, D. M.; Yang, L.; Young, A. N.; Wang, M. D.; Nie, S. *Nature Biotechnology* **2008**, *26*, 83.

(380) Kim, D. J.; Kang, S. M.; Kong, B.; Kim, W.-J.; Paik, H.-j.; Choi, H.; Choi, I. S. *Macromol. Chem. Phys.* **2005**, *206*, 1941.

(381) Dong, H.; Zhu, M.; Yoon, J. A.; Gao, H.; Jin, R.; Matyjaszewski, K. *J. Am. Chem. Soc.* **2008**, *130*, 12852.

(382) Holzinger, D.; Liz-Marzan, L. M.; Kickelbick, G. *J. Nanosci. Nanotechnol.* **2006**, *6*, 445.

(383) Li, D.; He, Q.; Cui, Y.; Wang, K.; Zhang, X. L., J. *Chem. Eur. J.* **2007**, *13*, 2224.

(384) Raula, J.; Shan, J.; Nuopponen, M.; Niskanen, A.; Jiang, H.; Kauppinen, E. I.; Tenhu, H. *Langmuir* **2003**, *19*, 3499.

(385) Wei, Q.; Ji, J.; Shen, J. *Macromol. Rapid Commun.* **2008**, *29*, 645.

(386) Lowe, A. B.; Sumerlin, B. S.; Donovan, M. S.; McCormick, C. L. *J. Am. Chem. Soc.* **2002**, *124*, 11562.

(387) Zhang, T.; Zheng, Z.; Ding, X.; Peng, Y. *Macromol. Rapid Commun.* **2008**, *29*, 1716.

(388) Shen, Y.; Kuang, M.; Shen, Z.; Nieberle, J.; Duan, H.; Frey, H. *Angew. Chem. Int. Ed.* **2008**, *47*, 2227.

(389) Roth, P. J.; Theato, P. *Chem. Mater.* **2008**, *20*, 1614.

(390) Wang, B.; Li, B.; Zhao, B.; Li, C. Y. *J. Am. Chem. Soc.* **2008**, *130*, 11594.

(391) Sumerlin, B. S.; Lowe, A. B.; Stroud, P. A.; Zhang, P.; Urban, M. W.; McCormick, C. L. *Langmuir* **2003**, *19*, 5559.

(392) McCormick, C. L.; Lowe, A. B. *Acc. Chem. Res.* **2004**, *37*, 312.

(393) Li, Y.; Smith, A. E.; Lokitz, B. S.; McCormick, C. L. *Macromolecules* **2007**, *40*, 8524.

(394) Smith, A. E.; Xu, X.; Abell, T. U.; Kirkland, S. E.; Hensarling, R. M.; McCormick, C. L. *Macromolecules* **2009**, *42*, 2958.

(395) Kim, B. J.; Bang, J.; Hawker, C. J.; Chiu, J. J.; Pine, D. J.; Jang, S. G.; Yang, S.-M.; Kramer, E. J. *Langmuir* **2007**, *23*, 12693.

(396) Park, S. C.; Kim, B. J.; Hawker, C. J.; Kramer, E. J.; Bang, J.; Ha, J. S. *Macromolecules* **2007**, *40*, 8119.

(397) Merican, Z.; Schiller, T. L.; Hawker, C. J.; Fredericks, P. M.; Blakey, I. *Langmuir* **2007**, *23*, 10539.

(398) Nuopponen, M.; Tenhu, H. *Langmuir* **2007**, *23*, 5352.

(399) Fustin, C. A.; Colard, C.; Filali, M.; Guillet, P.; Duwez, A. S.; Meier, M. A. R.; Schubert, U. S.; Gohy, J. F. *Langmuir* **2006**, *22*, 6690.

(400) Duwez, A. S.; Guillet, P.; Colard, C.; Gohy, J.-F.; Fustin, C.-A. *Macromolecules* **2006**, *39*, 2729.

(401) Hotchkiss, J. W.; Lowe, A. B.; Boyes, S. G. *Chem. Mater.* **2007**, *19*, 6.

(402) Roth, P. J.; Kessler, D.; Zentel, R.; Theato, P. *Macromolecules* **2008**, *41*, 8316.

(403) Scales, C. W.; Convertine, A. J.; McCormick, C. L. *Biomacromolecules* **2006**, *7*, 1389.

(404) York, A. W.; Scales, C. W.; Huang, F.; McCormick, C. L. *Biomacromolecules* **2007**, *8*, 2337.

(405) Li, M.; De, P.; Gondi, S. R.; Sumerlin, B. S. *J. Polym. Sci. Part A: Polym. Chem.* **2008**, *46*, 5093.

(406) Boyer, C.; Bulmus, V.; Davis, T. P. *Macromol. Rapid Commun.* **2009**, *30*, 493.

(407) Peer, D.; Karp, J. M.; Hong, S.; Farokhzad, O. C.; Margalit, R.; Langer, R. *Nature Nanotechnology* **2007**, *2*, 751.

(408) Kah, J. C. Y.; Wong, K. Y.; Neoh, K. G.; Song, J. H.; Fu, J. W. P.; Mhaisalkar, S.; Olivo, M.; Sheppard, C. J. R. J. *Drug Targeting* **2009**, *17*, 181.

(409) Prencipe, G.; Tabakman, S. M.; Welsher, K.; Liu, Z.; Goodwin, A. P.; Zhang, L.; Henry, J.; Dai, H. *J. Am. Chem. Soc.* **2009**, *131*, 4783.

(410) Liu, Y.; Shipton, M. K.; Ryan, J.; Kaufman, E. D.; Franzen, S.; Feldheim, D. L. *Anal. Chem.* **2007**, *79*, 2221.

(411) Chanana, M.; Jahn, S.; Georgieva, R.; Lutz, J.-F.; Baumler, H.; Wang, D. *Chem. Mater.* **2009**, *21*, 1906.

(412) Veronese, F. M.; Harris, J. M. *Advanced Drug Delivery Reviews* **2008**, *60*, 1.

(413) Harris, J. M.; Chess, R. B. *Nature Review Drug Discovery* **2003**, *2*, 214.

(414) Ryan, S. M.; Mantovani, G.; Wang, X.; Haddleton, D. M.; Brayden, D. J. *Expert Opin. Drug Delivery* **2008**, *5*, 371.

(415) Nicolas, J.; San Miguel, V.; Mantovani, G.; Haddleton, D. M. *Chem. Commun.* **2006**, 4697.

(416) Yusa, S. I.; Fukuda, K.; Yamamoto, T.; Iwasaki, Y.; Watanabe, A.; Akiyoshi, K.; Morishima, Y. *Langmuir* **2007**, *23*, 12842.

(417) Ishii, T.; Otsuka, H.; Kataoka, K.; Nagasaki, Y. *Langmuir* **2004**, *20*, 561.

(418) Shan, J.; Chen, J.; Nuopeponen, M.; Tenhu, H. *Langmuir* **2004**, *20*, 4671.

(419) Shan, J.; Nuopponen, M.; Jiang, H.; Kauppinen, E.; Tenhu, H. *Macromolecules* **2003**, *36*, 4526.

(420) Zhu, M. Q.; Wang, L. Q.; Exarhos, G. J.; Li, A. D. Q. *J. Am. Chem. Soc.* **2004**, *126*, 2656.

(421) Boyer, C.; Bulmus, V.; Liu, J.; Davis, T. P.; Stenzel, M. H.; Barner-Kowollik, C. *J. Am. Chem. Soc.* **2007**, *129*, 7145.

(422) Kujawa, P.; Segui, F.; Shaban, S.; Diab, C.; Okada, Y.; Tanaka, F.; Winnik, F. M. *Macromolecules* **2006**, *39*, 341.

(423) Van Durme, K.; Rahier, H.; Van Mele, B. *Macromolecules* **2005**, *38*, 10155.

(424) Zhou, Y.; Jiang, K.; Chen, Y.; Liu, S. *J. Polym. Sci. Part A: Polym. Chem.* **2008**, *46*, 6518.

(425) Zheng, P.; Jiang, X.; Zhang, X.; Zhang, W.; Shi, L. *Langmuir* **2006**, *22*, 9393.

(426) Bhattacharjee, R. R.; Chakraborty, M.; Mandal, T. K. *J. Phys. Chem. B* **2006**, *110*, 6768.

(427) Dong, Y.; Ma, Y.; Zhai, T.; Zeng, Y.; Fu, H.; Yao, J. J. *J. Nanosci. Nanotechnol.* **2008**, *8*, 6283.

(428) Jeon, H. J.; Go, D. H.; Choi, S.-y.; Kim, K. M.; Lee, J. Y.; Choo, D. J.; Yoo, H.-O.; Kim, J. M.; Kim, J. *Colloids Surf., A* **2008**, *317*, 496.

(429) Tang, T.; Krysmann, M. J.; Hamley, I. W. *Colloids Surf., A* **2008**, *317*, 764.

(430) Salmaso, S.; Caliceti, P.; Amendola, V.; Meneghetti, M.; Magnusson, J. P.; Pasparakis, G.; Alexander, C. *J. Mater. Chem.* **2009**, *19*, 1608.

(431) Ernst, O.; Lieske, A.; Hollaender, A.; Lankenau, A.; Duschl, C. *Langmuir* **2008**, *24*, 10259.

(432) Lutz, J. F.; Akdemir, O.; Hoth, A. *J. Am. Chem. Soc.* **2006**, *128*, 13046.

(433) Lutz, J. F.; Hoth, A. *Macromolecules* **2006**, *39*, 893.

(434) Lutz, J. F. *J. Polym. Sci. Part A: Polym. Chem.* **2008**, *46*, 3459.

(435) Wischerhoff, E.; Uhlig, K.; Lankenau, A.; Boerner, H. G.; Laschewsky, A.; Duschl, C.; Lutz, J.-F. *Angew. Chem. Int. Ed.* **2008**, *47*, 5666.

(436) Frens, G. *Nature Physical Science* **1973**, *241*, 20.

(437) Bradford, M. M. *Anal. Biochem.* **1976**, *72*, 248.

(438) Lutz, J.-F.; Hoth, A. *Macromolecules* **2006**, *39*, 893.

(439) Ghosh, P.; Han, G.; De, M.; Kim, C. K.; Rotello, V. M. *Advanced Drug Delivery Reviews* **2008**, *60*, 1307.

(440) Schneider, G.; Decher, G. *Nano Letters* **2004**, *4*, 1833.

(441) Schneider, G.; Decher, G. *Langmuir* **2008**, *24*, 1778.

(442) Schneider, G. F.; Decher, G. *Nano Letters* **2008**, *8*, 3598.

(443) Beamson, G.; Briggs, D. *High resolution XPS of organic polymers*; John Willey and Sons: Chichester, 1992.

(444) Zhou, C.; Khlestkin, V. K.; Braeken, D.; De Keersmaecker, K.; Laureyn, W.; Engelborghs, Y.; Borghs, G. *Langmuir* **2005**, *21*, 5988.

(445) Zareie, H. M.; Boyer, C.; Bulmus, V.; Nateghi, E.; Davis, T. P. *ACS Nano* **2008**, *2*, 757.

(446) Boyer, C.; Bulmus, V.; Priyanto, P.; Teoh, W. Y.; Amal, R.; Davis, T. P. *J. Mater. Chem.* **2009**, *19*, 111.

(447) Hirsch, L. R.; Stafford, R. J.; Bankson, J. A.; Sershen, S. R.; Rivera, B.; Price, R. E.; Hazle, J. D.; Halas, N. J.; West, J. L. *Proceedings of the National Academy of Sciences U.S.A.* **2003**, *100*, 13549.

(448) Gao, X.; Yang, L.; Petros, J. A.; Marshall, F. F.; Simons, J. W.; Nie, S. *Curr. Opin. Biotechnol.* **2005**, *16*, 63.

(449) Ballou, B.; Lagerholm, B. C.; Ernst, L. A.; Bruchez, M. P.; Waggoner, A. S. *Bioconjugate Chem.* **2004**, *15*, 79.

(450) Zheng, M.; Davidson, F.; Huang, X. *J. Am. Chem. Soc.* **2003**, *125*, 7790.

(451) Kohler, N.; Fryxell, G. E.; Zhang, M. *J. Am. Chem. Soc.* **2004**, *126*, 7206.

(452) Herrwerth, S.; Eck, W.; Reinhardt, S.; Grunze, M. *J. Am. Chem. Soc.* **2003**, *125*, 9359.

(453) Lee, H.; Lee, E.; Kim, D. K.; Jang, N. K.; Jeong, Y. Y.; Jon, S. *J. Am. Chem. Soc.* **2006**, *128*, 7383.

(454) Li, L.; Chen, S.; Zheng, J.; Ratner, B. D.; Jiang, S. *J. Phys. Chem. B* **2005**, *109*, 2934.

(455) Brewer, S. H.; Glomm, W. R.; Johnson, M. C.; Knag, M. K.; Franzen, S. *Langmuir* **2005**, *21*, 9303.

(456) Kaufman, E. D.; Belyea, J.; Johnson, M. C.; Nicholson, Z. M.; Ricks, J. L.; Shah, P. K.; Bayless, M.; Pettersson, T.; Feldotoe, Z.; Blomberg, E.; Claesson, P.; Franzen, S. *Langmuir* **2007**, *23*, 6053.

(457) Rezwan, K.; Meier, L. P.; Rezwan, M.; Voeroes, J.; Textor, M.; Gauckler, L. J. *Langmuir* **2004**, *20*, 10055.

(458) Zhang, Y.; Jiang, M.; Zhao, J.; Chen, D. *Eur. Polym. J.* **2007**, *43*, 4905.

(459) Kalyanasundaram, K.; Thomas, J. K. *J. Am. Chem. Soc.* **1977**, *99*, 2039.

Conclusions

Chapter 7

1. Conclusions

Along this thesis different polymers have been synthesized with a common characteristic, the thermoresponsive behavior. Controlled radical polymerization has been successfully utilized in order to obtain polymers with well defined architecture for diverse applications. Many techniques have been employed for characterizing and for analyzing these new materials. Also, it has been developed and adapted a new technique such as temperature modulated differential scanning calorimetry for characterizing the micelle formation process as well as the phase change process like lower critical solubility temperature. The main conclusions of the work undertaken in this thesis are detailed below:

Hierarchically Organized Micellization of Thermoresponsive Rod-coil Copolymers based on Poly[oligo(ethylene glycol) methacrylate] and Poly(ε-caprolactone)

1. A series of amphiphilic triblock copolymers, poly [oligo(ethylene glycol) methacrylate]$_x$ - *block* - poly (ε-caprolactone) – *block* – poly [oligo(ethylene glycol) methacrylate]$_x$, POEGMA$_{Co}$(x), has been successfully synthesized by ATRP with narrow polydispersity.

2. The cmc of these materials is governed by hydrophilic-lipophilic balance, thus cmc decrease as hydrophilic moiety increase. The values obtained are in good agreement with the expected for amphiphilic block copolymers as well as the partition coefficients.

3. A new technique of temperature modulated differential scanning calorimetry (Topem) has been successfully adapted for measuring the changes in the aggregation states of amphiphilic polymers and the results fit perfectly the thermoresponsiveness studied by turbidimetry.

4. It has been found that temperature and concentration of copolymers POEGMA$_{Co}$, containing a central PCL block, have influence on self-assembly mechanism as opposed to the homopolymer. As concentration increases the

cmt diminished for the copolymers and remained constant for the homopolymer.

5. The copolymers synthesized present a specific architecture (topology, relative block lengths) formed by blocks of different nature showing an unprecedented structural diversity. This has allowed us to identify a range of two-dimensional ordered particles which may be tuned by changing both the temperature and the concentration of polymer solutions.

6. The interplay of two hydrophobic chains and one thermoresponsive macromolecular chain offers the chance to more complex morphologies with potential applications for lipid-like drug delivery systems. The aggregates formed by these coil-rod-coil amphiphilic polymers have been found as cubic shape structur*e.*

Water-soluble, Thermoresponsive, Hyperbranched Copolymers based on PEG-Methacrylates: Synthesis, Characterization and LCST Behavior

1. Well defined PEGMA based hyperbranched copolymers using EGDMA as crosslinker have been successfully designed by reversible addition-fragmentation chain transfer polymerization. These polymers are water soluble and present thermoresponsive properties.

2. The ideal ratio for monomer/crosslinker is 40/3 because less proportion of crosslinker agent leads to non total hyperbranched polymers remaining high amount of linear polymers while more quantity of crosslinker forms a gel not soluble in water.

3. The LCST temperature depends on the hydrophilic-lipophilic balance, therefore controlling these parameters we have been able to design materials with LCST temperature adjusted. This was achieved by changing the monomer-to-macroinitiator ratio from 27:1 to 75:1.

4. The LCST values for hyperbranched copolymers based in PEGMA are between 7 and 9 °C below their analogues linear copolymers.

5. As expected, the addition of salts in the solution decrease the LCST of hyperbranched copolymers as it happens with the linear copolymers.

6. The characterization of the aggregates was done by DLS and TEM showing two different distributions, one in the range of 10 nm corresponding to the micelles and other distribution circa 200 nm corresponding to the aggregates. The data obtained by both techniques, DLS and TEM are in very good agreement.

Thermal studies and chromium removal efficiency of thermoresponsive hyperbranched copolymers based on PEG-methacrylates

1. The characterization of the LCST by temperature modulated differential scanning calorimetry (Topem) for hyperbranched polymers has been successfully achieved and they fit perfectly with those obtained by turbidimetry.

2. The thermal stability of hyperbranched polymers was slightly enhanced respect to linear structures, as it was evidenced by thermogravimetric analysis and chemiluminescence emission.

3. On hexavalent chromium removal from aqueous solution, hyperbranched polymers at temperature below LCST do not work, and above LCST its behaviour is excellent. At temperature above the lower critical solution temperature the polymers form aggregates and porous structures may be formed with nanocavities where the metal ions can get into them.

4. The values of chromium captured for hyperbranched are close to 40 mg per gram of polymer.

5. Hyperbranched thermoresponsive polymers could be used as an effective adsorbent, with the advantage that they can be separated from the medium.

Design and Synthesis of Dual Thermo-Responsive and Anti- Fouling Hybrid Polymer/Gold Nanoparticles

1. A new class of hybrid polymer-gold nanoparticles have been successfully designed/developed. These hybrid material have been obtained by grafting thermosensitive copoly(oligoethylene oxide) acrylates with narrow polydispersities prepared by the copolymerization of oligo(ethylene oxide) acrylate and di(ethylene oxide) ethyl ether acrylate using reversible addition-fragmentation chain transfer polymerization (RAFT) onto the surface of gold nanoparticles previously synthesized.

2. The thermoresponsive character of the gold/polymer hybrid nanoparticles in aqueous solutions (LCST) was demonstrated by nonisothermal turbidity measurements and DLS. These materials present two different LCSTs transition, one for each copolymer grafted to the nanoparticles. Thus, once the temperature goes beyond the lower LCST that polymer chains collapse and they form a hydrophobic layer on the particle while the chains of the polymer with higher LCST are stabilising the particle avoiding the formation of aggregates. This situation has been successfully proved by designing an experiment to determine the polarity of the environment of the particles.

3. For this new material, the presence of the thermoresponsive polymer attach to the gold nanoparticles is easily confirmed due to the color change of the solution, when the temperature is higher than the LCST the solution turns from red to purple because its dimensions and environment has changed.

4. The aggregates formed above the LCST were characterized using DLS and TEM measurements, confirming the presence of aggregates with sizes of 200 nm.

5. By choosing specific polymers it has been demonstrated that it is possible to control the hydrophilic/hydrophobic character of the surface layers surrounding the gold nanoparticles.

6. The system achieved shows anti-fouling/protein resistant surfaces which are evaluated by Bradford assays using BSA as model protein.

Resumen de la Tesis Doctoral en Castellano

Chapter 8

1. Introducción

El objetivo de esta tesis ha consistido en preparar polímeros inteligentes con estructuras bien definidas y sensibles a la temperatura mediante polimerización radical controlada. El interés por el desarrollo de los materiales inteligentes ha incrementado en muy diversos sectores como por ejemplo el farmacéutico o el biomédico, en los que las aplicaciones potenciales en las que podrían ser utilizados estos materiales incluyen liberación de fármacos, genes y células, ingeniería superficial y remediciación de aguas.

Los polímeros sintetizados en esta tesis se han obtenido mediante polimerización por transferencia de cadena vía fragmentación-adición reversible (RAFT), polimerización radical por transferencia de átomo (ATRP) y polimerización por apertura de anillo (ROP). Para su caracterización se han utilizado diversas técnicas como calorimetría diferencial de barrido, análisis termogravimétrico, quimioluminiscencia, microscopía electrónica, cromatografía liquida o dispersión de luz polarizada entre otras.

2. Resumen por Publicaciones

Hierarchically Organized Micellization of Thermoresponsive Rod-Coil Copolymers based on Poly[oligo(ethylene glycol) methacrylate and Poly(ε-caprolactone)

En este trabajo se describe la síntesis por polimerización radical controlada mediante transferencia de átomo de una serie de copolímeros anfifílicos tribloque del tipo ABA donde el bloque B está basado en policaprolactona y los bloques A laterales están formados por metacrilato de poli(oligo etilen glicol). Se ha estudiado el comportamiento autoasociativo en disolución acuosa de este tipo de copolímeros por distintas técnicas. Es importante destacar que el control de la organización que presentan los polímeros de naturaleza anfifílica se rige fundamentalmente por la interacción de las cadenas hidrofóbicas e hidrofílicas que dota a la macromolécula de la propiedad de responder a estímulos de temperatura aunque parámetros como la arquitectura y la naturaleza de los bloques también modifican dicho comportamiento.

Cabe resaltar que en este artículo se desarrolla el uso de una nueva metodología para la determinación de la temperatura crítica de micelización mediante la técnica de Calorimetría Diferencial de Barrido con Temperatura Modulada. Por otra parte, mediante Microscopía Electrónica de Transmisión de Alta Resolución, se ha detectado la formación de estructuras cúbicas con geometría cristalina.

Water-soluble, Thermoresponsive, Hyperbranched Copolymers based on PEG-Methacrylates: Synthesis, Characterization and LCST Behavior

En este estudio se han obtenido polímeros formados por metacrilatos de polietilenglicol (PEG) con una temperatura crítica mínima de solubilidad (LCST) bien definida. La precisión de la LCST se ha conseguido modificando tanto la composición de los polímeros como variando la longitud de las cadenas laterales de PEG. Por tanto, se han sintetizado polímeros con diferente arquitectura con la intención de evaluar como influye la estructura interna en sus propiedades de agregación en disolución acuosa.

Thermal studies and chromium removal efficiency of thermoresponsive hyperbranched copolymers based on PEG-methacrylates

Los polímeros hiperramificados sensibles a estímulos de temperatura sintetizados anteriormente se han aplicado en el campo de la remediación de aguas. Dada la propiedad que poseen de autoasociación en función de la temperatura se han evaluado como materiales cuya función es encapsular átomos de metales pesados en el interior de los agregados. Se han realizado ensayos para determinar su capacidad como agentes adsorbentes de átomos de cromo presentes en aguas contaminadas. Otra ventaja de estos materiales es que son reutilizables ya que la propiedad de micelización en función de la temperatura es reversible por lo que permite la recuperación de los polímeros una vez se haya purificado el agua contaminada.

Adicionalmente, se ha estudiado tanto el comportamiento térmico como su estabilidad frente a la temperatura mediante las técnicas de Quimioluminiscencia y Análisis Termogravimétrico.

Design and Synthesis of dual Thermo-Responsive and Anti-Fouling Hybrid Polymer/Gold Nanoparticles

El objetivo de este estudio ha sido la obtención de nanopartículas de oro sensibles a estímulos de temperatura y evaluar las propiedades de estos materiales híbridos en disolución acuosa. Para ello se han sintetizado por polimerización radical controlada mediante transferencia de cadena vía adición-fragmentación polímeros termosensibles, con diferente LCST, bien definidos de polidispersidad estrecha que se han injertado en la superficie de las nanopartículas de oro. De este modo, las nanopartículas poseen doble carácter en cuanto a su respuesta a variaciones de temperatura.

3. Conclusiones

A lo largo de esta tesis se han sintetizado polímeros de distinta índole con una característica común, su respuesta a estímulos de temperatura. La polimerización radical controlada ha sido utilizada de manera exitosa para obtener polímeros con una arquitectura controlada y bien definida para su uso en diversas aplicaciones. Se han utilizado una gran variedad de técnicas para caracterizar y analizar estos nuevos materiales. También se ha desarrollado y adaptado una nueva técnica basada en la calorimetría diferencial de barrido modulada para caracterizar el proceso de formación de micelas, así como, el proceso de cambio de fase como la temperatura mínima crítica de solubilidad.

La polimerización ATRP del macromonómero OEGMA (8-9 unidades de repetición) usando como un macroiniciador bifuncional basado en PCL nos ha llevado a obtener una serie de copolímeros de bloque varilla-hélice-varilla, dónde las varillas están

formadas por fragmentos densamente ramificados. Como la longitud del bloque de PCL está fijado, el balance hidrofílico-hidrofóbico de estos copolímeros de bloque se ha controlado variando el grado de polimerización del bloque POEGMA; esto se ha realizado modificando la relación monómero-macroiniciador de 27:1 a 75:1

El comportamiento autoasociativo está regido por el balance hidrofílico-lipofílico así como de efectos topológicos. De esta manera, los valores de cmc fueron suficientemente bajos como cabe esperar de copolímeros de bloque anfifílicos y tanto las cmc como los coeficientes de partición disminuyen según aumenta el grado de polimerización. Esta propiedad es explicada debido a la inclusión de las cadenas de oligoetilen glicol en el interior de la micela debido a repulsiones estéricas provocadas por los fragmentos altamente ramificados.

La cualidad de responder a estímulos de temperatura que poseen estos copolímeros se ha estudiado por MTDSC y turbidimetría. A diferencia de los homopolímeros POEGMA, se ha comprobado que el comportamiento autoasociativo de los copolímeros POEGMA que contienen un bloque central de PCL depende tanto de la temperatura como de la concentración y para estos copolímeros se ha observado que la CMT disminuye al aumentar la concentración, mientras que para los homopolímeros la cmt permanece constante a diferentes concentraciones.

Debido a su específica arquitectura (topología, relación de longitud de bloques) y la naturaleza de los bloques de la macromolécula se ha observado una diversidad y multifuncionalidad estructural única. Esto nos ha permitido identificar partículas ordenadas bidimensionalmente las cuales pueden ser modificadas cambiando la temperatura o la concentración de los polímeros en disolución. La interacción de las dos cadenas hidrofóbicas y la cadena sensible a estímulos de temperatura nos ofrece la oportunidad de crear morfologías más complejas con gran potencial en aplicaciones para formar sistemas de liberación de fármacos liposolubles.

La LCST de los polímeros basados en PEGMA se ha controlado con gran precisión variando la composición de los copolímeros y cambiando la longitud de las cadenas de PEG. En esta investigación se ha estudiado el impacto tanto de la topología como de la

composición sobre la LCST. Para este propósito se han sintetizado vía RAFT polímeros hiperramificados y sus análogos lineales determinando que una disminución de la relación monómero/monómero multifuncional o CLA nos lleva a la formación de un gel mientras que si incrementamos dicha relación obtenemos principalmente el polímero lineal. Se ha comprobado que los polímeros hiperramificados se dispersan en agua y son perfectamente estables, es decir, no se dio sedimentación. Estos polímeros hiperramificados solubles en agua poseen una LCST de aproximadamente 8 grados inferior a la de sus análogos lineales. Esta diferencia está causada por la restricción en la movilidad en las cadenas que presentan los polímeros hiperramificados.

Se ha evaluado la adición de sal (ej. NaCI y Na_2SO_4) en la disolución de polímero obteniendo una disminución en la LCST tanto para los polímero lineales como para los ramificados.

La caracterización de los agregados que forman en disolución acuosa los polímeros ramificados por encima de su LSCT se ha llevado a cabo mediante DLS y TEM, cuyos resultados son concordantes. Los resultado muestran que por debajo de la LCST los tamaños de los agregados son de 10 nm y el PDI es 0.4 y por encima de la LCST los tañamos de los agregados aumentan hasta 200 nm (con una disminución importante de PDI) y la disolución se vuelve turbia.

La determinación de la temperatura mínima crítica de solubilidad de los polímeros lineares e hiperramificados se ha realizado mediante MTDSC obteniendo valores muy próximos a aquellos obtenidos mediante espectroscopia UV.

Se ha determinado que la estabilidad térmica de los polímeros hiperramificados es ligeramente superior que los que poseen estructuras lineales, tal y como se ha evidenciado mediante análisis termogravimétrico y emisión de quimioluminiscencia.

Se ha encontrado que estos polímeros poseen la capacidad de adsorber átomos de cromo hexavalente. Esta cualidad se da únicamente cuando el polímero está formando agregados por encima de su LCST. Aprovechando esta característica se han estudiado estos materiales para su aplicación en la remediación de aguas contaminadas con metales pesados. Los polímeros hiperramificados ofrecen resultados más eficientes

que los lineales. Los valores de cromo capturado por los polímeros hiperramificados son aproximadamente de 40 mg por gramo de polímero, lo cual significa que estos polímeros podrían ser utilizados como adsorbentes efectivos con la capacidad de poder ser fácilmente separados del medio y así poder ser reutilizados en numerosas ocasiones.

Se han obtenido materiales híbridos a través de la unión de un polímero y un material inorgánico. Esta unión se ha realizado injertando copolímero sensible a la temperatura sobre nanopartículas de oro, controlando tanto la composición del polímero para ajustar las propiedades térmicas así como el tamaño de la partícula para obtener una nueva clase de nanopartículas híbridas polímero/GNP. Estas nuevas nanopartículas que poseen en su superficie capas de polímero anfifilíco nanoestructurado, además de poseer un comportamiento que responde a estímulos térmicos poseen una superficie con propiedades anti-fouling. En este sistema la presencia del polímero termosensible unido a la nanopartícula de oro se confirma por el cambio de color de disolución, cuando la temperatura es superior a la LCST la solución cambia de rojo a violeta debido a que las dimensiones de las nanopartículas y su entorno han cambiado.

Combinando polímeros de diferente LCST en la superficie de la partícula se hace posible cambiar las propiedades del sistema, se ha observado que diferente ratios de polímero provoca cambios en la LCST resultando también un ensanchamiento de la transición. De esta manera cuando la temperatura sobrepasa la LCST menor, las cadenas de este polímero colapsan y forman una capa hidrofóbica, mientras que las cadenas del polímero con mayor LSCT estabilizan la partícula evitando la formación de agregados.